Development of Atmospheric Pressure Plasma Based Desorption-Ionisation Sources for Mass Spectrometry

by

Carl Fletcher

UNIVERSITY OF LIVERPOOL

Department of Electrical Engineering and Electronics

Thesis submitted in accordance with the requirements of the University of Liverpool for the degree of Doctor of Philosophy

March 2018

Declaration

I hereby declare that this thesis is my own work and no further sources of information have been used other than the references cited. Neither this thesis nor any part of it have been submitted to any other university or institution for the application of another degree or qualification.

Signed: _____(Carl Fletcher)

Date: _____

Abstract

Ambient ionisation mass spectrometry is a rapidly increasing field, largely dominated by ambient ionisation sources that are dependent upon plasma formation. This thesis discusses attempts to create a plasma based ionisation source used at atmospheric pressure to be integrated with mass spectrometry for small molecule analysis such as drugs and explosives detection. The important features of the plasma ionisation source were to provide a rapid analysis technique which required little or no sample preparation, minimal consumables and a large sampling surface area.

The plasma sources developed in this study were used to treat various surface types replicating banknotes for drugs on money analysis, ensuring that plasma treatment was not detrimental to their integrity. Furthermore, the plasma sources were all coupled with various mass spectrometers for sample analysis and were successfully able to detect various drugs and explosives in both positive and negative ion modes at low nanogram to picogram detection limits. The evidence that these plasma sources are capable of ionising in both positive- and negative-ion modes suggests the possibility of other applications within small molecule analysis.

Most importantly, these plasma sources are able to detect drugs and explosives with very minimal sample preparation even from UK polymer banknotes without destroying them. This technique reduces consumable costs; whilst affording great sensitivity, speed, high-throughput, selectivity and specificity. As these plasma sources have been coupled with various mass spectrometers, it is possible that they will be readily coupled with other detectors such as ion mobility spectrometry.

Acknowledgements

Firstly I give thanks to my PhD supervisor, Professor James Bradley, for putting his faith in me and offering me this great opportunity to further my career and also for providing me with support, guidance and know how to progress throughout this project. Secondly, a big thank you to Mass Spec Analytical Ltd (MSA) for providing me with unlimited use of an analytical mass spectrometer, samples and computer. Without MSA this project would not have been as successful. A special thanks to Dr. Richard Sleeman for his advice and guidance, John Luke for helping with modifications of plasma sources and interfacing them with the mass spectrometer and Peter Luke for technical guidance and his assistance throughout.

During my PhD I have had the pleasure to work alongside many people whom without, this PhD would not have been as enjoyable and so my thanks go to TJ, Zaenab, Mo, Francis, Mike, Paddy, Ni, MJ, Kirsty, Mark, Tom Farley, Fred, Tom Hardiment, Ali, James Walsh, Paul, Brandon, Bryony, Aaron, Peter, Dave, Chris, Jenny, Lykourgos, Taiwo, Darren, Tom, Reino, Larry, Jill and Phil. An additional thank you to Sam Harrison for keeping me sane outside of work and showing me the Scouse way of life. In addition to the friends and colleagues from Liverpool, I must say thanks to the staff at MSA for making me feel welcome and part of the team making my time there very enjoyable, so thank you Byron, Jade, Vicki, Beth, Fay, Amy, Erin, Steve, Susanne, Sandra, Lance, Jonathan and Steve Grant.

I would also like to thank Alan Roby and Gareth Blacoe for their help in the workshop and making my attempted drawings come to life, whilst always being up for a laugh. Thank you to Harm Van Zalinge for training me how to use the AFM and understand my data, and also for being patient with me in learning. A big thank you to Fiona McBride, Alan Massey and Prof. Raval for their help on surface measurements and data manipulation they have acquired for me.

Thank you to the Bank of England for supplying dummy polymer £50 banknotes to allow the study of surface modification.

Thank you to Sciex for allowing access to their Sciex X500R QTOF at Warrington, UK to allow integration of the DBD ion source to their instrument for sample analysis.

Another thanks must be given to Dr. Ortori and Prof. Barrett of the University of Nottingham for allowing me to visit and acquire data on their Thermo Exaactive Orbitrap.

My deepest gratitude goes to all my friends and family who have supported me throughout my PhD, to whom I will be forever indebted, and to Jade and Aurora for all their love and patience.

Thank you to the Innovative Research Call 2016 for Explosives and Weapons Detection, Phase I, for funding the initial development of the DBD ion source for explosive detection. This is a Cross-Government programme sponsored by a number of Departments and Agencies under the UK Government's CONTEST strategy in partnership with the US Department of Homeland Security, Science and Technology Directorate.

Finally, I must give thanks to EPSRC for funding my studentship and the University of Liverpool for giving me the platform to allow me to partake in this fantastic opportunity.

Publications

The research carried out during the course of this study has, thus far, led to the following publications and patents

- **C. Fletcher**, R. Sleeman, J. Luke, P. Luke, J. W. Bradley, "Explosive Detection Using a Novel Dielectric Barrier Discharge Ionisation Source for Mass Spectrometry", *Journal of Mass Spectrometry* **53**, 214-222 (2017).
- **C. Fletcher**, R. Sleeman, J. Luke, P. Luke, J. W. Bradley, "Mass Spectrometric Analysis of Polymer Banknotes for the Presence of Controlled Drugs using a Dielectric Barrier Discharge Ion Source ", Submitted to *Rapid Communications in Mass Spectrometry*, March 2018, manuscript number RCM-18-0097.

Conferences

- British Mass Spectrometry Society (BMSS) Ambient Ionisation Special Interest Group (SIG) - National Physics Laboratory, Teddington, UK, 27th November2014.
- NiCE-MSI Science and Technology Day and 3D OrbiSIMS Launch Event **(Poster Presentation)** - National Physics Laboratory, Teddington, UK, 29th November 2016.
- Explosives Analysis Using High Resolution Accurate Mass - Thermo Fisher Scientific, Hemel Hempstead, UK, 8th September 2016.
- British Mass Spectrometry Society (BMSS) Ambient Ionisation Special Interest Group (SIG) - Keele University, Keele, UK, 18th January 2017.
- 38th British Mass Spectrometry Society Annual Meeting 2017 **(Poster Presentation)** - Royal Northern College of Music, Manchester, UK, 7th September 2017.
- 12th International Symposium on the Analysis and Detection of Explosives (ISADE) **(Poster Presentation)** - Keble College, Oxford, UK, 17-21st September 2017.
- UK Security EXPO 2017 **(Exhibitor and Poster Presentation for IRC 2016)** - Olympia, London, UK, 29-30th November 2017.
- British Mass Spectrometry Society (BMSS) Ambient Ionisation Special Interest Group (SIG) **(Oral Presentation and Poster Presentation)** - Syngenta, Bracknell, UK, 31st January 2018

Intellectual Property

- The foreground IP for the DBD plasma ionisation source is covered by British Patent Application No. 1717618.1

Nomenclature

Provided here is a list of commonly used abbreviations and notations

Abbreviations

MS Mass Spectrometer

MS/MS Tandem Mass Spectrometry or Mass Spectrometry/Mass Spectrometry

AI-MS Ambient Ionisation Mass Spectrometry

TD-MS/MS Thermal Desorption Mass Spectrometry/Mass Spectrometry

TD Thermal Desorption

APCI Atmospheric Pressure Chemical Ionisation

LTP Low Temperature Plasma

AFM Atomic Force Microscopy

WCA Water Contact Angle

XPS X-ray Photoelectron Spectroscopy

FTIR Fourier Transorm Infrared Spectroscopy

UoL University of Liverpool

PP Polypropylene

DBD Dielectric Barrier Discharge

SBD Surface Barrier Discharge

DART Direct Analysis in Real Time

DESI Desorption Electrospray Ionisation

PTFE Polytetrafluoroethylene

TEIS Thermal Extraction Ionisation Source

TNT Trinitrotoluene

RDX Cyclotrimethylenetrinitramine

PETN Pentaerythritol tetranitrate

HMTD Hexamethylene triperoxide diamine

4-MEC 4-methylethcathinone

MDMA 3,4-methylenedioxymethamphetamine

THC Δ^9-Tetrahydrocannabinol

Mephedrone 4-methylmethcathinone (4-MMC)

MeOH Methanol

AcCN Acetonitrile

mL Millilitre

μL Microlitre

μg Microgram

TRL Technology Readiness Level

LOD Limit of Detection(s)

Contents

List of Figures

List of Tables

Chapter 1

Introduction

As services for routine analysis of all kinds require high-throughput, speed and sensitivity, the techniques used have to be cheap and easy to use, whilst being reliable and reproducible. Conventionally, techniques used for screening purposes in many applications rely upon the use of chromatography [1–3], ion mobility spectrometry and mass spectrometry [4, 5]. Whilst there are other techniques available[Moore2004], these core technologies are ubiquitously used within the majority of applications. As the need for analyses to be quicker and cheaper increases, techniques involving chromatography have started to become slightly less favourable for some users. The reason for this is that traditionally, chromatographic methods require a lot of sample preparation and the analysis time can be hours for some analytes and applications. Despite this, there has been some effort in dramatically reducing the method time for chromatographic methods but, there still remains the underlying issue of sample preparation and consumable costs and also co-elution of some compounds due to a reduced separation time [6, 7].

Ion mobility spectrometry (IMS) is widely used for screening purposes, especially within the security sector such as airports [8]. IMS is a rapid technique with very few consumables or sample preparation however, IMS does not possess a very high specificity and therefore, affords a relatively high false positive rate [9]. False positives can prove costly, especially within an environment such as an airport, where if for example an IMS returned a positive result for explosives on a passenger suitcase, the customs officer would be required to fully search the suitcase contents and person carrying them which consumes a significant amount of time and man-power, especially if the result was a false positive. False positives discourage security agencies from using IMS as a robust form of security and instead, screen a percentage of people/possessions as opposed to 100%. Despite this though, IMS is relatively inexpensive and rapid hence, it is widely used for many screening applications.

Mass spectrometry can be coupled to chromatography such as gas chromatography

(GC) or liquid chromatography (LC) to create hyphenated techniques GC/MS or LC/MS. The benefits of the addition of mass spectrometry are an increased sensitivity, specificity and selectivity but the use of chromatography still possesses lengthy run times and high consumable costs. Efforts to use mass spectrometry without chromatography are becoming more popular especially with tandem mass spectrometry (MS/MS) and accurate mass as they have great sensitivity, speed, specificity and selectivity without the compromises of chromatography. Unfortunately though, tandem mass spectrometry tends to come at a higher capital cost and therefore, is seldom seen for screening applications but is used for final confidence checks within a laboratory environment.

This thesis discusses the development of several atmospheric pressure plasma based ionisation sources typically designed for mass spectrometry but with the potential of being readily coupled with other technologies such as chromatographic techniques and IMS. The aims of the plasma based sources were to have a large sampling surface area and to operate at atmospheric pressure with as few consumables and little sample preparation as possible.

This thesis begins with chapter 2 which provides an overview of plasma and existing plasma based ionisation sources, justifying the hypotheses for this research. Chapter 3 thoroughly documents the experimental set-up that was used for all experiments. Chapter 4 discusses data that was obtained using an atmospheric pressure plasma jet with various mass spectrometers. Additional development led to two additional plasma based ionisation sources called a plasma brush and plasma jet array which are discussed in chapter 5. These various plasma sources were used with various surfaces such as polypropylene for the application of analysing drugs on money which is discussed in chapter 6. In addition to the before mentioned sources, another plasma based ionisation source was developed based on a surface dielectric barrier discharge which is discussed in chapter 7. Finally, the data from the surface barrier discharge ionisation source is thoroughly detailed in chapters 8 and 9 for explosive and drug detection respectively, before concluding the findings in chapter 10.

Chapter 2

Literature Review

This chapter will thoroughly discuss the previous literature surrounding atmospheric pressure plasmas within this scope of research.

2.1 Atmospheric Pressure Plasma Based Ionisation Sources for Mass Spectrometry

Plasma in physics is described as a fourth state of matter, but unlike solids, liquids and gases, plasma does not exist freely on Earth under standard conditions [10]. Atmospheric pressure plasma sources are nonthermal, which is described as a plasma that is not in thermodynamic equilibrium due to discrepancies within the electron and ion temperatures or the velocity distribution of one of the species in relation to the Maxwell-Boltzmann distribution [11]. Plasma is an ionised or excited gas such as helium, that largely consists of ions, neutrals and free electrons. Atmospheric pressure plasmas have attracted significant attention due to their wide variety of applications without need for vacuum systems and so allows for direct interaction with the sample or surface that is to be analysed.

It is the species within the plasma that can be attributed to the characteristics that allow for atmospheric pressure desorption and ionisation. The mechanisms of these are still only vaguely understood as the processes is fairly complex. Firstly, within the plasma there is an abundance of electrons, and when an electron is directed with a large amount of energy at a surface, it can induce ionisation through electron impact [12, 13]. This is important within atmospheric plasmas because the temperature of a non-equilibrium plasma is always lower than the ionisation potential in regards to the Maxwell-Boltzman distribution [13]. The avalanche of electrons to the surface allows for an atmospheric pressure plasma to ionise a molecule despite the ionisation potentials and temperatures being low.

Electron impact ionisation can ionise a molecule (M) into a cation as shown in the equation below.

$$M + e^- = \mathrm{M}^{+\bullet} + 2e^- \tag{2.1}$$

Furthermore, an atmospheric pressure will contain various other species such as metastables (excited state of an atom) at these metastables are responsible for further ionisation mechanisms such as metastable induced ionisation [14]. Penning ionisation is the interaction of an excited gas phase atom (metastable) and the target molecule. The collisions between the target molecules and excited species result in ionisation of the target molecule, such as in the equation below.

$$G^* + M \rightarrow \mathrm{M}^{+\bullet} + e^- + G \tag{2.2}$$

The metastables and electrons are responsible for the ionisation of a target molecule, but also play a large role in the desorption of the molecule from a surface. The energy imparted onto a surface from a plasma results in a disturbance between the molecule and the surface, resulting in liberation. Additionally, within a non-equilibrium plasma, there are also ions, neutrals and radical which are all responsible for some of the desorption-ionisation.

Mass spectrometry has attracted significant attention in research and industrial environments over recent years due to an increased desire for high-throughput and rapid analysis. The most ubiquitous method is ambient ionisation mass spectrometry (AI-MS), which enables analysis to be very versatile, cheap and potentially portable. AI-MS combines the selectivity and sensitivity of mass spectrometry with direct analysis of samples with little or no preparation [15]. The first of its kind, introduced in 2004, was desorption electrospray ionisation (DESI) which utilizes an electrospray containing charged solvent ions directed at the sample surface, these collisions create gaseous ions of the sample present, desorbing them from the surface [16]. Shortly after the innovation of DESI was direct analysis in real time (DART), which is similar to DESI in terms of versatility and time of analysis [14]. DART ionises analytes upon collision from electronically excited molecules such as helium metastables [He^*].

Since the introduction of DART and DESI, the field of AI-MS has developed rapidly producing more than a dozen new techniques such as low temperature plasma (LTP) [17], dielectric barrier discharge ionisation (DBDI) [18], plasma assisted desorption ionisation (PADI) [19], atmospheric pressure plasma jet (APPJ) [20], micro-plasma

in a micro-hollow cathode discharge (MHCD) [21], high-power pulsed microplasma jet (HPPMJ) [22], atmospheric pressure glow discharge (APGD) [23], and flowing atmospheric pressure afterglow (FAPA) [24, 25], to name a few. However, as AI-MS is relatively novel there are still many limitations in its understanding and application. Previous literature, focused on mass spectrometry, outlined its importance in many analytical fields such as environmental monitoring [26], public security [27], tissue biopsy analysis [28], and forensic science [29]. Therefore, it is important to reinforce the understanding of new ionisation techniques as it could potentially benefit a wide variety of applications.

2.1.1 Low Temperature Plasma (LTP)

Low temperature plasma (LTP) probes have seized the majority of attention since they were first described in 2008 [17]. An LTP is usually a glass or quartz tube which has a grounded electrode inside and an outer electrode where the glass wall serves as a dielectric barrier. A high voltage power supply providing kV (at a frequency in the region of 10s of kHz) to the outer electrode produces a dielectric barrier discharge (DBD) with the discharge gas (usually either helium, argon, nitrogen or air). The discharge gas is delivered through the glass tube providing transport for gaseous ions. An LTP probe requires a much lower gas flow than DART and DESI which is more cost efficient and could potentially be easily portable [30]. Despite the LTP employing a DBD, it differs from DBDI due to the orientation of the electrodes within the probe, promoting analysis of samples without placing them between two electrodes.

Many different configurations of LTP probes have been described, some with differing results and parameters. For example, Martinez-Jarquin *et al.*, [31], reports an LTP based on a similar design as above [17], but regards it as a safer design. This design incorporates two glass tubes, one inside the other to prevent arcing. Both designs utilise a low power input and output, however, the gas temperatures are different. Harper *et al.*, [17], reports temperatures of around 30 ^{o}C whereas Martinez-Jarquin *et al.*, [31], reports a temperature of 70 ^{o}C without the second tube and 48 ^{o}C with the second tube, probably due to a higher power and frequency used.

It is possible to operate an LTP probe using a pulsed power source which decreases power consumption even further, this may also lower the gas temperature of the plasma [32]. However, every parameter will have an effect on the LTP probes' ability for desorption/ionisation from temperatures to incidence angle [33, 34]. Different waveforms can also affect the plasma characteristics as well as the reagent ion formation; optimisa-

tion of these parameters as well as a good understanding will help to produce a better, more efficient plasma source [35–37]. Furthermore, understanding the ion chemistry of the ionisation process is important in optimising these parameters, but it is also crucial to gain a sound knowledge of what is happening when the plasma interacts with the air such as the formation of water clusters [33–38].

Recent developments of LTP probes have shown that achieving very low limits of detection (LODs) is possible although difficult without thermal desorption [39]. When thermal desorption is used in conjunction with an LTP, the LODs achieved are much lower and more reproducible. However, thermal desorption would not be suitable for analysis on living tissues or heat sensitive samples as heating the surface may cause damage or degradation. Harper *et al.*, [17], recorded detection limits as low as 5 pg for solid samples and 1 ppb for aqueous solutions; the samples used in this experiment were RDX, TNT and PTFE. Chen *et al.*, [39], operated a halogen lamp as a heat source providing thermal aid to desorption of solid samples, in this experiment LODs of 10-20 pg were observed for TNT, RDX, PETN, HMX, Tetryl and TNB.

Unfortunately, much of the previous literature does not offer a wide range of compounds to show the versatility of the plasma ion sources; typically compounds of a similar type in either positive or negative mode are described as opposed to a variety of compounds in both positive and negative modes. Furthermore, many papers also show that the plasma, coupled to a detection device such as a mass spectrometer, merely detect samples and do not always report LODs and other limitations such as matrix effects. Therefore, it is observed that there are gaps in the research in regards to LTP probes but they have potential as a desorption/ionisation source. An LTP can be operated at low power and low temperature showing its definite potential to be a fully portable device [40–42], in addition to a rapid method for screening a large quantity of samples allowing for high-throughput analysis; an LTP probe has been reported to be capable of analysing roughly 600 samples in 1 hour [30].

2.1.2 Dielectric Barrier Discharge Ionisation (DBDI)

In addition to LTP, significant interest has been invested into dielectric barrier discharge ionisation (DBDI) as it has great potential as a desorption/ionisation device. In DBDI, a capacitively coupled dielectric barrier discharge (DBD) is produced between two electrodes (a pin and a plate) in a design not too dissimilar to an LTP probe. The difference is, in DBDI, the sample is placed directly between the electrodes [18, 43]. Although there is an increasing awareness of the interactions within the DBD such as

plasma bullet formation [44], and propagation of the plasma [45], there is limited research into the application of DBDI as an ionisation source. A DBDI source was developed for use with liquid chromatography/mass spectrometry (LC/MS) which demonstrated that it was a reasonably soft ionisation technique useful for analysing polar compounds [46]. Further to this, a DBDI source was coupled with a tandem mass spectrometer for the analysis of TNT, RDX and PETN with LODs of 10 pg, 0.1 ng and 0.1 ng respectively (lower than with ion mobility spectrometry (IMS)) and also reported a gas flow 10 times lower than DART and DESI [18].

Unfortunately however, there has been little advancement in recent years in the application of DBDI. The reason for this could be because DBDI, despite its low gas flow operation, results in a higher degree of fragmentation regarding it as a slightly 'harder' ionisation technique. Harder ionisation results in unwanted fragmentation and thus reducing the overall intensity of the molecular ion. For mass spectrometric methods such as tandem mass spectrometry, the highest sensitivity of the precursor ion is desired and therefore, a softer ionisation mechanism is preferred. Furthermore, by exposing the sample to the direct discharge between the electrodes, the characteristics of the plasma such as the electric field may be altered, possibly resulting in limited reproducibility, matrix effects and depletion of sensitivity [32]. For this reason, LTP probes based on a DBD are preferred as direct contact with the plasma can be avoided or controlled.

2.1.3 Plasma Assisted Desorption Ionisation (PADI)

Another recent development of plasma sources includes plasma assisted desorption ionisation (PADI). The initial introduction of PADI was in 2002 for the surface treatment of (bio)materials [20] and since, there have been recent developments for PADI sources to be coupled with mass spectrometry (MS) for analytical purposes. Ratcliffe *et al.*, [19], reported a comparison of a PADI/MS device with DESI and DART, outlining the advantages gained by using PADI. Firstly, DART uses a high-voltage/low-current to produce its corona discharge whereas PADI utilises a lower operating voltage and higher current, often powered by radio frequencies. Furthermore, PADI is operated with low voltages in the region of 300 V peak-to-peak, and low power ranges less than 5 W resulting in a cold, non-thermal plasma that is also low in ion energies, roughly less than 5 eV. This enables the plasma to directly interact with the samples without heating or degrading them, and unlike DART, it does not depend upon the removal of highly energetic species, resulting in a simpler ionisation source [19].

Although Ratcliffe *et al.*, reports a cold/non-thermal plasma, there are no temperature

measurements recorded but there are optimised values for incidence angles and power used to achieve the highest signal intensities [19]. The samples were over-the-counter and prescription drugs. There is no evidence of LODs, however the mass spectra is much cleaner in comparison to DART and DESI. A further study of a micro-PADI device shows an even cleaner mass spectrum suggesting an even softer ionisation mechanism which is very promising [47]. PADI also requires a lower voltage supply than LTP and DBDI as it requires only hundreds of volts in comparison to kV [17–19].

A study by McKay *et al.*, [48], reinforces the understanding of the plasma ion chemistry, what is happening in the plasma and its interaction with the surroundings, such as the importance of water cluster ion formation. Additionally, the effects of the duty cycle on the plasma is further understood as by decreasing the duty cycle, the yield of positive ions is shifted towards higher mass clusters as a result of a decrease in gas temperature which in return increases hydration reactions [48]. It is suggested that cluster ions are very important in plasma mechanisms, and fragments were seen using PADI that had not been previously reported, showing a higher degree of fragmentation suggesting that PADI is not as 'soft' as DESI in terms of ionisation.

A recent study has compared PADI to an LTP and a radio-frequency plasma needle and it suggests that the ion intensities achieved by PADI are 10 times higher than LTP and 100 times higher than a plasma jet [33]. PADI definitely has potential as an ambient desorption/ionisation device and after more extensive research into the LODs that may be achievable, it could potentially supersede other ionisation sources due to its ability to be low powered, pulsed and non-thermal. However, further development is required to appreciate its potential.

2.1.4 Micro-Hollow Cathode Discharge (MHCD)

Developments similar to atmospheric pressure plasma jets (such as LTP and PADI) have been introduced called micro-plasma discharges as an ionisation source for mass spectrometry. The first technique called micro-hollow cathode discharge (MHCD) incorporates a silicon wafer chip with a 200 μm circular hole through the middle which enables the discharge gas to flow through at a low flow rate of only 0.28 L/min, and operates a low negative voltage in the range of -300 and -350 V [21]. This study also discusses the likely ionisation processes that the plasma employs such as proton transfer ionisation, electron-impact ionisation, photoionisation due to vacuum ultraviolet light (VUV), and also metastable-induced penning ionisation. However, understanding whether these ionisation processes take place simultaneously requires further research and also whether any process is more dominant than the other, for example ionisation caused by VUV may be

harder to achieve as not all of the plasma may be within the VUV region. It is observed by this study that the LODs are in the range of 0.4 and 14.3 ng/mm^2 for the samples analysed which is encouraging for its use as a desorption/ionisation device however, it is also clear that matrix effects may need to be understood further as paracetamol (acetaminophen) in two different matrices had very different LODs [21].

2.1.5 High-Power Pulsed Micro-Plasma Jet (HPPMJ)

A more recent study explored the use of a touchable high-power pulsed micro-plasma jet (HPPMJ) as a desorption/ionisation source for ambient ionisation mass spectrometry [22]. The HPPMJ was based on the design used in Symonds *et al.*, [21], but the plasma jet was coupled to a high power pulsed supply rather than a DC power supply. The benefit of using a pulsed power supply is that it can produce a much lower temperature plasma, unlike a DC glow discharge which tends to produce high-temperature afterglows exceeding 200 ^{o}C that may cause damage or degradation to thermally sensitive samples [14, 21, 25]. The HMPPJ was a molybdenum-glass-molybdenum layered structure containing a 500 μm circular opening for the discharge gas to be introduced through at only 200 mL/min. An average power density of 0.6 W per Hz was observed for plasma generation suggesting that a portable version could be produced with a battery operated power source. This HPPMJ shows significant ability to be a suitable desorption/ionisation source due to its capacity to produce a gas excitation temperature of nearly 7000 K which favours ionisation for AI-MS. In addition to a high electron density more than 100 times higher than an LTP recorded by Chan *et al.*, [32], and low plasma gas temperatures not exceeding 60 ^{o}C [22]. This study suggests that this HPPMJ is a 'harder' ionisation technique than the previously reported micro-plasma by Symonds *et al.*, [21], however the parameters were not completely optimised for all the samples.

The HPPMJ was also able to analyse a sample of isoproplantipyrine (50 ppm) from a finger successfully but further research into the safety of analysing from living tissue will be required before further exploration [22]. Finally, the LODs were not quite as good as previous studies, but this could be improved by using tandem mass spectrometry (MS/MS), a more sensitive and specific technique as well as optimisation of the HPPMJ conditions and parameters [22].

2.1.6 Atmospheric Pressure Glow Discharge (APGD)

Atmospheric pressure glow discharge (APGD) is generated by a radio frequency power between two electrodes with a steady flow of gas similar to PADI, however, APGD uses higher applied radio-frequency (rf) discharge potentials and often a mixture of gases. The afterglow is allowed to directly interact with the sample for desorption/ionisation. APGD

is a relatively well researched area with a good understanding of how parameters such as the waveform affect the plasma; pulsed plasma has more potential than sinusoidal [35], and linear-field plasma jets have a plasma chemistry that is more active than cross-field plasma jets as well as containing a larger electron mean energy which has been shown to improve ionisation ability [36].

In more recent studies however, APGD has been coupled to MS as a desorption/ionisation source [49]. This set-up uses APGD/MS to eliminate the need for sample preparation and chromatographic separation for drug identification. Although samples of over-the-counter drugs and drugs of abuse were correctly identified, there is no report of LODs. It may be suggested though that the LODs are slightly lower than other plasma techniques as further optimisation is obviously required due to the mass spectra being dominated by the molecular ion, resulting in a low abundance of product ions. This issue could potentially be resolved by using tandem mass spectrometry (MS/MS), allowing for greater sensitivity and specificity. Temperature related issues arose when a power greater than 75 W was used, as charring and damage was caused to the surface of the analyte [49]. Despite observing a hotter plasma than other techniques, it is shown that the ionisation process is similar to DART and PADI, however, this APGD ionisation source can be regarded as softer than an electrospray ionisation source used by the National Institute of Standards and Technology (NIST) to create a database of mass spectra [49].

Another study using liquid sampling-atmospheric glow discharge (LS-APGD) coupled with mass spectrometry shows promise for rapid sampling of solids and liquids using a technique not too dissimilar to DESI, EI/ESI and atmospheric-pressure chemical ionisation (APCI) [50]. A low operation power of less than 10 W and solution delivery rates less than 50 μL/min are used to produce a discharge between an anode and an electrolytic liquid cathode composed of nitric acid. The electrolytic fluid flows through a glass capillary angled towards the sample surface desorbing and ionising target molecules [50], a design initially used for elemental mass spectrometry [51]. Initially, this study contains promise for an LS-APGD source which can also compliment other techniques such as laser ablation to be used with mass spectrometry. This study also reports limits of detection of caffeine to be as low as 10 pg which is comparable to and even better than some peer devices [39–41], however the gas temperature range is between 195-315 ^{o}C [50]; high gas temperatures are good as it aids desorption, but they cannot be used with thermally sensitive materials. This unique LS-APGD device requires more research and optimisation to reach full potential and efficacy by examining the use of other gases, electrolytes and other operating parameters but it has the ability to compete with other plasma sources.

2.1.7 Flowing Atmospheric Pressure Afterglow (FAPA)

Finally, flowing atmospheric-pressure afterglow (FAPA), a similar technique to APGD has also shown its ability to be coupled with mass spectrometry as a desorption/ionisation source. FAPA was first described in 2008 as an enclosed chamber consisting of a pin cathode and a plate anode, powered by DC voltage with a power consumption less than 13 W [24, 25]. Reactive species are created through an orifice in the plate electrode and the direct current is proportional to the gas temperature. Since 2008, other variations of FAPA have been described. A configuration where the plate electrode has been replaced by a capillary electrode reports reduced background signals and analyte oxidation which as a result produces better LODs [52].

In another arrangement, plasma is generated between two concentric capillary electrodes which enables the introduction of a gaseous or aerosol sample, this is called the halo-FAPA [53]. In the pin-to-capillary FAPA, the study performed a mass spectrometric analysis of explosives which shows that, as with other plasma sources, it can be coupled to mass spectrometry for mass analysis [52]. Furthermore, FAPA/MS was used for drug analysis and showed that it was successful in identification but no limits of detection were recorded. This study explains that FAPA has limitations such as a difficulty in detecting high mass ions (greater than m/z 400).

In another study, a novel design of FAPA was utilised by incorporating a drop-on-demand sample introduction system of liquid samples [54]. This study reports very low and promising LODs of 1 μg/mL of drugs of abuse but more importantly, an extremely reproducible method of sample introduction (4 % RSD) which looks promising for drug quantification [54].

FAPA has the ability to oxidise aromatic compounds, unsaturated hydrocarbons and polymers similar to the way in which an LTP can. However, newer versions of FAPA have a lower oxidation rate due to the reduced diffusion of atmospheric oxygen in the discharge region [52, 53, 55]. A comparison drawn between DART, FAPA and LTP shows that although plasma sources generally produce few fragmentation ions suggesting that they are 'soft' ionisation techniques, DART can be regarded as the 'softest', followed by FAPA and then LTP [56]. FAPA is another rapidly developing source and it is clear that it has capacity to be competitive to similar devices, offering good desorption/ionisation capabilities as well as a reproducible sample introduction but as with the majority of plasma sources, further research and optimisation is still required.

2.1.8 Discussion

A thorough examination of the literature has shown that plasma desorption/ionisation sources for AI-MS are forever improving and developing, with many variations and applications. It is apparent that plasma sources are very versatile and although very well researched, there are still limitations and gaps which need to be addressed. Mainly, more work is required in order to improve precision, accuracy and repeatability of AI-MS, as well as ensuring long-term stability, improving linear dynamic ranges and also attempting to overcome matrix effects and ion suppression. Ultimately, reinforcing the understanding of fundamental mechanisms such as reactive species formation, gas-phase reactions and also desorption/ionisation of analytes themselves will lead to more reliable and reproducible methods.

Additionally, all of these plasma sources have a common limitation for some applications in that they all operate with a relatively small sampling surface area. A small sampling surface area is beneficial for some applications such as imaging or tissue treatment, but for applications where a large surface is analysed such as in a screening procedure which utilises swabs or in the analysis of drugs on banknotes, a much larger sampling surface area is required. A larger sampling surface area enables the whole, or at least a significantly larger sample of the swab or sampling media to be analysed in one analysis as opposed to several analyses which would be required for a small sampling surface area.

The application focus for this project is to develop a reliable ambient ionisation source that can be coupled to mass spectrometry, that consists of a large sampling surface area and possesses the ability to detect drugs of abuse from polymer banknotes, and explosive residues from various swabbing matrices.

This study aimed to investigate the size of plasma that is created by developing the existing knowledge of these ambient ionisation techniques. As previously explored in Dalgleish *et al.*, [57], increasing the surface area of the sample analysed, the selectivity was increased and surface temperatures remained low. Furthermore, another study reports on the tube diameter of an APPJ suggesting that decreasing the tube diameter increases the excitation temperature and the electron density [58]. This project will explore whether increasing the tube diameter is a viable option or whether increasing the number of ionisation sources would render better results.

Similar to increasing the tube diameter, a recent study reported a design referred to as plasma brush [59]. This study was used for disinfection and sterilisation of bacteria

but it could have an application within this area of study. In Chen *et al.*, [59], a design 80 mm wide was used but with a very high gas flow of 4.5 L/min however, this may be too large and 40 mm might be more suitable to reduce the gas requirements. Having a linear plasma source 40 mm wide will provide the ability to sample a large surface area whilst hopefully creating higher excitation temperatures and electron densities as suggested in previous literature [58].

This study also explores the potential of a surface barrier discharge (SBD) as an ionisation source, which is novel for its application with mass spectrometry. A surface barrier discharge is the same concept as a DBD except the plasma forms on the surface of the dielectric material. A typical use for SBDs are for plasma actuation in which the plasma generated on the surface results in a chordwise ionic wind from the electrode, generating a force without any moving parts hence the name actuator. The use of a plasma actuator would allow for a large sampling surface area, dictated by the size of the dielectric surface and the electrodes but additionally, the chordwise ionic wind may provide ion transportation.

This project will develop a plasma device that can be used in conjunction with tandem mass spectrometry for increased sensitivity, specificity and selectivity, therefore increasing the limits of detection, linear ranges, reproducibility and precision. Developments in mass spectrometry enable speed and sensitivity to be coupled with *in-situ* analysis with little or no sample preparation. However, these methods are often restrained by the necessity of close spatial proximity between the sample and the mass spectrometer which limits the ability to analyse samples. For many of the ambient ionisation sources previously mentioned, the plasma source has to be aligned with the orifice of the mass spectrometer to allow for maximum ion transmission, the sample is then inserted between the plasma and the mass spectrometer for analysis. However, this method would be entirely unsuitable for a sample of a large surface area such as a swab, as the swab would physically block the path between the ionisation source and the mass spectrometer.

The samples themselves may increase understanding of the fundamental mechanisms within the plasma that are responsible for ionisation. Using APCI, there are many compounds such as ibuprofen, PTFE and polypropylene that are not detectable as positive ions. However, by using plasma devices, it has been reported that the mass spectra of these compounds can be obtained in positive mode very easily [17, 19]. This suggests that the ionisation process in plasma is very different from APCI and therefore, a plasma source could potentially detect a larger range of compounds. The ability to detect polymers and other compounds may further increase plasma devices' versatility by being able to detect plastics used in explosives and other samples that other atmospheric

methods cannot. Therefore, understanding of how samples undergo ionisation is very important.

This project was a collaboration with Mass Spec Analytical Ltd and their main focus is detecting drugs on banknotes [29]. As nearly every banknote in circulation contains some trace of illicit substance, it is possible to directly compare the amounts found on notes in general circulation to those on notes found at a crime scene. An inference can then be drawn as to whether the money found at a crime scene can be linked to drug related crime due to raised levels of contaminants. Currently, this analysis is undertaken on paper banknotes using a method of thermal desorption APCI at around 285 ^{o}C [29]. However, since the introduction of polymer banknotes in the UK in 2016, and previously elsewhere worldwide, it is realised that thermal based techniques would destroy the banknotes which have a melting point of roughly 120 ^{o}C. Therefore, a plasma desorption/ionisation source could resolve the issue by having a lower temperature method and additionally, using a larger, linear plasma such as a plasma brush could ensure that nothing is lost in regards to sampling surface area.

However, it must be proved that by exposing a polymer banknote to plasma, the surface properties are not changed greatly enough to cause long lasting damage. The modification in surface properties can be measured by atomic force microscopy (AFM), water contact angle measurements, x-ray photoelectron spectroscopy (XPS) and Fourier transform infrared spectroscopy (FTIR) which if used in corroboration could show any change in surface hydrophobicity and bond binding energies at the surface. Furthermore, and most importantly, it must be proven that when using a plasma source with a larger sampling surface area, any surface molecules such as illicit substances can be desorbed from a surface, ionised and detected in a mass spectrometer.

2.1.9 Conclusions

In conclusion, this project aims to adapt, improve and reinforce the understanding of already published plasma sources such as LTP and PADI whilst developing them into an ambient ionisation source that can be coupled with mass spectrometry. In doing so, an analysis of a much larger range of samples and sample type will be explored whilst optimising the parameters of the mass spectrometer and plasma source for improved results. Furthermore, the use of MS/MS itself will likely improve the results and deepen the level of research as few previous publications use MS/MS or even high-resolution MS. Also, by investing time into an already existing source and attempting to understand more of its fundamental mechanisms, it is hoped that a better, more reliable technique

would be available rather than producing a new technique with limited understanding. Finally, creating an integrated plasma desorption-ionisation source may produce a truly portable device that is attached to the mass spectrometer rather than another separate entity as in previous literature. The benefit of this is that it could potentially be downsized to smaller instruments as well being sold and transported as one item, but also not limiting the ionisation source to mass spectrometry but also offering capabilities for other detectors such as ion mobility spectrometry.

Chapter 3

Experimental Setup

This chapter will explain the technical specifications of each plasma source and mass spectrometer conditions used to obtain the data presented, what each sample was and from where it had been obtained.

3.1 Plasma Ionisation Sources

3.1.1 Atmospheric Pressure Plasma Jet

The plasma jet used for the purpose of this study was a linear-field dielectric barrier discharge (DBD) configuration based on a previous study by Walsh and Kong [36]. The jet consisted of a copper ring electrode attached 1 cm from the open end of a 7 cm glass capillary (OD 2.95 mm; ID 1.38 mm). A sinusoidal AC high voltage (6-8 kV, 20 kHz) was applied to the copper electrode using a commercial audio amplifier (IMG Stageline, STA-800, Monacor International GmbH & Co. KG, Bremen, Germany) which was driven using a digital function generator (TG2000; AIM-TTI Instruments, Huntingdon, Cambridgeshire, UK). A custom built voltage step-up transformer (Express Transformers, Runcorn, UK) was connected to the output stage to enable high voltages required for gas breakdown. The peak-to-peak voltage was varied between 6 kV and 8 kV the voltage measurements were recorded using a high voltage probe (Pintek Electronics, HVP-15HF, Pintek Electronics, Shulin, New Taipei City, Taiwan) and the frequency was fixed at 20 kHz. Voltage measurements were recorded using a Tektronix TDS3024B oscilloscope (Tektronix UK Ltd, Bracknell, Berkshire). The discharge gas used was pure helium (99.996%) at a flow rate of 1.4 SLPM controlled by an MKS PR400B digital mass flow controller (MKS Instruments, Andover, Massachusetts, USA). A schematic of the plasma jet and power supply is shown in Fig. 3.1.

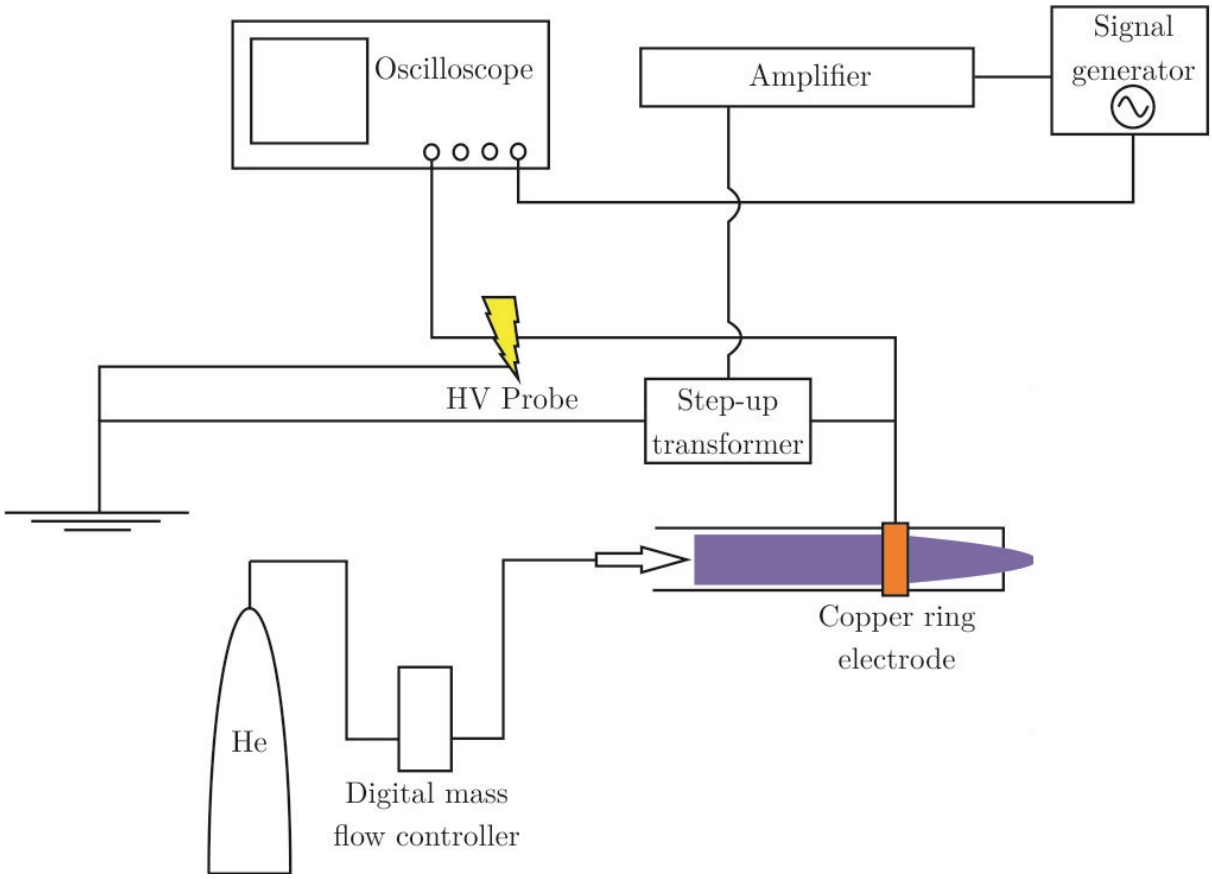

Figure 3.1. Schematic diagram of an AC high voltage linear field dielectric barrier discharge plasma jet.

3.1.2 Atmospheric Pressure Plasma Brush

The atmospheric cold plasma brush consisted of a discharge chamber 60 (l) x 30 (w) x 1 mm^3 which is made up by two pieces of polished quartz slides framed in a custom designed, 3D printed holder, which held the two quartz pieces apart by 1 mm creating the discharge gap. The electrodes were formed using copper tape 5 mm wide placed on the outside of both pieces of quartz and the gap between the inner edges of both electrodes was roughly 10 mm. The ground electrode was either inactive or was upstream of the brush whilst the powered electrode was downstream and roughly 5 mm from the open end of the chamber. A sinusoidal AC high voltage (6-8 kV, 20-40 kHz) was applied to the copper electrode using a commercial audio amplifier (IMG Stageline, STA-800) which was driven using a digital function generator (TG2000; AIM-TTI Instruments, Huntingdon, Cambridgeshire, UK). A custom built step-up transformer (Amethyst Designs Ltd, Bar Hill, Cambridge) was connected at the output stage to provide high voltages to the downstream electrode for excitation and sustaining the discharge. The peak-to-peak voltage was varied between 6-8 kV and the voltage measurements were recorded using a high voltage probe (Pintek Electronics, HVP-15HF) and the frequency was fixed at 40 KHz. Voltage measurements were recorded using an Tektronix TDS3024B

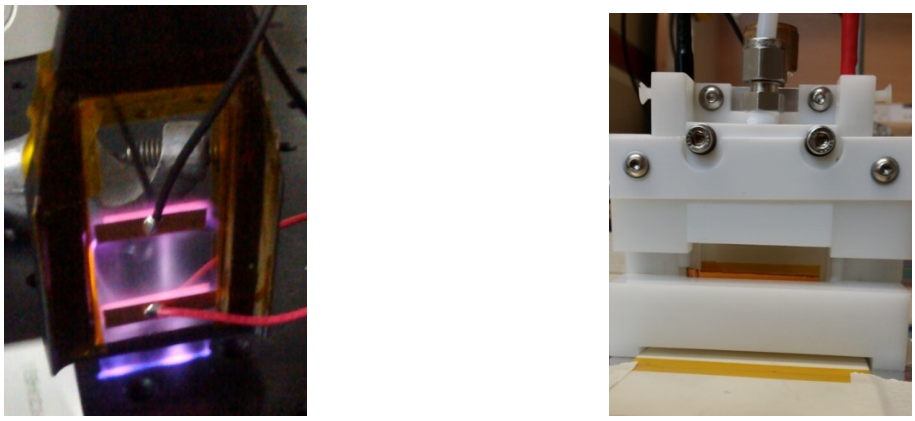

(a) **(b)**

Figure 3.2. Image of plasma brush in early stage of development (a), with powered electrode (downstream) and ground electrode (upstream) in its 3D printed holder; and second plasma brush prototype with quartz block in PTFE (b).

oscilloscope (Tektronix UK Ltd, Bracknell, Berkshire). The discharge gas used was pure helium (99.996 %) at a flow rate of 1.4 SLPM controlled by an MKS PR400B digital mass flow controller (MKS Instruments, Andover, Massachussetts, USA). The visually uniform brush-shaped plasma extended approximately 5 mm from the discharge chamber.

It was found that a dielectric surface less then 5 mm from the end of the brush was required to allow for homogeneous breakdown of the plasma instead of arcing to ground. The dielectric surface was likely acting as a capacitor so that the current from the electrodes would be more evenly distributed across all of the discharge gas resulting in a more homogeneous plasma. This version of the plasma brush can be seen in Fig. 3.2.

The plasma brush was later developed to contain a continuous quartz rectangular block 43 mm x 3 mm with rectangular hole through the centre 40 mm wide, 1 mm thick and 60 mm long. The second plasma brush prototype can be seen in Fig. 3.2. The quartz was obtained from Multi-lab (Throckley, Newcastle upon Tyne, UK). The continuous block was developed to eliminate helium leaking through the sides which occurred in the earlier, 3D printed version. Furthermore, a continuous block should allow for improved power distribution as one electrode could be used rather than two electrodes (one on each quartz slide in previous version). The quartz block was housed in a PTFE block, secured by a reasonably tight push-fit. Helium (pure grade 99.996%) was purged through a 1/4" Swagelock fitting at a rate of 1.4 SLPM, into a small 45 x 5 mm block that contained several holes allowing the gas to be distributed into the quartz block. The electrodes were encased within the PTFE block to improve safety and secure the connections. As with the previous version, a 5 mm copper tape was wrapped around the quartz block acting

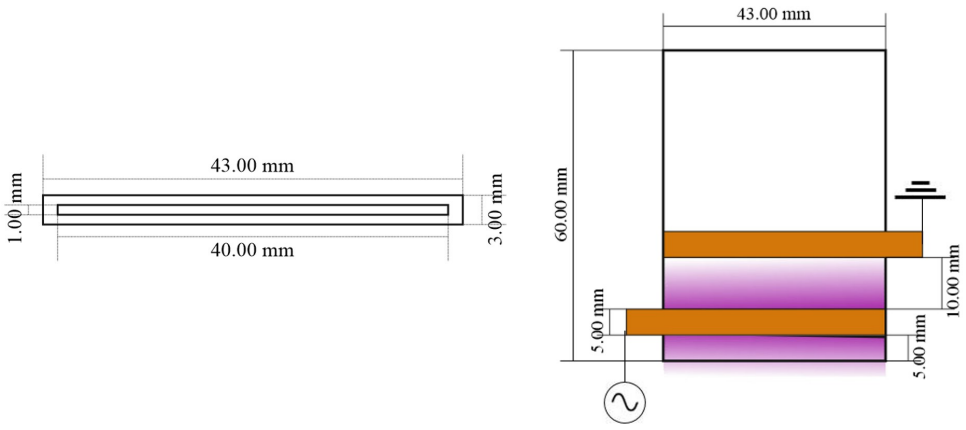

Figure 3.3. Schematic diagram of the second prototype plasma brush made from one continuous piece of quartz from the birds eye view (left) and front view (right) with electrodes.

as an electrode. The powered electrode was 5 mm from the end of quartz block in the downstream direction whilst the ground electrode was 10 mm apart from the powered electrode in the upstream direction. See Fig. 3.3 for schematic of plasma brush.

3.1.3 Atmospheric Pressure Plasma Jet Array

A plasma jet array consisting of 32 quartz tubes (OD 3 mm; ID 1 mm) (Robson Scientific, Sawbridgeworth, Hertfordshire, UK) was housed within PTFE block to create a large surface area ionisation source. The PTFE block was 100 (L) x 60 (W) x 75 (H) mm and was fitted with a brass electrode 45 mm (L) x 34 mm (W) containing 32 holes (3.5 mm diameter) for the quartz tubes, separated by 2 mm. The quartz tubes were in four columns, each containing eight tubes, and protruded from the end of the PTFE block by 0.5 mm. Looking at the source front on in Fig. 3.4, the four columns were at a 75^o angle instead of heading straight back (Straight would have been 90^o or perpendicular in relation to the front). Helium (99.996%) was purged into a gas chamber 44 x 36 x 22 mm at a flow rate of 4 SLPM controlled by a Dwyer variable area flow meter (Dwyer Instruments Limited, High Wycombe, Buckinghamshire, UK). The brass electrode was subjected to a sinusoidal AC high voltage (6-8 kV, 20 kHz) using a commercial audio amplifier (IMG Stageline, STA-800) which was driven using a digital function generator (TG2000; AIM-TTI Instruments, Huntingdon, Cambridgeshire, UK). A custom built voltage step-up transformer (Express Transformers, Runcorn, UK) was connected to the output stage to enable high voltages required for gas breakdown. The peak-to-peak voltage was varied between 6-8 kV and the voltage measurements were recorded using a high voltage probe (Pintek Electronics, HVP-15HF) and the frequency was fixed at 20 kHz.

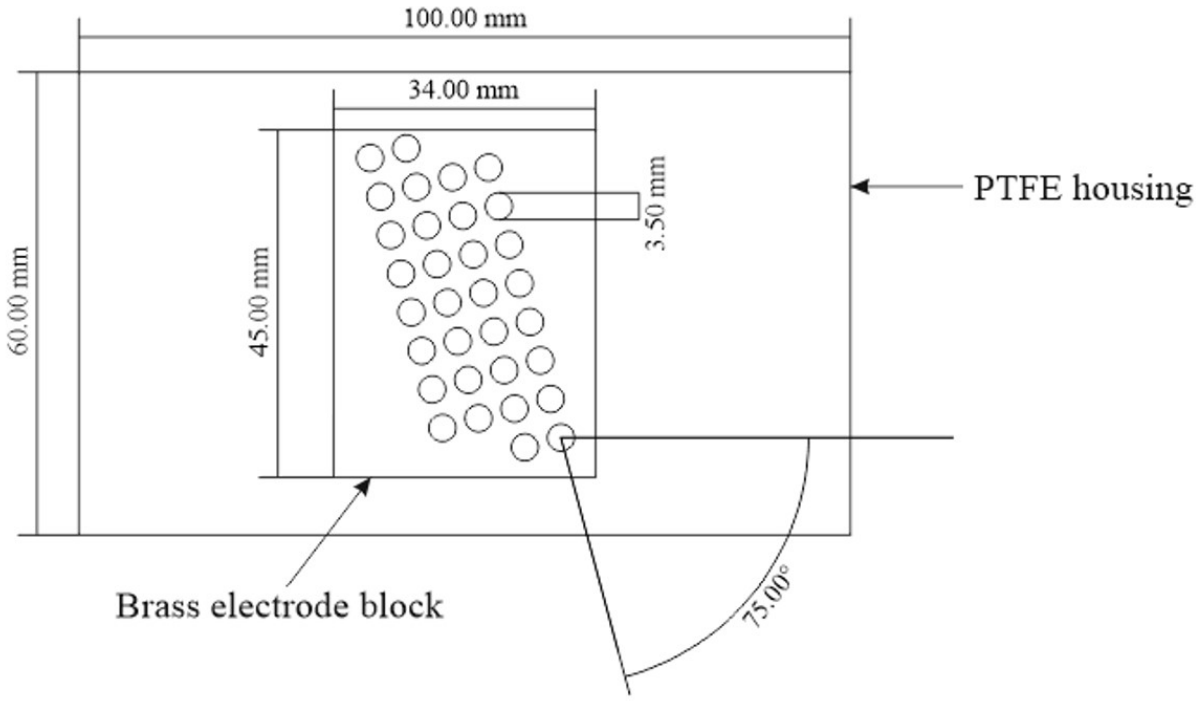

Figure 3.4. Schematic of plasma jet array housing and electrode block.

The plasma jet array unit was fixed to a custom made plenum chamber which allowed full integration of the source to the front of the mass spectrometer. The plenum chamber was similar to that described in Ebejer *et al.*, and Fletcher *et al.*, [29, 60]. The plenum chamber housed an APCI needle which could be disconnected. The plenum chamber incorporated a sample pump which was used to draw air through the transfer line of the plenum chamber towards the mass spectrometer; the flow was varied between 5 and 25 SLPM. Furthermore, attached to the plenum chamber was a single brass plate used as the ground electrode and to create a gap of 4 mm from the array and the ground. Plasma jet array schematic is depicted in Fig. 3.4.

It was found that a dielectric surface less then 5 mm from the end of the array was required to allow for homogeneous breakdown of the plasma instead of arcing to ground. This was likely to allow an even share of the current to be distributed across each jet, enabling successful breakdown of every jet instead of only a few.

3.1.4 Surface Barrier Discharge Ionisation Source

Initial experimentation of a surface barrier discharge (SBD) began by applying an exposed powered electrode on one side of a ceramic surface, and a ground electrode on the opposite side of the electrode. The electrodes were offset from one another but overlapped by roughly 1 mm and the ground electrode was encapsulated in a dielectric

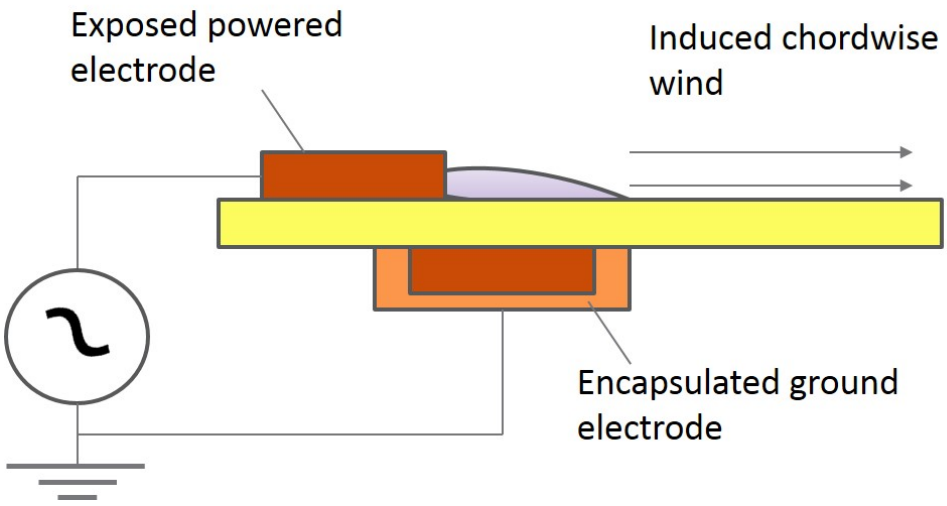

Figure 3.5. Schematic representation of a surface barrier discharge.

material, Kapton tape. This experiment was similar to other plasma actuators that have been previously developed [61, 62]. The offset electrodes result in an ionic wind, largely consisting of electrons, neutrals and ions, which travels in the direction of the ground electrode shown in Fig. 3.5. These initial experiments gave the indication that an SBD could be used as an ionisation source with mass spectrometry and consequently led to the development of SBD prototype ionisation sources.

It was decided that mica would be used as the dielectric surface because it is relatively cheap, has a good dielectric constant, is generally quite thin and it is translucent allowing the user to be able to view the plasma. The mica sheets were obtained from Dean and Tranter Ltd. (Dean and Tranter Ltd., Fordingbridge, UK) and were 100 x 100 x 0.15 mm. The SBD consisted of two mica sheets and on each sheet there were three powered electrodes and three ground electrodes, all of which were 60 mm long and 5 mm wide composed of adhesive copper tape. The three powered electrodes were on the same side of the mica separated by 7 mm and the ground electrodes were in the same configuration on the reverse side of the mica similar to Fig. 3.5. The ground and powered electrodes were slightly offset from one another but overlap by 1 mm. The offset electrodes result in the production of a chordwise ionic wind in the direction of the ground electrodes, with the plasma forming on the leading edge and extending a few mm. It can be seen in Fig. 3.7 that the chordwise ionic wind travels in the direction of the ground electrode and therefore, the flow of the plasma can be directed towards the orifice of a mass spectrometer for analysis. The two SBD plates were identical to one another and were separated by 4 mm; however the powered electrodes on each SBD were positioned opposite each other creating a plasma actuator tunnel.

The mica SBD, seen in Fig. 3.6, was housed on a holder that was tailored to allow

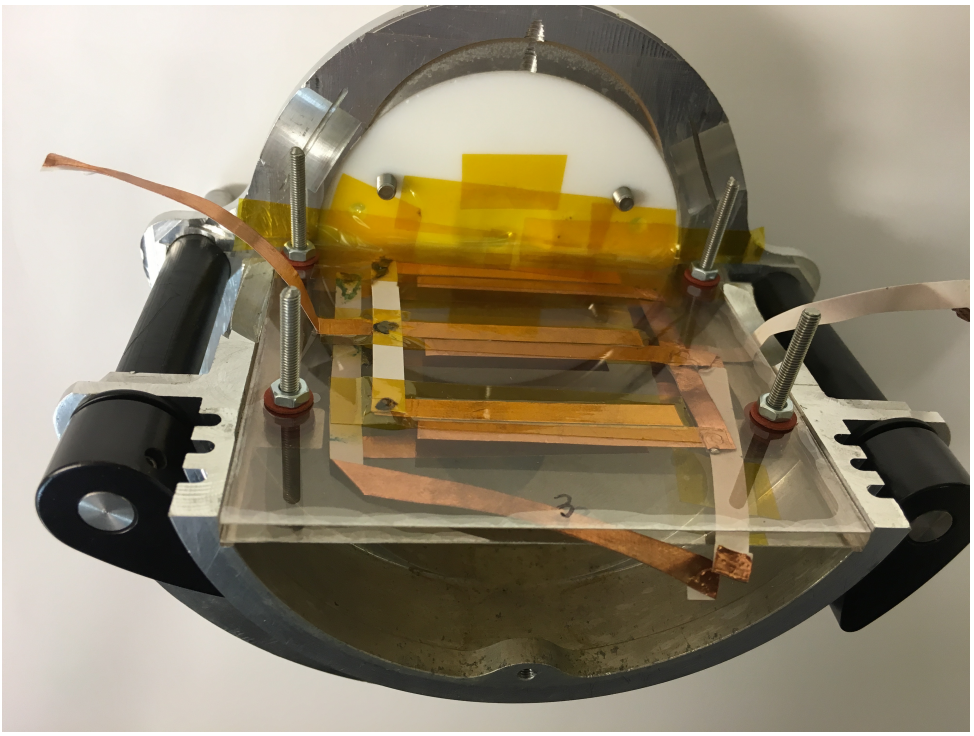

Figure 3.6. Early prototype of SBD with mica as the dielectric.

for coupling with a mass spectrometer. Although this prototype initially worked as an ionisation source, the capabilities were minimal due to some of the properties of the mica. Firstly, the mica delaminated easily resulting in a modified surface structure and air gaps between layers of material which caused arcing. Secondly, the mica was quite flexible and when subjected to the heat that was produced by the electrodes/plasma, the mica began to bend making it difficult to transport ions towards a mass spectrometer. Therefore, mica was discontinued and alumina was used as the dielectric instead.

The surface barrier discharge consisted of two alumina plates 91 x 79 x 0.5 mm (Ceramic Substrates & Components Ltd, Newport, Isle of Wight, UK). On each plate there were three powered electrodes and three ground electrodes, all of which were 60 mm long and 5 mm wide composed of adhesive copper tape. The three powered electrodes were on the same side of the alumina separated by a 7 mm gap and the ground electrodes were in the same configuration on the reverse side of the alumina. The ground and powered electrodes were slightly offset from one another but overlap by 1 mm. The offset electrodes result in the production of a chordwise ionic wind in the direction of the ground electrodes, with the plasma forming on the leading edge and extending a few mm. It can be seen in Fig. 3.7 that the chordwise ionic wind travels in the direction of the ground electrode and therefore, the flow of the plasma can be directed towards the orifice of a mass spectrometer for analysis. The two SBD plates were identical to one another and were separated by 4 mm; however the powered electrodes on each SBD

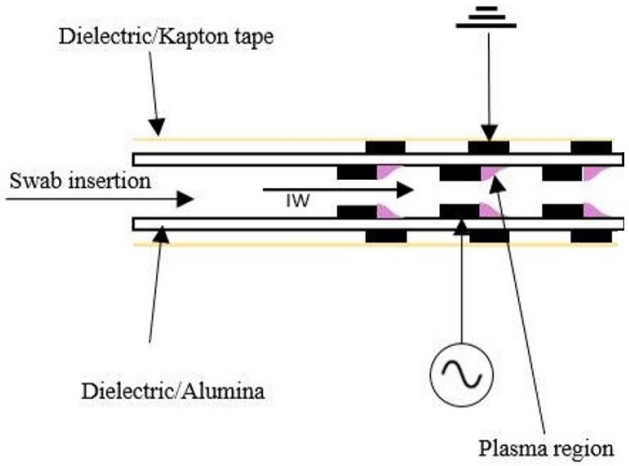

Figure 3.7. Schematic representation of SBD ion source with two alumina sheets each containing three pairs of electrodes. Chordwise ionic wind direction is labelled by IW.

were positioned opposite each other creating a plasma actuator tunnel. The resulting tunnel was open at the front and sides and was 91 mm wide, 79 mm long with a gap of 4 mm between each sheet. Finally, the powered electrodes remained exposed, whereas the ground electrodes were encapsulated in a dielectric material, Kapton tape in this case, to prevent a breakdown of plasma on the grounded surface. The flow generated by the resulting ionic wind was not recorded but previous literature of a similar electrode configuration would suggest it to be 2 m/s [63]. Literature reports suggest that having additional actuators can increase the flow up to 10 m/s [61,64]. Other than the chordwise ionic wind, no special gases are added to affect ion transport.

A sinusoidal AC high voltage (6-8 kV, 20 kHz) was applied to the powered copper electrodes using a commercial audio amplifier (IMG Stageline, STA-800) which was driven using a digital function generator (TG2000; AIM-TTI Instruments, Huntingdon, Cambridgeshire, UK). A custom built voltage step-up transformer (Express Transformers, Runcorn, UK) was connected to the output stage to enable high voltages required for gas breakdown. The optimum peak-to-peak voltage was found to be 7 kV and the voltage measurements were recorded using a high voltage probe (Pintek Electronics, HVP-15HF) and the frequency was fixed at 20 kHz. Voltage measurements were recorded using a Gould OS300 20 MHz dual trace oscilloscope (Gould, Ilford, Essex, UK). The current monitored was 20 mA using a Fluke 79 Series III multimeter (Fluke Europe B.V., Eindhoven, Netherlands). Schematic of SBD set-up shown in Fig. 3.7. The operating temperature of the SBD is roughly 100 ^{o}C which allows for direct analysis from thermally labile surfaces such as polypropylene. The temperature was measured using a hand-held infra-red thermometer (Titan Power Tools (UK) Ltd, BA22 8RT) on

the ground electrodes on the top of the alumina plate. Therefore, it is likely that the electrodes and resulting plasma inside are slightly above 100 ^{o}C, but is not sufficient to result in damage to a polypropylene swab that has been subjected to the plasma for three seconds. The liberation of a sample from a polypropylene surface is not likely to be via thermal desorption, but through other mechanisms. It is possible that the oxygen, nitrogen and other excited species in the air, as a result of plasma interactions, are responsible for desorption through a transfer of their potential energy to the surface, similar to that with helium in PADI [65]. Salter et al., recently studied the effect of thermal desorption with PADI and suggested that while thermal desorption does contribute to the overall desorption in PADI, the main desorption process must be due to more complicated plasma mechanisms [34], which have been previously suggested to be excited species such as (He*) helium metastables [14].

The current measured across the SBD is not an accurate reading of the discharge current within the plasma itself and therefore, more accurate and thorough power measurements were obtained to create a Lissajous curve in an attempt to better estimate the charge within the plasma itself. These measurements were obtained using a sinusoidal AC high voltage (7 kV, 20 kHz) applied to the powered copper electrodes using a commercial audio amplifier (IMG Stageline, STA-800) which was driven using a digital function generator (TG2000; AIM-TTI Instruments, Huntingdon, Cambridgeshire, UK). A custom built voltage step-up transformer (Express Transformers, Runcorn, UK) was connected to the output stage to enable high voltages required for gas breakdown. The peak-to-peak voltage was 7 kV and the voltage measurements were recorded using a high voltage probe (Pintek Electronics, HVP-15HF) and the frequency was fixed at 20 kHz. The oscilloscope used was a Tektronix TDS 3012 (Tektronix UK Ltd., Berkshire, UK). The current was measured on the powered electrode using a Pearson current monitor model 2877 (Pearson Electronics, California, USA). Added to the circuit on the ground electrode was a 4 k Ohm resistor and a 10 nF capacitor and the voltage across the capacitor was monitored using a Tektronix 06139A voltage probe (Tektronix UK Ltd., Berkshire, UK). Using a Lissajous curve the estimated power of the plasma is calculated to be 26 W.

3.2 Mass Spectrometric Techniques

3.2.1 Hiden HPR-60 Molecular Beam Mass Spectrometer

A study of the ion production from each plasma source was monitored using a HPR-60 molecular beam mass spectrometer (MBMS) (Hiden Analytical Ltd, Warrington, UK).

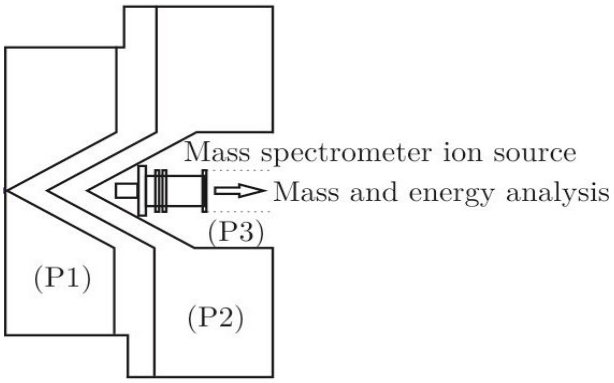

Figure 3.8. Schematic of molecular beam mass spectrometer and various pressure regions separated by skimmer cones.

The HPR-60 has a mass range of m/z 0-1000. For the majority of this study, the mass spectrometer was fitted with a 200 μm grounded extraction orifice, which reduces the chances of electric field penetration beyond the grounded orifice plate. Electric field penetration may result in modified chemistry of the ions detected due to creating a discharge inside the low pressure region of the mass spectrometer and therefore, the ions that would be detected may no longer be from the external atmospheric pressure plasma.

The Hiden MBMS utilises a single-stage quadrupole mass spectrometer (QMS). The MBMS is capable of sampling ions directly without the need for an internal ionisation source. The instrument can sample radical and neutral species using an internal electron beam ionisation source. The MBMS was operated in ion detection mode (no internal ionisation source) and so any ions that were detected must have originated from an external ionisation source. The MBMS samples species via a multi-stage differentially pumped skimmer inlet and transferred through the mass spectrometer with minimal interaction with other species and without wall collisions. The pressure reduction stages are separated by various skimmer cones which allows for a free-jet expansion from atmospheric pressure into the low pressure region resulting in a molecular beam [19, 60, 66]. The various pressure stages P_1, P_2 and P_3 are shown in Fig. 4.1 where behind the first cone (P_1 orifice plate) the pressure is nearly atmospheric, 10^{-1} Torr, the second pressure region (P_2) is 10^{-5} Torr and the final pressure region reaches ultra high vacuum (P_3) 10^{-7} Torr.

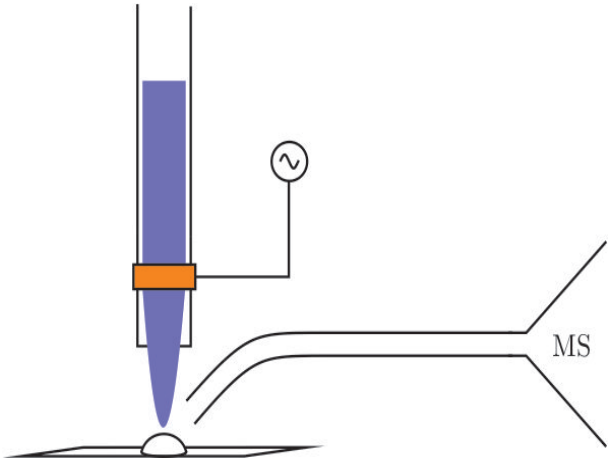

Figure 3.9. Schematic diagram of the plasma jet and its orientation with the Thermo Exactive Orbitrap with attached "sniffer".

3.2.2 Thermo Exactive Orbitrap

Samples containing cocaine, trinitrotoluene (TNT), nitroglycerin (NG), pentaerythritol tetranitrate (PETN) each at 10 ng/μl and 100 ng/μL were analysed using a Thermo Exactive Obitrap. The samples used for this analysis were received from Mass Spec Analytical Ltd and were blotted onto paper and allowed to dry. Paracetamol was analysed by scraping the surface of a 500 mg tablet and directly sampling, polytetrafluoroethylene (PTFE) was analysed by wrapping PTFE around a glass slide and directly analysing. Lidocaine was analysed by dissolving approximately 2 mg in 1 mL of water and allowing to dry on a glass slide which was directly analysed. Samples of PTFE, lidocaine and paracetamol were obtained from Boots school of pharmacy, University of Nottingham. For these studies, a Thermo Exactive Orbitrap mass spectrometer was operated in both positive and negative mode with accurate mass. The software used was the Thermo Xcalibur software; samples were introduced into the MS via a "sniffer" tube attached to the orifice of the mass spectrometer to directly transport ions (See Fig. 3.9).

3.2.3 AB Sciex API 2000 Tandem Mass Spectrometer

For these studies, an AB Sciex API 2000 triple quadrupole tandem mass spectrometer (AB Sciex, Concord, Ontario, Canada) was utilised by removing the original ionisation source. The software used was AB Sciex Analyst 1.4.1 and 1.6.1. The optimised global parameters were: Curtain Gas (CUR): 20.0 psi, Collision-Induced Dissociation Gas (CID/CAD): 3 V, Nebulizer Current (NC): 2.0 μA, Q1 resolution (ion energy): 0.7 V, Q_3 resolution (ion energy): 4.0 V, Deflector: 100.0 V, Channel Electron Multiplier (CEM): 2200 V and the sample flow was approximately 18 mL/min. The resolution used was unit resolution with

a dwell time of 7 ms for SRM/MRM measurements.

3.2.4 Sciex X500R Quadrupole Time-of-Flight (QTOF)

A Sciex X500R QTOF was used for accurate mass measurements for explosive detection (AB Sciex, Concord, Ontario, Canada). A sequential windowed acquisition of all theoretical fragment mass spectra (SWATH) method was implemented for this study. A SWATH acquisition is an expanded mass isolation window which is stepped across the whole mass range of interest, and a composite MS/MS spectrum of all precursor masses from each mass window is obtained during each mass step [60].

The X500R used the following conditions: Firmware: ATLAS_QTOF_ICX_v0 03 (0 03), Software: SCIEX OS 1.2, Scan type: SWATH (sequential windowed acquisition of all theoretical masses), Polarity: negative, Ionspray (v): -4300 V, CAD gas: 7 V, TOF/MS start mass: 100 (Da), TOF/MS stop mass: 500 (Da), Accumulation time: 0.05 (s), Declustering potential (DP): -20 V, DP spread: 0 V, Collision energy (CE): -5 V, CE spread: 0. For TOF/MS/MS the parameters used were: Start mass: 30 (Da), Stop mass: 500 (Da), Accumulation time: 0.03 (s), Rolling CE: False, Charge state: 1, DP: -10 V, DP Spread: 0, CE: -30 V, CE spread: 15 V.

3.3 Surface Analysis Techniques

3.3.1 Atomic Force Microscopy (AFM)

AFM measurements were obtained in contact mode with a silicon tip over various scanning regions using a Veeco CP-II (Veeco Digital Instruments, Veeco UK, St Ives, Cambridgeshire, UK, PE27 5JL) whilst acquiring the data using ProScan software. Data anlalysis was conducted using WSxM 5.0 Develop 7.0 [67]. Samples of cotton paper, polypropylene, paper banknotes and polymer banknotes (10 x 10 mm samples) were held in place on a glass slide by double sided tape before analysis.

3.3.2 X-Ray Photoelectron Spectroscopy (XPS)

The XPS data were taken on an Axis-Supra instrument from Kratos Analytical using monochromatic Al Kα radiation (1486.7 eV, 225 W) and a low-energy electron flood source for charge compensation. Survey scan spectra were acquired using a pass energy of 160 eV and a 1 eV step size. Narrow region scans (O 1s, and C 1s) were acquired using a pass energy of 20 eV and a 0.1 eV step size. Narrow region scans for N 1s were acquired using a pass energy of 20 eV and a 0.1 eV step size for samples PBBC, PBB, PBJ, and PBJC, for all other samples a pass energy of 160 eV and a 0.1 eV step size was used (due to

the lower concentration of nitrogen at the surface). The hybrid lens mode was used for all the data acquired. The samples were attached to the sample bar using beryllium copper (BeCu) plates and screws. The data was processed using ESCApe software (supplied by Kratos), data was re-calibrated so the hydrocarbon C 1s peak maximum appeared at a binding energy of 285.0 eV.

3.3.3 Fourier Transform Infra-red Spectroscopy (FTIR)

FTIR spectra were obtained with a JASCO FT/IR 4100 (JASCO, Essex, UK) fitted with aMIRacle ATR accessory (Pike Technologies, US). A blank, untouched sample of each surface type (polypropylene, cotton paper and polymer banknote) was acquired as a blank/background. Data was acquired in a wavelength range of 700-4000 cm^{-1} and analysed using Spectra Manager Version II software (JASCO, Essex, UK).

3.3.4 Contact Angle Measurements

Water contact angle measurements were acquired by accurately dispensing 1 μL of distilled water via the Sessile drop method onto the surface and measuring the contact angle using CAM100 software (KSV Instruments Ltd., Biolin Scientific UK, Trinity Way, Manchester, M3 7BG, UK). Unfortunately, paper banknotes were not analysed using this technique as they were too porous to get an accurate measurement.

3.4 Samples, Reagents and Chemicals

The polypropylene used in this study was Rayoface C50 (50 μm thickness) supplied by Innovia Films (Wigan, UK). The polypropylene had a side pre-treated by a corona discharge which was shown to be more consistent and most likely to be used in polymer banknotes thus, this side was chosen for analysis. Cotton paper samples used in this study were obtained from Cranes Crest (Dalton, MA) and were 100% cotton, 210 x 297 mm and 90 gsm. Finally, the polymer banknotes used in this study were obtained from the Bank of England and were £50 prototypes obtained before the release of polymer £5 notes in the UK on the 13^{th} September 2016.

The explosives used for this study were obtained from Kinesis Ltd (Kinesis Ltd, St. Neots, Cambridgeshire, UK) and contained TNT 1 mL 1000 μg/mL in MeOH:AcCN (1:1), RDX 1 mL 1000 μg/mL in MeOH:AcCN, PETN 1 mL 1000 μg/mL in MeOH and HMTD 1 mL 100 μg/mL in AcCN. For analysis, the samples were spotted onto a glass slide, left to dry, and then swabbed with polypropylene (Rayoface C50 50 μm) (Innovia, Wigton, Cumbria, UK), the swab was then placed directly in the plasma for 2-3 seconds for liberation/ionisation. Where real-world samples are referenced, these consist of

samples from a real explosive composition of Semtex 1H provided by a UK government stakeholder, the exact composition was unknown. These samples were collected by handling a heavily contaminated mobile phone, wearing gloves, before depositing the sample in a series of fingerprint depositions.

The controlled substances used for this study were obtained from Kinesis Ltd (Kinesis Ltd, St. Neots, Cambridgeshire, UK). Cocaine hydrochloride, ketamine hydrochloride, mephedrone hydrochloride, 3,4-methylenedioxymethamphetamine hydrochloride, amphetamine sulfate were all at 1 mg/mL in MeOH and diamorphine was at 1 mg/mL calibrated in AcCN. Fentanyl 1 mg/mL in MeOH was obtained from Sigma Aldrich Company Ltd. (Sigma Aldrich Company Ltd. Dorset, UK). All solutions of drugs and explosives were diluted using methanol (>95% HPLC grade) from Charlton Scientific (Charlton Scientific Ltd, Charlton, Oxon, OX17 3DR, UK). For analysis, the samples were spotted onto a glass slide, left to dry, and then swabbed with polypropylene (Rayoface C50 50 μm) (Innovia, Wigton, Cumbria, UK), the swab was then placed directly in the plasma for 2-3 seconds for liberation/ionisation. During the optimisation process, solutions were infused by glass capillary at a rate of 0.60 mL/hr directly onto the very front electrode (furthest powered electrode in the downstream direction) for volatilisation/ionisation.

Chapter 4

Evaluation of an Atmospheric Pressure Plasma Jet with Mass Spectrometry

This chapter will describe the results and development of a plasma jet as described in section 3.1.1.

4.1 Introduction

As previously discussed in the literature review (Chapter2), there are many forms of plasma desorption/ionisation sources, some of which were commercially available such as DART and DESI. Therefore, it was decided that this project would focus on some existing technologies that were not commercially available, and develop them into improved ionisation sources with a valid application such as drugs and explosives detection. PADI and LTP are very similar techniques based on a dielectric barrier discharge, covered well within the literature and so it was decided that this would be the plasma source on which to form the focus of what should be technologically developed. However, it was imperative that similar results to that presented in the literature could be achieved using similar designs before any major changes were to take hold. Providing similar results were obtained, it would then be important that the plasma source would be fit for the specific applications of drug and explosive detection with an analytical instrument.

This project was in collaboration with Mass Spec Analytical Ltd, Bristol, UK who specialise in the analysis of drugs on money. When money is seized as part of a criminal investigation such as possession of drugs with intent to supply, it is possible to analyse the drug contamination and compare the amounts and patterns found to what would usually be seen in general circulation. This comparison between the exhibit and general circula-

tion can provide support as to whether the money was likely to have come from a general circulation source such as a bank or automated teller machine (ATM), or from a crime source. Current methods for this analysis rely on thermal desorption to volatilise the drug molecules on the banknote which can then be ionised and detected with a mass spectrometer [29, 68, 69]. However, thermal desorption requires temperatures over 250 ^{o}C and due to the introduction of polymer banknotes in the UK in 2016, thermal methods would be too destructive as polymer banknotes cannot withstand temperatures higher than 120 ^{o}C.

Therefore, plasma based methods may be useful to replace thermal based methods for the detection of drugs on money providing it can be shown that the plasma is not destructive to the banknote. This chapter will discuss experiments regarding plasma treatment of several surfaces such as paper and polymer banknotes in an attempt to measure the damage, if any, that is caused by a plasma source.

4.2 Experimental Method

A plasma jet based on the design previously discussed in Walsh and Kong was constructed using a 7 cm glass capillary [36], with a copper ring electrode 1 cm from the exit of the tube. The other end of the capillary was connected to a PTFE tube which delivered pure grade helium at 1.4 SLPM as previously discussed in section 3.1.1. To ensure that similar results could be obtained using the plasma jet, it was coupled with a Hiden HPR-60 molecular beam mass spectrometer (MBMS) which enables measurement of the reactive species generated within an external ionisation source i.e. the plasma jet. The plasma jet was aligned with the 200 μm front cone of the mass spectrometer and was located approximately 1 cm from the orifice as shown in Fig. 3.1. An AC high voltage was applied to the copper ring electrode of 7 kV with a frequency of 20 kHz and the front cone of the mass spectrometer was connected to earth to act as a ground.

The Hiden MBMS utilises a single-stage quadrupole mass spectrometer (QMS). The MBMS is capable of sampling ions directly without the need for an internal ionisation source. The instrument can also sample radical and neutral species using an internal electron beam ionisation source. The MBMS was operated in ion detection mode (no internal ionisation source) and so any ions that were detected must have originated from the external plasma jet. The MBMS samples species via a multi-stage differentially pumped skimmer inlet and transferred through the mass spectrometer with minimal interaction with other species and without wall collisions. The pressure reduction stages are separated by various skimmer cones which allows for a free-jet expansion from atmospheric pressure into the low pressure region resulting in a molecular beam [19,60,66].

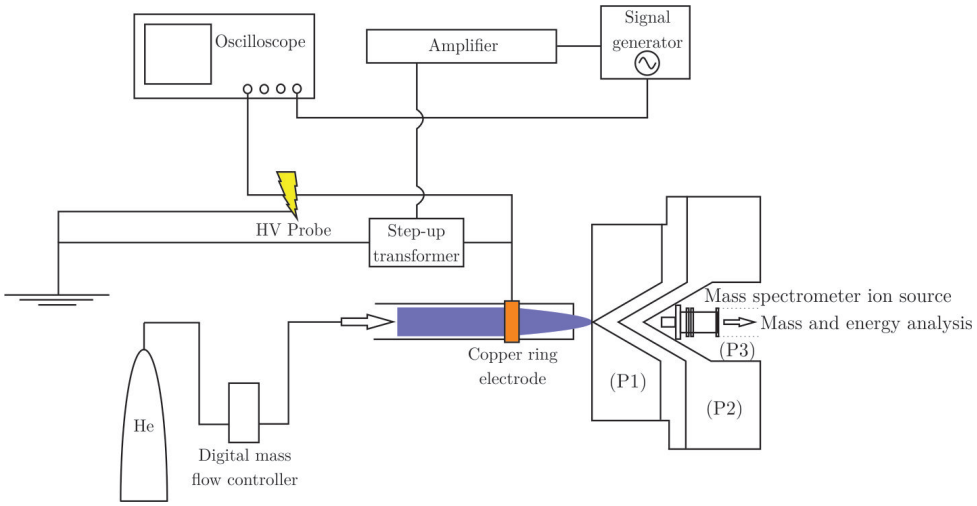

Figure 4.1. Schematic of plasma jet, circuit diagram of the equipment used to supply a high voltage AC sine wave and Hiden HPR-60 mass spectrometer. The Hiden HPR-60 contains a differentially pumped skimmer inlet demonstrated here by the various pressure regions labelled as P1, P2 and P3.
.

Once satisfied that the plasma jet was capable of reproducing data previously obtained in the literature, it would then be possible to undertake experiments using various surfaces in relation to banknotes to measure the damage that may be caused during plasma treatment. For these experiments, the surfaces were subjected to the plasma source for various amounts of time and examined using several techniques such as Fourier-transform infra-red spectroscopy (FTIR) to determine the potential bond formation at the surface, atomic force microscopy (AFM) to measure the surface roughness, water contact angle (WCA) measurements to measure changes in hydrophobicity and x-ray photoelectron microscopy (XPS) to determine the changes within the bonds at the surface, as mentioned in section 3.3.2.

4.3 Results and Discussion

4.3.1 Plasma Jet with a Molecular Beam Mass Spectrometer

The MBMS was used to investigate the effects that variable power, frequency and flow rate would have on the ionic (positive and negative) and neutral species generated within the plasma. To ensure accurate measurements, the instrument was tuned before every set of experiments to ensure that the mass spectrometer was optimising the amount of ions that are securely transported to the detector. The differentially pumped skimmer inlet described above consists of three metal cones of varying size orifices; each cone is

pumped down to different pressures to provide a pressure reduction from atmospheric pressure to 10^{-7} Torr as described by various authors [43, 48, 70, 71]. Furthermore, each cone can be biased with a voltage to encourage ions to travel through in a straight line, followed by several other lens and focussing voltages. Once optimised, measurements of negative, positive and neutral species were taken under various conditions to establish the best working parameters for the plasma jet.

The variable conditions of the jet were frequency (5-35 kHz), voltage (6-8 kV), helium gas flow (0.4-2.4 SLPM) and distance of the jet to the orifice (0, 0.5 & 1.0 cm). These conditions were decided because the breakdown voltage of the plasma was roughly 4-5 kV and a distance greater than 1 cm from the orifice resulted in an unsustainable plasma below 6 kV. For all species (negative, positive and neutral) a frequency of 20 kHz was the most reproducible as well as resulting in a higher intensity of ions that could be detected. A voltage of 7-8 kV produced comparable intensities of ions, however, 7 kV was chosen as the optimum operating voltage as it resulted in a larger spread of high and low mass ions unlike 8 kV. A distance of 1 cm from the orifice was deemed to be the most appropriate resulting in a high intensity of ions and a broad spectrum of high and low mass ions, likely due to the interaction of the plasma to the ambient air resulting in more collisions and therefore, more ions. Flow rates below 0.8 SLPM were not considered as optimum as the plasma plume did not extend long enough to reach the mass spectrometer orifice despite ions of low intensity being detected. A flow rate of 1.4 SLPM gave a better spectrum containing high intensity of high and low mass ions whilst producing a very stable plasma plume. Therefore, the final operating conditions of the jet were 7 kV, 20 kHz, 1.4 SLPM (helium) and 1 cm away from the orifice. Finally, in this case the plasma was directly aligned with the orifice to ensure as many of the ions enter the orifice as possible, for this reason, the plasma jet was at 180^{o} to the orifice.

The results obtained using MBMS suggest that this plasma jet produced ions that were to be expected when compared to previous literature [33]. In Fig. 4.2 it can be seen that oxygen and nitrogen species dominate both the positive and negative ion spectra as a result of plasma interaction with the ambient air. The dominant positive ions are N^+, O^+, $N_2{}^+$ and $O_2{}^+$ whilst the dominant negative ions are O^-, $O_2{}^-$, $NO_2{}^-$ and $NO_3{}^-$. This ion production is evidence to show that a plasma jet is capable of ionisation in ambient air and therefore indicates the application as an ionisation source. The suggested ionisation mechanisms are slightly more complex than other conventional techniques and could be attributed to several ionisation pathways such as (a) penning ionisation: due to the helium metastables in the plasma; (b) gas-phase charge-transfer reactions similar to those experienced in DART; (c) proton transfer; and (d) photoionisation due to the possible presence of vacuum ultraviolet light (VUV) [17,55].

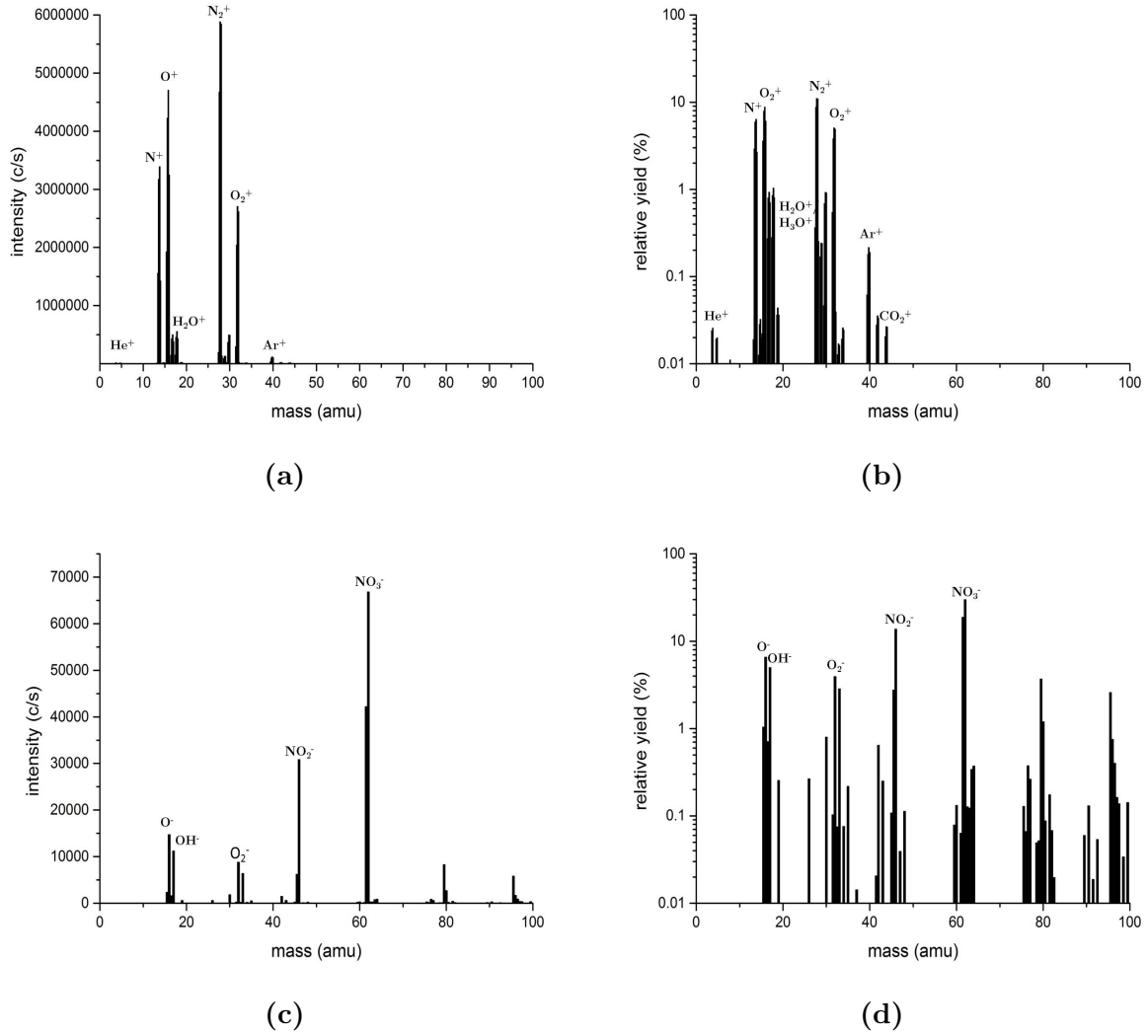

Figure 4.2. Mass spectra acquired for ions generated in ambient air with a plasma jet coupled to a Hiden MBMS in positive mode for the signal intensity (a) and relative yield (b) and the negative ion spectrum for intensity (c) and relative yield (d).

These results provided the necessary information to suggest that the plasma jet was suitable as an ionisation source, however, this data is only of air species and would not represent the plasma jet performance for the detection of analytes within an actual sample. To reinforce the satisfaction that the plasma jet could be used as an ionisation source, some analytes would have to be considered where the plasma jet would be required to perform both desorption and ionisation simultaneously to liberate a sample from a surface or from within a matrix. The analysis required to detect an analyte from an actual sample would require an analytical instrument as opposed to the MBMS.

4.3.2 Thermo Exactive Orbitrap

Investigative analysis of the plasma jet was performed on a Thermo Exactive Orbitrap mass spectrometer at the Boots school of pharmacy, University of Nottingham. This analysis was performed in an attempt to detect samples of drugs and/or explosives from a surface or within a matrix using a plasma jet. For this study, the plasma jet was operated in the above conditions and the samples analysed were cocaine, lidocaine, paracetamol, trinitrotoluene (TNT), and nitroglycerin (NG). Samples of cocaine, TNT and NG were blotted on to paper and allowed to dry at a concentration of 100 ng. Unfortunately, these samples were undetected by the orbitrap mass spectrometer. There are various explanations as to why no signal was detected for these samples. Firstly, 100 ng is a low concentration but previous literature has reported limits of detection (LODs) lower than this [17]. However, these LODs were reported obtained by liberating samples from a hard non-porous surfaces such as glass whereas the matrix chosen for this study was paper; a porous surface renowned for being a complex matrix. The paper would have likely required a higher temperature to liberate the sample out of the matrix and as the plasma jet operates at approximately 30 ^{o}C it is likely that the temperature was not great enough to overcome the complex matrix.

Despite the cocaine, TNT and NG samples not being detected, mass spectral data of polytetrafluoroethylene (PTFE), lidocaine (lignocaine) and paracetamol (acetaminophen) was obtained (the difference is likely due to concentrations of paracetamol, lidocaine and PTFE being within the milligram range0. The mass spectral data obtained in these experiments are shown in figure 4.3. The negative ion mass spectral results produced by direct interaction of PTFE and a plamsa jet are shown in figure 4.3 in the range of *m/z* 80 to *1000*. The results correlate to the same major ion species that were previously documented in Bowfield *et al* [47], in regards to a PADI *needle*. It can be seen in figure 4.3 that a series of ions separated by *m/z* 49.9968 (50 Da) is beginning *m/z* 146.9874. This species is identified as $[C_2F_3 + [CF_2]_n + (O)]^-$ where the peak at *m/z* 146.9874 represents n=1, and the loss of 50 Da corresponds to CF_2 which is half of a PTFE polymer unit. This species is identified in Bowfield *et al* [47], but the main species recorded by Bowfield *et al* is $[C_3F_2 + [CF_2]_n + (OH)]^-$.

Furthermore, these results also confirm the plasma jet as a soft ionisation technique due to the mass spectrum containing more high mass fragments, also reported in Bowfield *et al* [47]. A soft ionisation technique is much more preferable because it reduces the chance of in-source fragmentation (thus reducing the amount of molecular ion available) which shows promise for the plasma jet as a desorption-ionisation source. However, a harder ionisation technique may have been more capable of detecting the

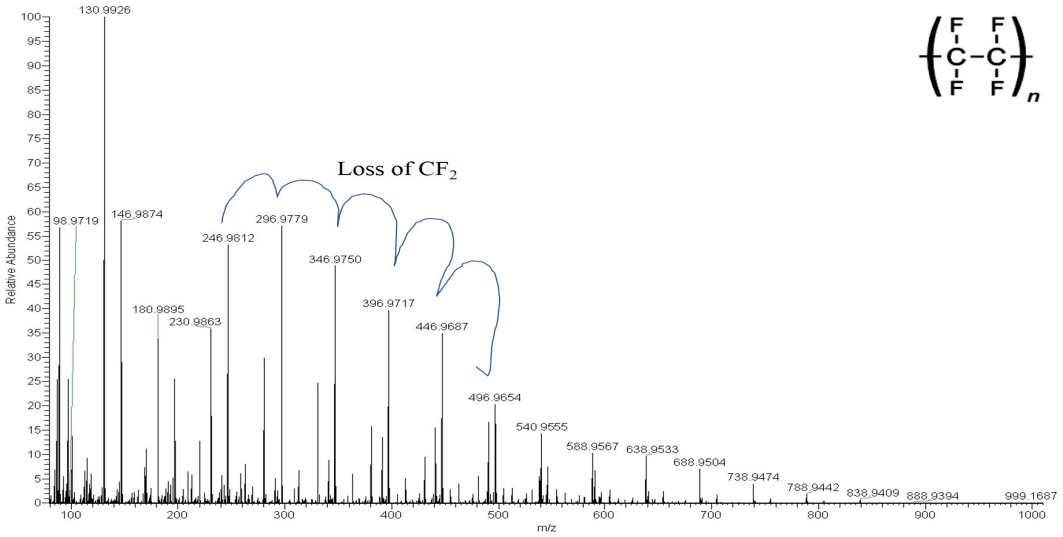

(a)

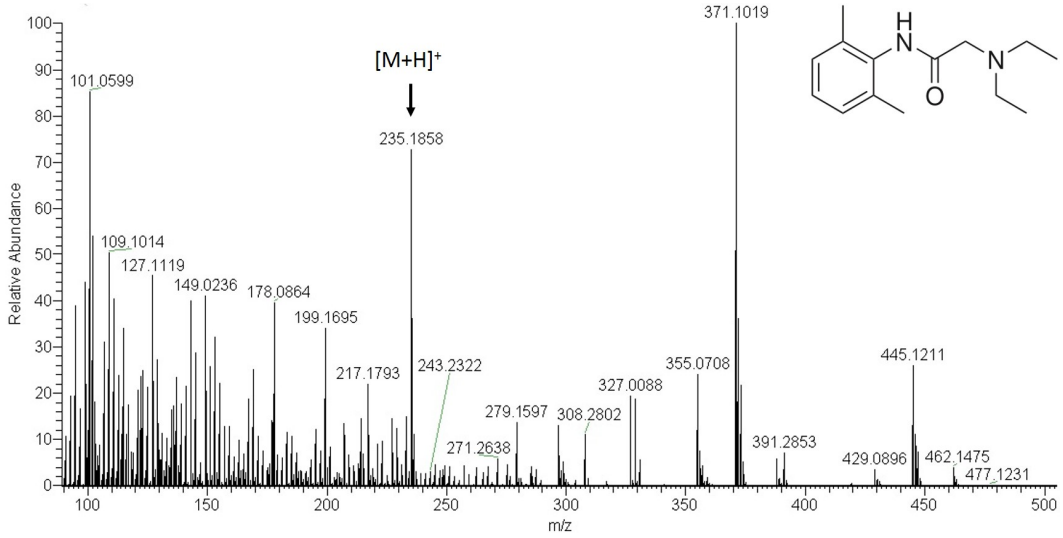

(b)

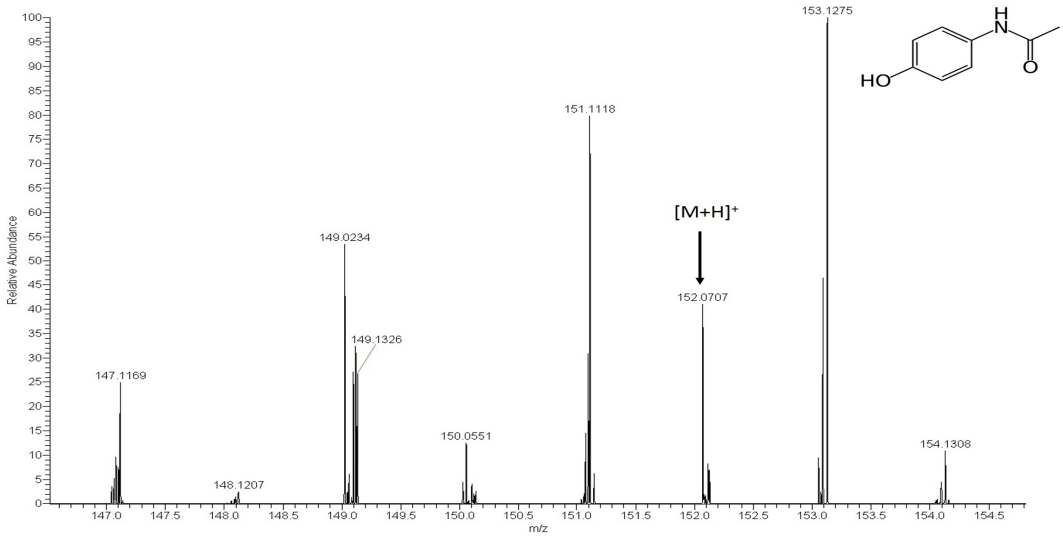

(c)

Figure 4.3. Mass spectral data acquired on the Thermo Exactive Orbitrap for (a) PTFE in negative acquisition mode showing the repeat units of PTFE 50 Da apart, (b) lidocaine at m/z 235.1858 for the $[M+H]^+$ ion and (c) paracetamol at m/z 152.0712 for the $[M+H]^+$ ion, both in positive acquisition mode.

low concentration samples not detected in this study. The positive ion mass spectral data showing successful identification of lidocaine can be seen in figure 4.3 (b) where the protonated molecular ion $[M+H]^+$ can be seen in high abundance at m/z 235.1858 (theoretical monoisotopic mass of m/z 235.1810, mass error of roughly 20 ppm), and the detection of paracetamol is shown in (c) at m/z 152.0707 (theoretical monoisotopic mass of m/z 152.0712, mass error of roughly 3.29 ppm) for the protonated molecular ion $[M+H]^+$.

The results obtained on the Orbitrap, although not perfect (containing some calibration shifts), provided the indication required that the plasma jet could be a viable ionisation source to couple with mass spectrometry for the detection of drugs, explosives and many other types of analyte. It is important to note that PTFE is not a compound that is readily ionised by other conventional ionisation methods such as APCI and therefore, a plasma source may be useful for a wide variety of applications. Currently though, the aim is to develop a plasma based ionisation source for mass spectrometry primarily for the detection of drugs on money and explosives detection therefore, real samples of drugs and explosives were obtained for analysis and detection with an analytical mass spectrometer.

4.3.3 Analytical Data

The plasma jet showed potential as an ionisation source however, it was important to develop the technique and apply it to the application of drugs and explosives detection. The results were all obtained in collaboration with Mass Spec Analytical Ltd (MSA) in Bristol, UK, using an AB Sciex API 2000 tandem mass spectrometer. Tandem mass spectrometry is a technique that offers a very high level of selectivity and specificity which results in a high level of confidence that the corresponding peaks obtained are the analytes of interest. Tandem mass spectrometry, or MS/MS, separates ions (formed in the plasma jet ionisation source) by their mass-to-charge ratio (m/z) in the first quadrupole of the mass spectrometer (MS1). In the example of cocaine, the ionisation results in a protonated molecule $[M+H]^+$ at m/z 304 and during the first stage of MS/MS in a selected reaction monitoring (SRM) method, any ions that do not have an m/z value of 304 are filtered out of the mass spectrometer. The ions that do have the m/z value of 304 are focussed into the collision cell (second quadrupole). Once in the collision cell, the precursor ions are accelerated by an electrical potential causing collisions with neutral molecules (nitrogen in this case) which results in bond breakage and fragmentation of the precursor ions into smaller, product ions. This process is called collisionally induced dissociation (CID). The characteristic product ions such as m/z 182 and 105 are then

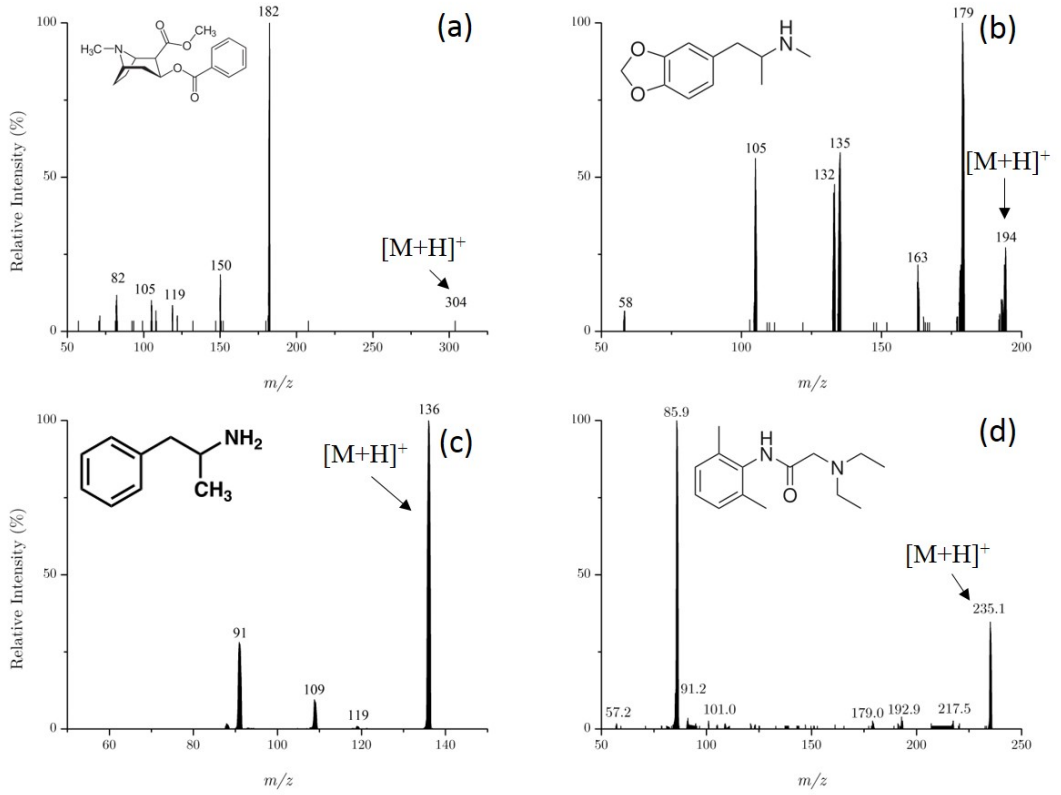

Figure 4.4. Positive product ion spectra of cocaine at m/z 304 for the $[M+H]^+$ ion (a), MDMA m/z 194 for the $[M+H]^+$ ion (b), amphetamine m/z 136 for the $[M+H]^+$ ion (c) and lidocaine m/z 235 for the $[M+H]^+$ ion (d) obtained using an atmospheric pressure plasma jet at 100 ng/μL.

separated and detected by the third quadrupole (MS2).

The plasma source was coupled to the mass spectrometer at an approximate distance of 1 cm from the orifice and at an angle of 45^o for analysis of samples. The samples were introduced by spotting a known amount onto a glass slide and allowing to dry. The dry sample spot on the glass slide was then positioned in front of the mass spectrometer about 0.2 mm below the orifice. The plasma was then able to directly interact with the dry sample spot initiating desorption/ionisation so that the sample could enter the mass spectrometer in gaseous form for detection. Some changes to the mass spectrometer were required to aid detection such as the curtain gas. The mass spectrometer has a curtain plate roughly 5 mm from the orifice plate and this gap is filled with nitrogen to act as a curtain gas. This curtain gas is essential to prevent dirt, debris or solvents from entering the orifice. However, the curtain gas had to be reduced to ensure safe transportation of ions into the mass spectrometer (from 20 psi to 10 psi) as it seemed to prevent the ions entering the mass spectrometer, affecting sensitivity. It was not possible to remove the curtain plate or curtain gas because that would enable the helium to enter the mass spectrometer which could result in mechanical failure of the instrument.

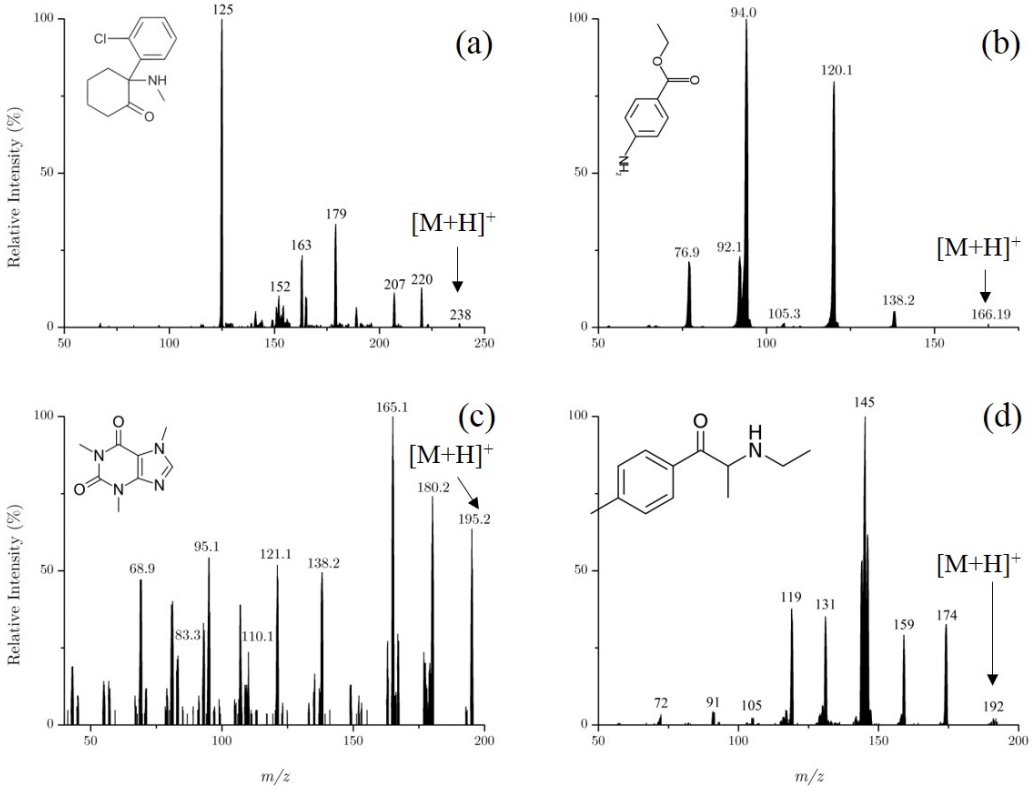

Figure 4.5. Positive product ion spectra of ketamine at m/z 238 for the $[M+H]^+$ ion (a), benzocaine at m/z 166 for the $[M+H]^+$ ion (b), caffeine at m/z 195 for the $[M+H]^+$ ion (c) and 4-MEC at m/z 192 for the $[M+H]^+$ ion (d) obtained using an atmospheric pressure plasma jet at 100 ng/μL.

In Fig. 4.4 are product ion spectra obtained in positive ion mode for cocaine, 3,4-methylenedioxymethamphetamine (MDMA), amphetamine and lidocaine. All samples were prepared using 100 ng in methanol by spotting 1 μL of 100 ng/μL solution onto a glass slide and allowing to dry. The precursor ion in all cases was the $[M+H]^+$ ion as this was the most dominant. The characteristic ions for cocaine can be seen in Fig. 4.4 (a), at m/z 304 for the precursor ion and m/z 182 and 105 for the characteristic product ions. MDMA can be seen in Fig. 4.4 (b) at m/z 194 for the precursor ion and the characteristic product ions can be found at m/z 163 and 105. The precursor ion for amphetamine is shown in Fig. 4.4 (c) at m/z 136 and the characteristic product ions at m/z 119 and 91. Finally, the lidocaine precursor ion can be seen in Fig. 4.4 (d) at m/z 235 with product ion at m/z 85. It is evident by Fig. 4.4 that other product ions could be chosen instead of the ones mentioned. These product ion spectra have been obtained at various collision energies and have not been optimised to achieve the highest signal intensity of each product ion and therefore, will encompass some losses in sensitivity.

The product ion spectra for ketamine, benzocaine, caffeine and 4-methylethcathinone

(4-MEC) are all shown in Fig. 4.5 where the precursors for ketamine are at m/z 238 (a), benzocaine at m/z 166 (b), caffeine at m/z 195 (c) and 4-methylethcathinone (4-MEC) at m/z 192. These results suggest that the plasma jet is capable of desorption/ionisation of major drug compounds from a glass surface. A similar study was conducted with a few well known explosives such as 2,3-dimethyl-2,3-dinitrobutane (DMNB), cyclotrimethylene trinitramine (RDX), pentaerythritol trinitrate (PETN), triacetone triperoxide (TATP) and trinitrotoluene (TNT). Explosives analyses are not quite as straight forward as drugs, for example, some explosives require an adduct to be formed with the explosive molecule, increasing identification confidence, and increasing sensitivity (detection probability). Routinely, for nitroesters such as pentaerythritol trinitrate (PETN) and nitroamines such as cyclotrimethylene trinitramine (RDX), a chloride ion can be used to form an adduct with the explosive molecule to form the $[M+Cl]^-$ species [72]. This is due to their electrophilic nature and the chlorine ion is highly electrostatic.

For RDX and PETN pure nitrogen gas was bubbled through dichloromethane and added to the helium stream to enable a mM concentration of chlorine to enter the plasma region to adduct to the explosive molecules, and for TATP, nitrogen was bubbled through a 10 mM solution of ammonium hydroxide to produce the NH_4^+ ion for adduction. The product ion spectra for DMNB and RDX can be seen in Fig. 4.6 where DMNB is detected in positive ion mode as a protonated precursor ($[M+H]^+$) at m/z 177 and RDX is detected in negative ion mode for the $[M+Cl]^-$ precursor ion at m/z 257. PETN is detected in negative ion mode as $[M+Cl]^-$ at m/z 351, whilst TATP is detected in positive ion mode with ammonium adduct to form the $[M+NH_4]^+$ precursor ion at m/z 240 as shown in Fig. 4.7.

Finally, in Fig. 4.8 TNT can be shown to be detected as the radical molecular ion $[M]^-$ and protonated molecular ion $[M-H]^-$ at m/z 227 and 226 respectively. The explosives data demonstrate that the plasma jet is a form of soft ionisation as for most explosives, the spectrum is dominated by the molecular ion and few products, suggesting a soft ionisation technique.

4.4 Conclusions

From these results, especially the explosives in negative ion mode, the plasma jet can be considered as a soft ionisation technique similar to APCI [46]. A soft ionisation technique is preferred because in-source fragmentation is reduced or eliminated, which in turn results in a higher sensitivity of the precursor ion that can be separated and fragmented into product ions. Despite APCI and the plasma jet both being soft ionisation techniques,

the plasma does have the potential for different or additional ionisation mechanisms to APCI and therefore, it is possible that a plasma ionisation source may be able to produce ions that were not possible with APCI as seen with PTFE in Fig. 4.3. Furthermore, it is also possible due to interaction with air, ozone and other excited species are generated which may result in more ions such as NO_x. Such ions could be used as adducts instead of introducing chlorine or ammonia.

Evidently, the plasma jet is capable of functioning as a desorption/ionisation source for mass spectrometry to detect drugs, explosives and likely, many other compounds. However, for the application of drugs and explosives detection, the surface area of the plasma jet is not sufficient in comparison to the size of a banknote or a swab. Therefore, the plasma jet was further developed to produce a plasma that could analyse a much larger surface area than 10 mm^2.

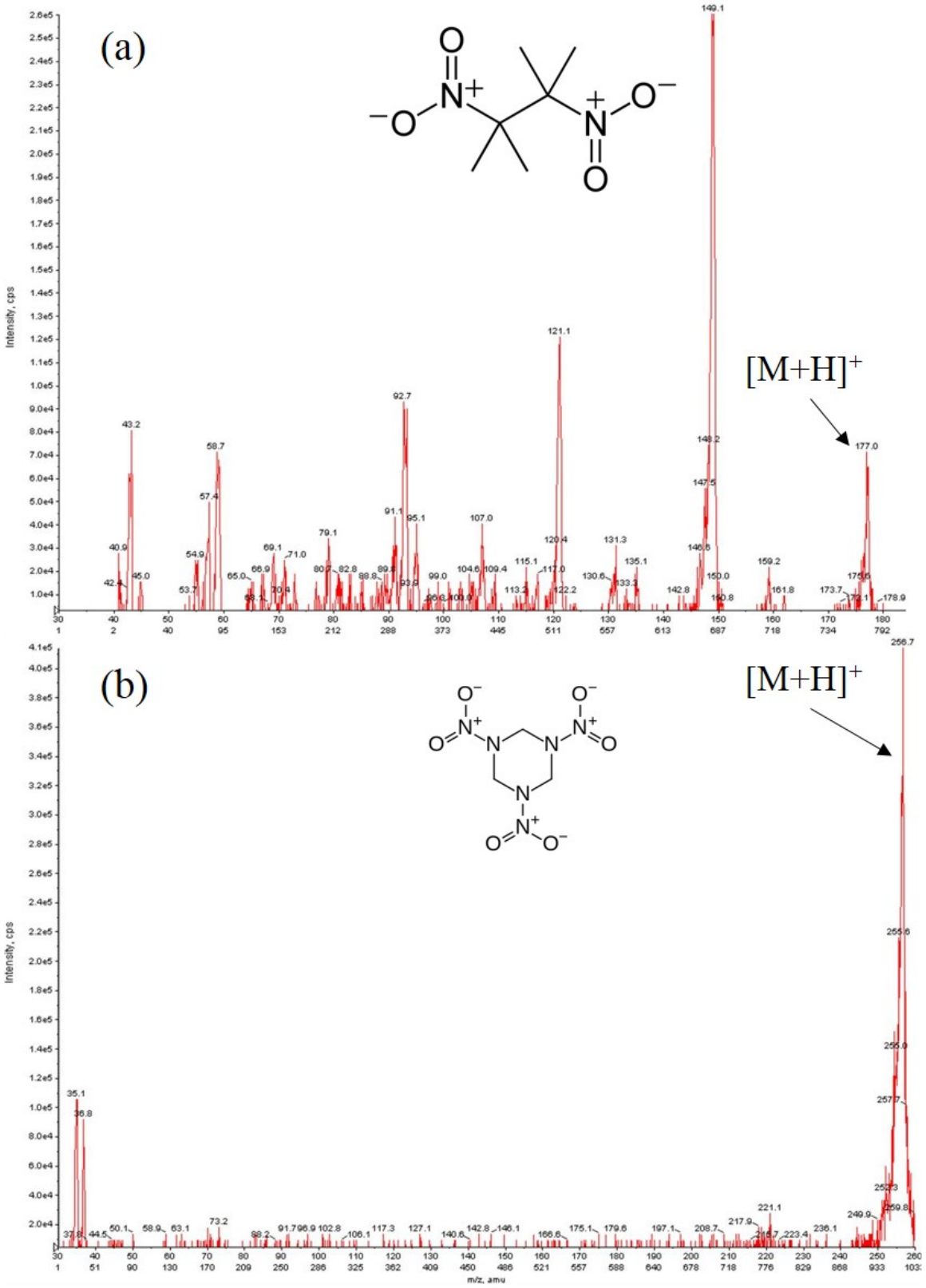

Figure 4.6. Positive product ion spectra of DMNB at m/z 177 for the $[M+H]^+$ ion (a) and negative product ion spectra for RDX at m/z 257 for the $[M+Cl]^-$ ion (b), obtained using an atmospheric pressure plasma jet at 100 ng/μL.

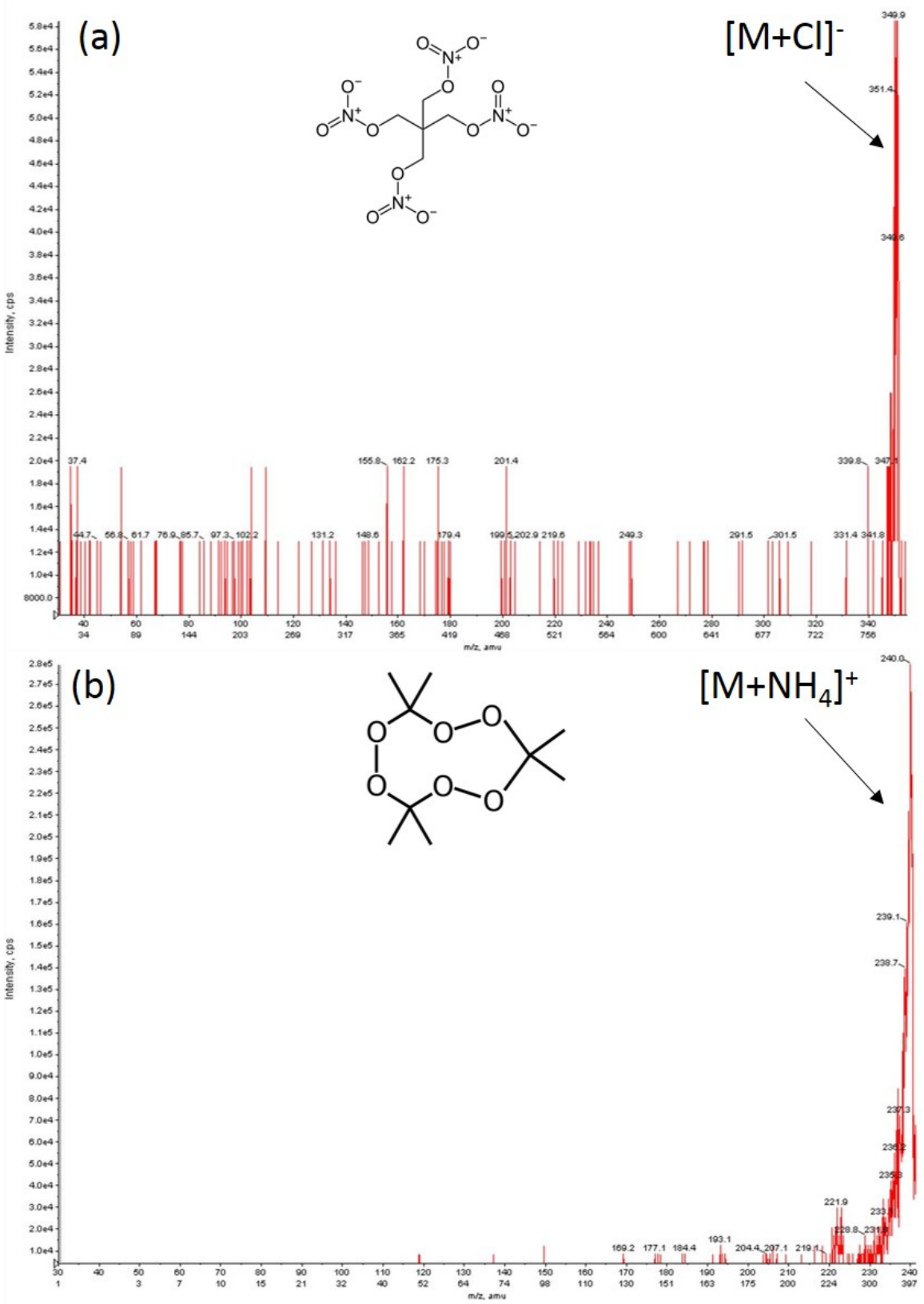

Figure 4.7. Negative product ion spectra of PETN at m/z 351 for the $[M+Cl]^-$ ion (a) and positive product ion spectra for TATP at m/z 240 for the $[M+NH_4]^+$ ion (b), obtained using an atmospheric pressure plasma jet at 100 ng/μL.

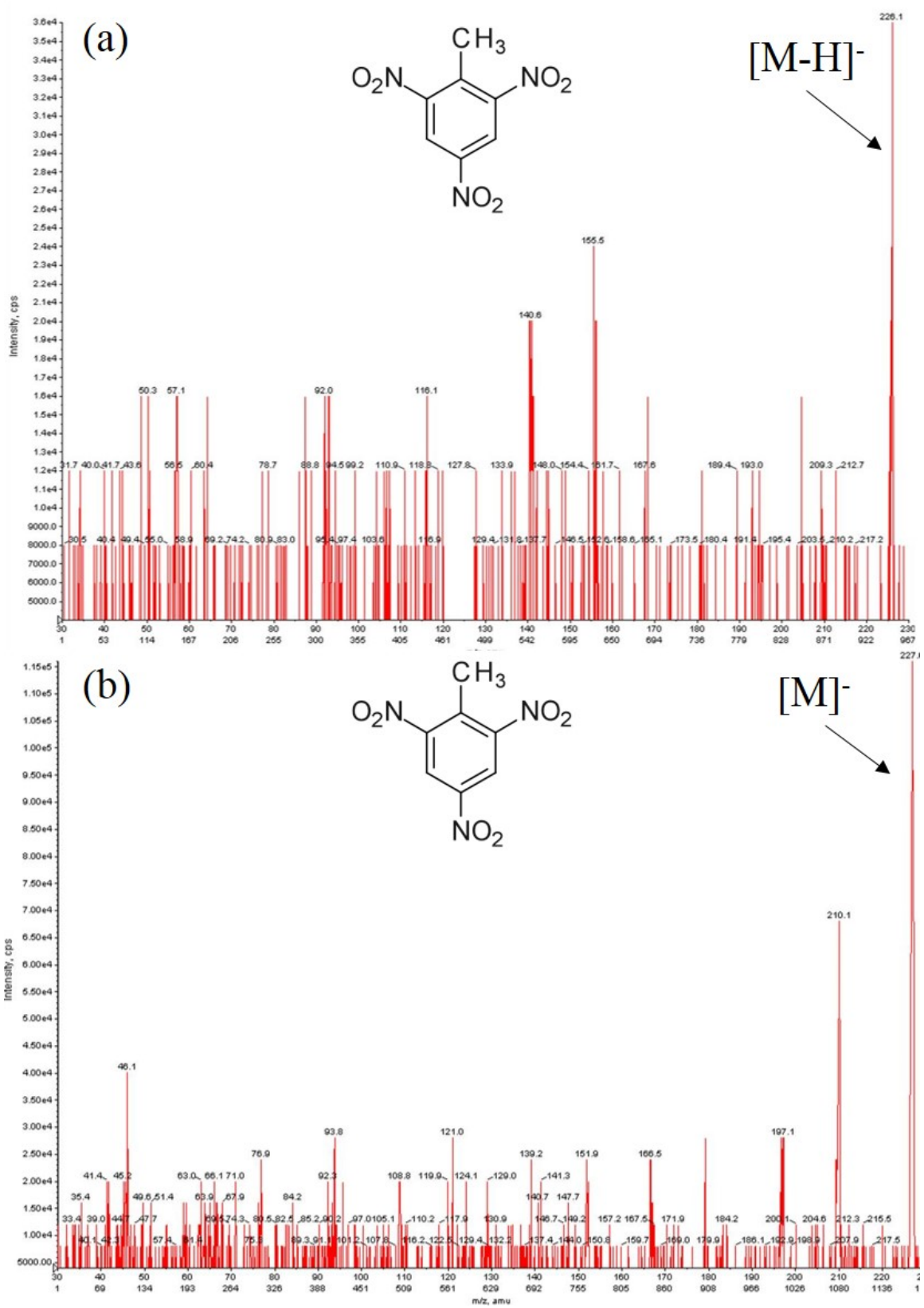

Figure 4.8. Negative product ion spectra of TNT at m/z 226 for the $[M]^-$ ion (a) and at m/z 227 for the $[M\text{-}H]^-$ ion (b), obtained using an atmospheric pressure plasma jet at 100 ng/μL.

Chapter 5

Development of an Atmospheric Pressure Plasma Brush and a Plasma Jet Array

This chapter will discuss the development from a plasma jet into a plasma brush and a plasma jet array as discussed in chapter 4.

5.1 Introduction

The plasma jet proved to be capable of desorption and ionisation for analytes of interest from a glass surface comparable to previous literature [18, 33]. However, the plasma jet is not capable of rapidly analysing a large surface area which would be required for the application of drugs on money and analysing swabs for explosives. Therefore, it was imperative that the plasma jet was developed further so that it could analyse a larger surface area. The majority of the plasma based ionisation sources have a small surface area and thus, a plasma ionisation with a large surface area may possess some novelty.

5.2 Plasma Brush

The plasma brush was created by extending the opening of a plasma jet to become a much wider plasma source. This innovation was based on the design of a plasma brush developed in Chen *et al* [59]. Other recent publications based on a similar concept were also taken into consideration when designing the plasma brush [73–76]. The initial design of the plasma brush utilised two quartz slides 30 mm wide, 65 mm long and 1 mm thick. The slides were housed within a 3D printed holder manufactured and designed by Michael John Lynch. The holder was made of a black polymer filament and contained

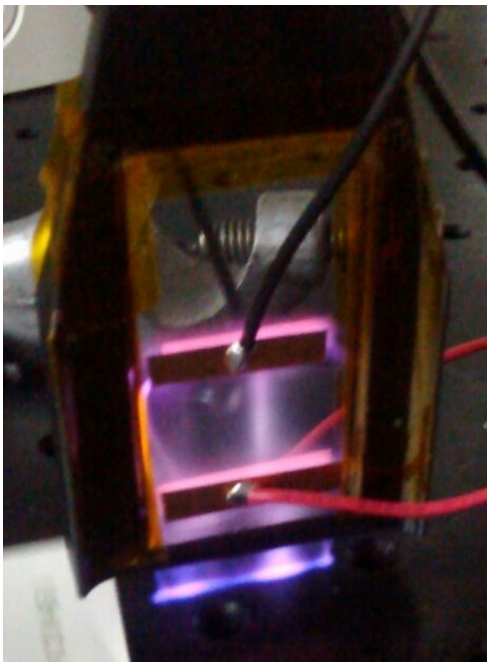

Figure 5.1. Image of plasma brush in original 3D printed holder. The black wires (top) are connected to an electrical ground provided a ground electrode, the red wires (bottom) are powered by a high voltage AC sine wave. The orange Kaptop tape around the edges of the 3D printed holder were placed to prevent helium leakage through the sides of the holder.

two grooves 1 mm wide for the quartz slides to fit in shown in Fig. 5.1. The grooves were separated by 1 mm to create an air gap between the two quartz slides. The top of the holder was funnel shaped and connected to a 1/4 ” Swagelock fitting for helium introduction.

The side of the quartz slides, where they meet the grooves, was sealed using Kapton tape to prevent any leaks or interference from the ambient air. On each slide, was a ground electrode and a powered electrode. All electrodes were composed of adhesive copper tape 5 mm wide and 20 mm long and each electrode were soldered in the centre to allow for a wire to connect the electrodes to either earth or an AC power supply. The powered electrodes were located 5 mm from the exit of the two quartz slides in the downstream direction whilst the ground electrodes were separated from the powered electrodes by 15 mm in the upstream direction. The powered electrodes were attached to a high voltage AC power supply at 6 kV and 20 kHz and the helium flow was 1.4 SLPM and a ground electrode (in this case a metal table electrically connected to earth) was located roughly 5 mm from the exit of the brush.

Various electrode arrangements were considered and tested such as 10 mm thick electrodes, 5 mm saw tooth electrodes and different spacing between the electrodes themselves and also the distance of the powered electrode from the exit. It was decided that the above electrode configuration was the most stable, reproducible and resulted in the most homogeneous plasma.

Unfortunately, this set-up contained many flaws. Firstly, at 20 kHz (chosen to replicate the conditions of the jet) the time-lapse fuse in the audio amplifier continuously blew and this is likely to be due to the current capacity of the transformer struggling to operate over this frequency, possibly resulting in current surges. In an effort to overcome this issue, a dielectric surface such as alumina was placed between the exit of the chamber and the grounded table. The dielectric surface acted as a capacitor resulting in a much more homogeneous plasma that could operate at 20 kHz without creating surges.

Despite overcoming the issue of power, there were other issues with the design. Firstly, the 3D printed polymer holder could not withstand any arcs or high temperatures and a couple of arcs caused permanent damage to the holder. These arcs were caused by being too close to the ground ground electrode and finally, the most crucial, helium leaks. As the sides of the holder were not air tight despite attempts to seal them with Kapton tape, it was possible for the helium to escape and this caused a potential difference between the electrodes and the excited helium causing arcing. Therefore, it was decided that the plasma brush would require further design improvements before it could be used as an ionisation source.

To counteract the problem caused by helium escaping the chamber, a custom made rectangular quartz tube was manufactured that was 43 mm wide, 3 mm deep and 60 mm long as described in 3.1.2 (Multi-Lab, Throckley, Newcastle upon Tyne, UK). The walls of the quartz were 1 mm to create a hollow centre that was 40 mm x 1 mm x 60 mm. The electrodes were still composed of adhesive copper tape, except they were a single continuous electrode around the entire block instead of one either side. The powered electrode remained in the downstream direction, 5 mm from the end and the ground electrode was in the upstream direction, with a separation distance of 10 mm. A gap of 10 mm was discovered as the optimum electrode gap for the quartz.

The powered electrode was connected to a high voltage AC power supply under the same conditions whist the ground electrode was connected to an electrical earth. To increase safety and eliminate exposed electrodes, the whole plasma brush was encompassed within a PTFE holder. The quartz block was connected at the top to

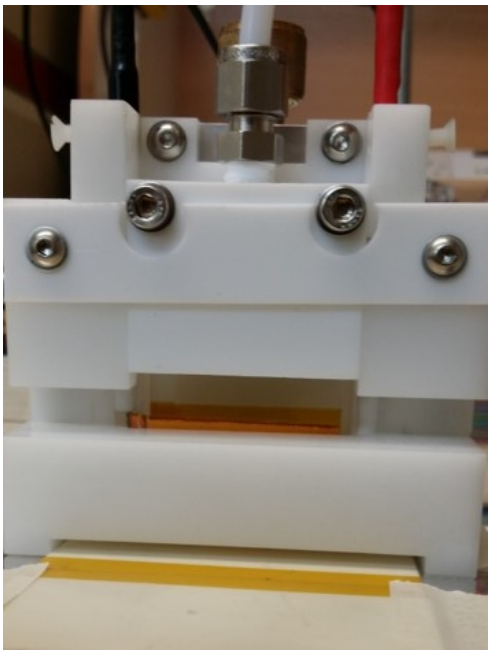

Figure 5.2. Image of plasma brush in PTFE housing with dielectric surface. The black wire (top left) provided an electrical ground to the top electrode and the red wire (top left) provided a high voltage AC sine wave to the bottom electrode. The Swagelock fitting shown at the tope of the image is the gas line connection to allow for a flow of helium. The yellow surface under the brush is a piece of alumina as a dielectric surface to allow for homogeneous plasma formation.

a hollow PTFE block to act as a gas chamber secured by a reasonably tight push-fit. Helium (pure grade 99.996%) was purged through a 1/4" Swagelock fitting at a rate of 1.4 SLPM, into the small PTFE block that contained several holes allowing the gas to be distributed into the quartz block. Finally, a micrometer was attached to the whole unit to allow for minor adjustments to be made to the gap between the exit of the brush and the dielectric surface (vertical height adjustment). The newly designed plasma brush can be seen in Fig. 5.2

Unfortunately, despite the design improvements, no meaningful data was obtained using the plasma brush which can be attributed to a couple of reasons. Firstly, it is difficult to align the plasma brush towards the mass spectrometer and if a pump was used to draw ions from the brush to the mass spectrometer, the influence on the helium was too great, resulting in an unstable plasma. Secondly, the plasma brush used the same power conditions as the plasma jet with the same flow rate but with a much larger

volume and consequently, the surface that was being analysed was being subjected to a reduced amount of helium metastables as they were now much more spread out. These factors were enough to prevent any signal being detected within the mass spectrometer and so the plasma brush was rejected, while a new idea was developed consisting of an array of plasma jets.

5.3 Plasma Jet Array

The plasma jet array was also based on the design of the plasma jet, but after it was discovered that making the jet itself larger was not advantageous, the idea of several jets became of interest. There were a few existing plasma jet arrays in previous literature mainly for surface treatment [77,78], but some were developed as an ionisation source for mass spectrometry [57]. The plasma jet arrays that were developed for surface treatment were linear, presumably to create a large surface area of plasma although a large surface area is essential, a linear pattern would prove problematic in ensuring safe transportation of the ions into a mass spectrometer.

The plasma jet array built as an ionisation source in Dalgliesh *et al* gave inspiration for the next design [57]. The design of the plasma jet array in Dalgleish *et al* consisted of up to 19 probes that were all 1.5 mm in their outer diameter and the overall surface area could not be much larger than 20 mm^2. Therefore, it was decided that the plasma jet array would consist of 32 plasma jets in four columns of eight (looking from the front). Unlike the plasma jet arrays for surface treatment which required an electrode for each individual jet [77, 78], a single electrode was used to excite all the jets in a similar way that others had [57, 79]. A dielectric surface also helped to ensure all plasma jets were ignited because it acted as a capacitor; this effect is described in Ghasemi *et al* where a ballast resistor between each electrode/jet enabled the ignition of every jet [78].

Each jet of the plasma jet array consisted of a quartz tube (OD 3 mm; ID 1 mm) that was housed within a PTFE block with 32 holes for a push-fit at the top. At the bottom of the quartz tubes, roughly 10 mm from the exit, was a 10 mm thick brass block with 32 x 3.5 mm holes which acted as the powered electrode. Each jet was spaced 2 mm from one another and looking at the source front on in Fig. 3.4 the four columns were at a 75^o angle instead of heading straight back (straight would have been 90^o or perpendicular in relation to the front). This angle was deemed important as it angled towards the orifice encouraging ions in that direction. All of the plasma jets/quartz tubes protruded from the end by 0.5 mm. A gas chamber which consisted of a hollow PTFE block was fitted over all 32 jets to act as the discharge gas supply. The plasma jet array can be seen in

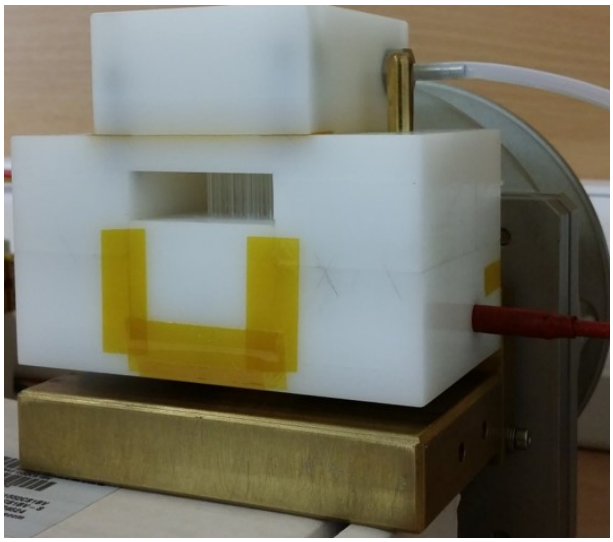

Figure 5.3. Image of plasma jet array in PTFE housing with brass block and plenum chamber attached. The brass block acts as a ground electrode for the plasma jets to breakdown against. The heliums is purged through the PTFE tube at the top into a small chamber containing holes for the jets. Finally, the powered electrode is connected via the right hand side using the red wire and a banana plug connection.

Fig. 5.3

Except for the helium flow of 4 SLPM, all other conditions of power and frequency remained the same as a single plasma jet. The higher flow was required to ensure a flow of helium into each jet, a lower flow resulted in only a few of the jets igniting into a plasma. Initial experiments were conducted with the plasma jet array coupled to the curtain plate but no ions were detected. The plasma jet array was then coupled to a plenum chamber and sample pump to draw the ions into the mass spectrometer. A brass block was fitted 4 mm away from the exit of the plasma jets to act as a ground electrode to enable plasma formation in the jets. A positive ion mass spectra of molecular ions generated in the plasma can be seen in Fig. 5.4, these ions are the result of direct interaction between the plasma jet array and ambient air.

Known concentrations of cocaine in methanol were spotted onto a glass slide and allowed to dry, the glass slide was then subjected directly to the plasma by inserting it between the ground electrode but no characteristic ions for cocaine were seen. Unfortunately, due to this, the plasma jet array development was discontinued and the development of another plasma source based on a dielectric barrier discharge that forms on the surface, which is described in chapter 7, was prioritised. However, it is

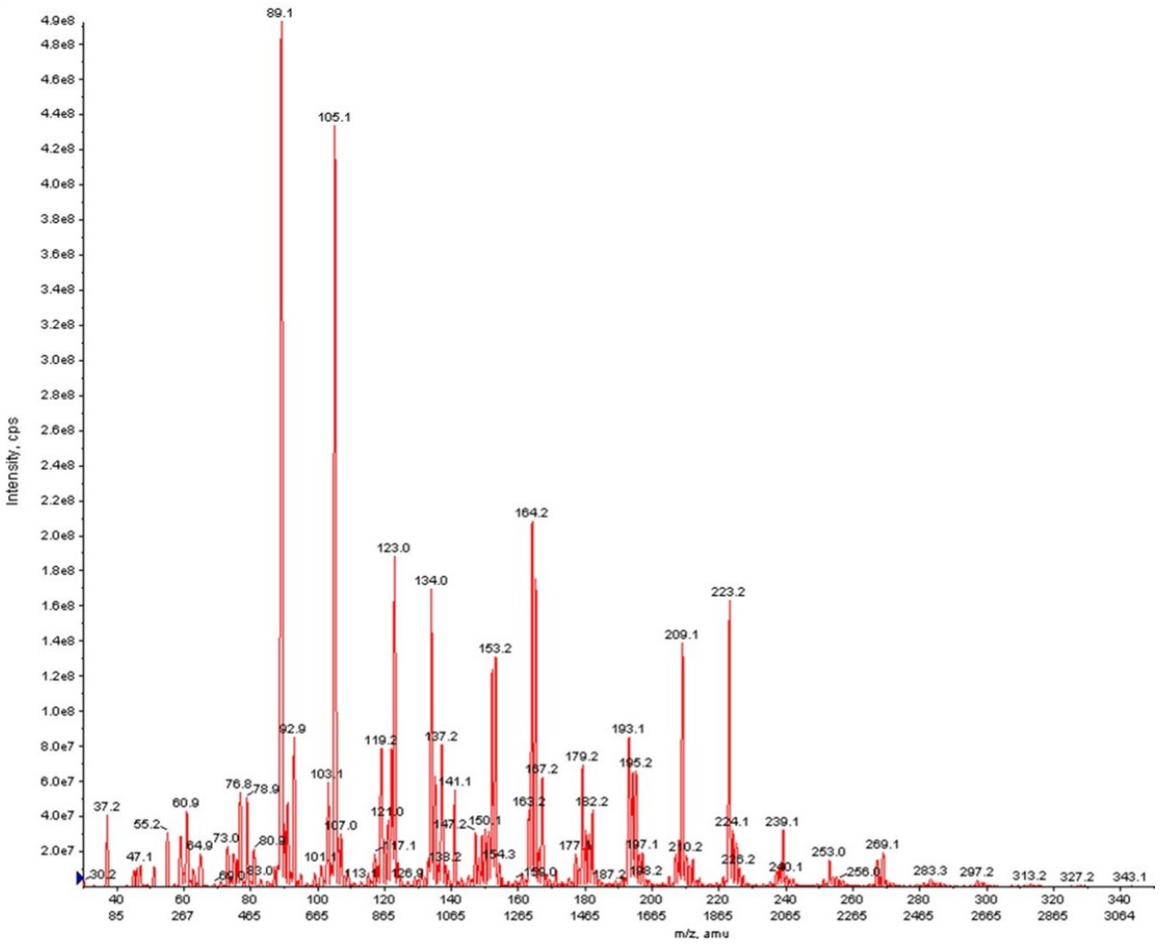

Figure 5.4. Positive ion mass spectra of $[M+H]^+$ ions detected in the air using the plasma jet array coupled with a plenum chamber.

likely that the plasma jet array would have been capable as a desorption ionisation source with additional development as it had rendered some positive ion data. Further development of the ion source would include tilting the jets to 45 ^oC in relation to the mass spectrometer orifice, replicating the alignment of a single jet.

As the plasma source ionises the sample, the ions then have to be transferred to the mass spectrometer but ions only have a very short lifetime and the distance that these ions had to travel between the plasma and the orifice may have been too great. As a result, the ions may have lost their charge through collisions with other species in the air or they may have formed clusters. There are at least two options that would help to overcome this. Firstly, the plasma array is currently located 90 ^{o} in relation to the orifice and therefore, the ions are not aligned at all and have freedom to travel in any direction. If the plasma jet array was tilted towards the orifice, the helium would act as a carrier gas towards the orifice and the sample pump would help to focus this flow.

Secondly, it would be possible to include a post-ionisation source before the orifice

plate such as an APCI needle. The APCI needle would be able to re-ionise any ions that had lost their charge through collisions and would also be able to break up any clusters that may have formed, increasing sensitivity. However, having said this, the plasma jet array would not be the perfect solution for the application of drugs on money but would be useful for other applications. The plasma jet array consists of 32 jets within close proximity to one another and because of this, there is a strong repulsion between the jets which results in a non-reproducible divergence of the jet. This divergence could result in small areas of the swab or banknote not being analysed at all and there would be limited confidence that the swab had been thoroughly analysed.

5.4 Conclusions

To conclude, during the course of this project, two potential plasma based ionisation sources were developed and coupled with mass spectrometry with limited results. The aim was to develop a plasma source with an increased surface area, which was successfully achieved. However, the plasma sources were not successful in producing ions for detection. Firstly, the plasma brush probably did not possess enough energy to liberate a sample from the surface and would therefore, not be a potential ionisation source. The plasma jet array was successful in generating ions and with further development could prove to be a useful plasma source. The plasma jet array does use a higher flow of helium to enable ignition of every jet; this flow could be reduced by reducing the diameter of the jets but this would, in turn, reduce the surface area. Using large amounts of helium is a concern as it is a finite source which is rapidly declining, additionally, it is a high cost consumable which limits the likelihood that the plasma array would become commercially viable.

As the plasma brush and plasma jet array did not render the desired results for drug and explosives detection, a new surface barrier discharge ionisation (SBD) source was developed and is discussed in chapter 7. The use of an SBD ionisation source with mass spectrometry is novel and so is its design.

Chapter 6

Measurement of Surface Modification due to Plasma Treatment

This chapter will describe the results obtained using various plasma sources to treat polypropylene, cotton paper and polymer banknote surfaces in an attempt to measure the surface morphology.

6.1 Introduction

The development of a plasma jet led to two additional plasma sources as described in sections 4 and 5 called a plasma brush and a plasma jet array, respectively. The main basis of their development was to be able to analyse a larger surface area than what was currently possible with other plasma based methods. The reason a larger surface area was required is because of the application of drugs on money and also to be able to analyse swabs for drugs and explosives or even many other types of compounds. Previous plasma sources had a surface area rarely larger than 10 mm^2 such as DART and DESI [14, 16] and hence, the development of the plasma brush and the plasma jet array.

6.1.1 Polymer Banknotes Introduction

In the UK in 2016, the Bank of England announced they would introduce polymer banknotes into the UK general circulation to replace the paper banknotes. The polymer banknotes are made to be cleaner, stronger and safer than paper banknotes, increasing the life cycle of a banknote in circulation as well as preventing counterfeits from being made as easily. The contamination on paper banknotes was possible to analyse using thermal desorption (TD) APCI with a temperature of over 250 ^oC to volatilise the

molecule into gaseous form for ionisation. However, these temperatures would melt the new polymer banknotes, composed of polypropylene, which cannot withstand temperatures greater than 120 ^{o}C. Therefore, a plasma ionisation source was proposed which operates at a much cooler temperature and is capable of desorption/ionisation.

It was therefore important to understand what would happen to the polypropylene surface following plasma exposure and determine whether or not this was minimal or destructive to the banknote. For these experiments, the plasma jet, jet array and brush were used to treat the surface of polypropylene, polymer banknotes and cotton paper (replicating paper banknotes). The polymer banknote samples were dummy banknotes printed by the Bank of England. These experiments included a time variable to see how much the surface changed over plasma treatment duration and the changes were measured using analytical techniques.

6.2 Results and Discussion

6.2.1 Water Contact Angle Measurements

Water contact angle (WCA) measurements are the angle where a water droplet meets a surface. For a hydrophobic surface, the contact angle is likely to be close to 90^{o} as the water droplet will retain its surface tension and not spread across the surface. However, a hydrophilic surface will have a much reduced angle below 90^{o}. This technique is capable of measuring whether the treatment of the surface with plasma is enough to change the hydrophilicity (or wettability) of the surface which will infer a change in the inter-molecular forces of the substrate. For these experiments, a static sessile drop method was utilised in which a drop of deionised water was dropped onto the surface. An optical system with a back-light would then be used to capture images of the droplet and measure the contact angles over several frames and average them out. In this case, 20 frames were taken and averaged to find the mean contact angle. Unfortunately due to the porous nature of cotton paper, WCA measurements were not possible.

It can be seen in Fig. 6.1 that the polymer control a) has a large contact angle with the surface in comparison to the polymer sample that has been treated by a plasma jet for 2 minutes b). This would suggest that the hydrophilicity of the surface had increased due to plasma treatment. The angles were measured over various treatment times (0-10 minutes) and the data for polypropylene can be seen in Table 6.1. The samples named *CSBKG* were control samples for polypropylene and were therefore not subjected to plasma treatment. The WCA for the controls were measured as 86.67^{o} and 82.47^{o}. For

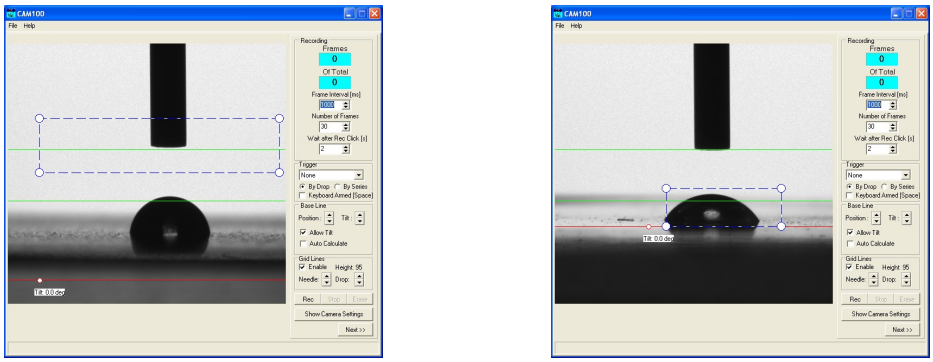

(a) **(b)**

Figure 6.1. Water contact angle images of a) a polymer control sample and b) a polymer surface that has been treated with a plasma jet for 2 minutes.

Table 6.1. Table showing water contact angles of the corona side of polypropylene samples treated by a plasma jet and plasma brush for various lengths of time, CSBKG_03 is the control for jet and CSBKG_04 is the control for the brush. Jet samples are JCSX and brush samples are BCSX.

Sample Name	**Time Treated (mins)**	**Average Contact Angle(^{o})**
CSBKG_03	0	86.7
CSBKG_04_Brush	0	82.5
JCS1_06_Jet	2	70.0
BCS1_17_Brush	2	71.3
JCS1_07_Jet	4	60.7
BCS2_18_Brush	4	70.2
JCS3_08_Jet	6	60.8
BCS3_19_Brush	6	73.1
JCS4_09_Jet	8	56.1
BCS4_20_Brush	8	58.3
JCS5_10_Jet	10	61.0
BCS5_21_Brush	10	53.8

all the other samples that were treated by a plasma source for at least 2 minutes, the contact angle was much reduced to roughly 70^o, suggesting an increase in hydrophilicity. It is interesting to note that neither the jet or the brush changes the surface more than the other which would suggest that the same surface modifications are happening at the surface. However, this is not surprising as they are both operating at exactly the same conditions.

When a 'real' sample is subjected to plasma for analysis of drugs on money, it is very unlikely that the surface will be subjected to the plasma for more than a few seconds, and therefore, a window of 2-10 minutes was considered too large. It was decided that a shorter treatment time should be used to replicate a scenario closer to reality. Samples of

Table 6.2. Table showing water contact angles of the corona side of polypropylene samples treated by a plasma source for various lengths of time, PPC is the polypropylene control.

Sample Name	Time Treated (seconds)	Average Contact Angle(^{o})
PPC	0	88.1
Jet	10	72.7
Brush	10	73.4
Array	10	45.3
Jet	30	70.5
Brush	30	78.6
Array	30	51.0
Jet	60	69.7
Brush	60	57.9
Array	60	74.5

polypropylene were treated by the plasma jet, array and brush for 10 seconds, 30 seconds and 1 minute and then measured using the same technique as before. The results of the reduced times can be seen in Table 6.2 where PPC is the polypropylene control sample. Even after only 10 seconds of plasma treatment there is a significant difference in the WCA, reinforcing the hypothesis that plasma treatment will increase the hydrophilicity. Interestingly, the surface modification happens extremely quickly and while it may increase over time, even 10 seconds is enough to modify the surface properties greatly.

It is evident in Table 6.2 that the plasma jet and the plasma array modify the surface to a similar extent over time. However, the jet array (excluding the 60 s measurement which may be erroneous) appears to increase the surface hydrophilicity to a higher degree than the brush and the jet which is not overly surprising considering that it is comprised of 32 plasma jets compared to a single jet. As the hydrophilicity was increased as would be expected, the plasma source was then used to treat samples of polymer banknotes.

Due to the nature of polymer banknotes having many varying surface types due to ink, holograms and textures etc. it is quite difficult to measure accurately any changes because there will always be an uncertainty that the varied surface was partially responsible for the change in result. However, preliminary studies were performed out of interest to see if there were any great changes but it is important to note that for these results to be truly meaningful, many repeats should be made to take into account the possible uncertainties and outliers in the data. Furthermore, it is difficult to draw comparison between the plasma sources as they each treated a different region of the banknote and therefore, the surfaces could have been very different in composition to one another. Instead, this exercise was useful to determine whether the hydrophilicity

Table 6.3. Table showing water contact angles of polymer banknote samples that have been treated by various plasma sources.

Sample Name	Time Treated (seconds)	Average Contact Angle(^{o})
Jet Control	0	73.55
Brush Control	0	78.22
Array Control	0	67.98
Jet	30	27.81
Brush	30	56.85
Array	30	61.98

would have been increased like polypropylene or whether the other factors as a whole would have prevented such surface modifications.

The water contact angle measurements for polymer banknote samples that have been treated by a plasma source is displayed in Table 6.3 where each sample other than the controls were subjected to plasma treatment for 30 s. It is clear that the WCA has reduced dramatically, which would suggest a large increase in hydrophilicity but this could be due to many other uncontrollable factors too. Therefore, not much weight should be applied to the amount of change in WCA but more a statement to the fact that it has reduced. This is due to obtaining very few data points resulting in a large uncertainty. To overcome this, an increased number of analyses would reduce the level of uncertainty and make it much easier to draw conclusions from the data.

The WCA measurements of the polypropylene and polymer banknotes would suggest that there was an increase in hydrophilicity, even after a short treatment time of 10 seconds. These results would indicate a modification of the inter-molecular forces on the surface allowing for the water molecules to interact more with the surface than before. However, this can only be assumed using WCA and should be corroborated using additional techniques. Therefore, further confirmatory techniques such as atomic force microscopy (AFM), Fourier-transform infra-red spectroscopy (FTIR) and x-ray photoelectron spectroscopy (XPS) were used to corroborate the data in addition to gaining some insight to what happens to cotton paper with plasma treatment as WCA was not suitable for the substrate type. The plasma jet array was not used for the following set of results because the samples of each surface (10 mm x 10 mm) were roughly the same surface area as each jet within the jet array and therefore, it would more or less replicate the results of the plasma jet.

The water contact angle measurements are important to show that the surface properties have been modified by the plasma making the surface more hydrophilic. The

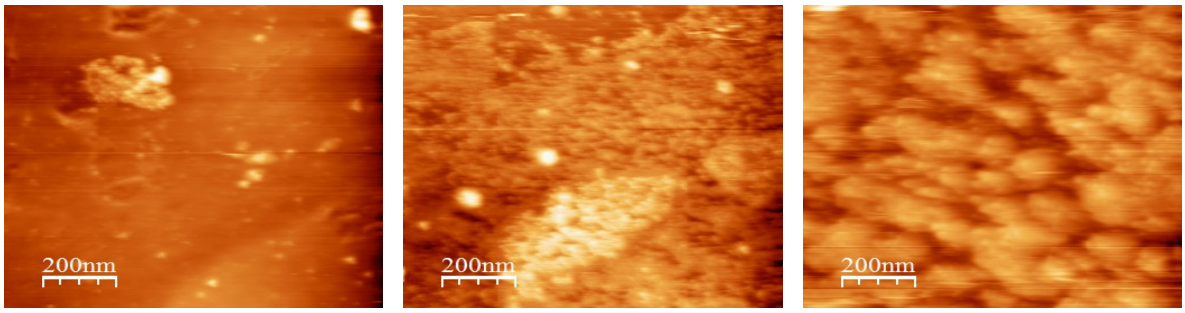

(a) (b) (c)

Figure 6.2. AFM analysis of a control sample of polypropylene at 40 μm (a), polypropylene samples treated by a plasma jet (b) and (c) at 40 μm and 10 μm respectively.

surface properties are likely changed due to breaking of the bonds of the surface, allowing for additional forces such as Van der Waals, resulting in increased hydrophilicity. This study was performed to ensure that the increase in hydrophilicity was not great enough to damage the banknote however, if plasma treatment was used in another application where it was important to have a hydrophobic surface, this study would suggest that plasma may not be suitable for such applications.

6.2.2 Atomic Force Microscopy

Atomic force microscopy (AFM) is a technique that uses a cantilever tip (silicon for these experiments) to scan a surface. If that tip is touching or close enough to the surface, the forces between the tip and surface lead to a deflection of the cantilever in accordance with Hooke's law [80]. In contact mode, the tip of the cantilever is slowly moved over the sample, measuring the contours of the surface and therefore, measuring the surface roughness. The signal that is received back to the detector is translated to a topographical representation of the surface to micro and nano-scale, portraying the peaks and troughs of the image as the surface roughness. A comparison of the topographical images of controls and treated samples should show a degree of change in the surface roughness indicating a change in surface structure. Unfortunately however, it was not possible to measure the piezoelectric displacement using this instrument, otherwise the forces such as Van der Waals forces could have been monitored. Topgraphical images and roughness measurements were produced using WSxM 4.0 software [67].

Figure 6.2 shows the topographical representations of a polypropylene control a) at 40 μm and polypropylene samples that have been subjected to the plasma for 2 mins at 40 μm (b) and 10 μm (c) respectively. The control sample a) is visually very smooth, especially in comparison with the treated samples (b) and (c) which show a distinctively rougher surface structure, suggesting surface modification. As the surfaces

of (b) and (c) do not look as smooth as the control, a), it is reasonable to suggest that the surface roughness has increased. The interaction of the surface with plasma results in a bombardment of ions, electrons and energetic species of neutrals and molecules on the surface which results in a removal of surface species such as contaminants and this process is called plasma cleaning [81, 82]. Following the cleaning process, shearing of the bonds, ablation and etching occurs resulting in a modification of surface properties and morphology [81, 82].

It has been well documented in the literature that surface roughness of polypropylene increases over time when treated by plasma [83], and therefore, results of treatment time of polypropylene are not presented here. However, the effect of treatment time using a plasma jet and a plasma brush on cotton is reported over 10-60 s. The surface topography for the cotton paper samples are shown in figure 6.3 where (a) is an untreated control, (b)-(d) have been treated by a plasma jet for 10 s, 30 s and 60 s and samples (e)-(g) have been treated by a plasma brush for 10 s, 30 s and 60s respectively. It is evident in figure 6.3 that an increase of plasma treatment time results in an increase in surface roughness and morphology. The surface does seem to appear rougher post-plasma treatment but there are a few things to bear in mind. Firstly, this is only a single measurement so caution has to be exerted before making conclusions. Secondly, these AFM images are taken at a scale of 5 μm as opposed to 10 μm in the polypropylene study due to technical difficulties with the instrument. In future experiments, it would be useful to re-analyse these samples with several repeats at an appropriate scan size.

However, the fibrous nature of the cotton paper is very apparent in Fig. 6.3 post-plasma treatment. This would suggest that the plasma is capable of breaking the bonds within the cotton surface which can be attributed to etching and has been reported to cause weight loss to cotton [84]. Unfortunately, weights of the samples were not recorded but it would be interesting for future studies to measure how much is lost over time and whether the different plasma sources vary in the amounts of weight loss they cause.

It is possible to conclude that the surface roughness does increase for polypropylene and cotton paper, however the AFM images in Fig. 6.4 for the polymer banknote samples does not reflect the same pattern. Again however, this could be due to the smaller scanning region and may be erroneous, unfortunately, there was not enough data for the polymer banknotes to provide a conclusion with too much certainty. However, they are made out of polypropylene and the data does suggest a surface modification which is backed up by the literature [81, 82, 85]. The change in surface morphology appears less extreme for polymer banknotes than for cotton and polypropylene but this could be due to so few samples taken.

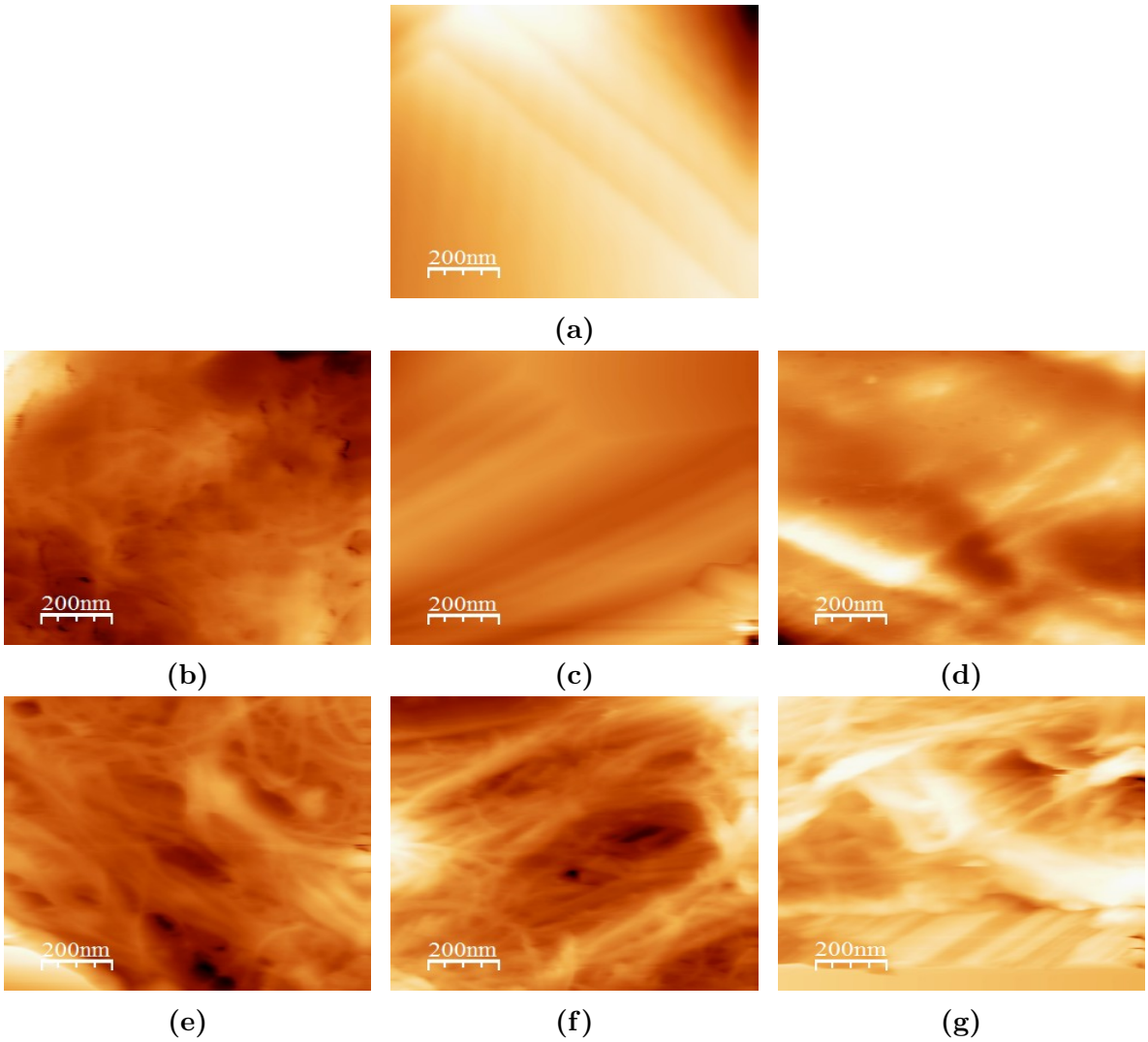

Figure 6.3. AFM topographic representation of cotton paper at 5 μm for different exposure times and plasma sources: (a) cotton paper control, plasma jet treatment: (b) 10 s, (c) 30 s and (d) 60 s and plasma brush treatment (e) 10 s, (f) 30 s and (g) 60 s.

Although some of these results give an indication of surface morphology, further examinations would still be required to be confident that the surface properties do change, especially when there are some outlying results and so few samples. Future research would be required to reinforce the understanding and confidence levels of the effects of the plasma, especially for polymer banknotes. Any future AFM measurements should include roughness measurements as these would give a true representation of the average roughness changes across the surface and despite it being possible to report them here, due to so few repeats, it was determined to be irrelevant. Additional techniques such as FTIR and XPS were conducted to examine the chemical properties of the surfaces to analyse any changes in chemical structures which could lead to a change in surface roughness and wettability.

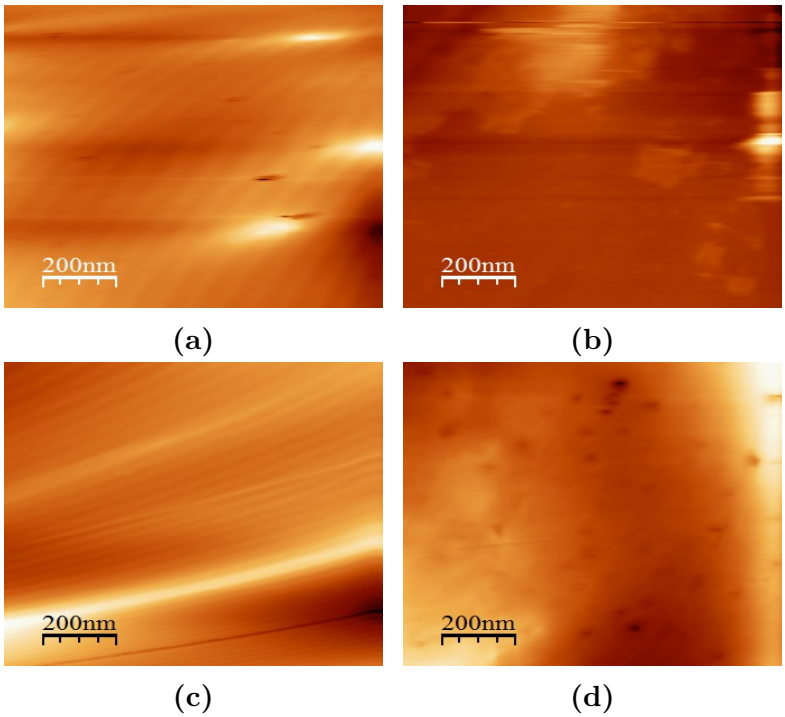

Figure 6.4. AFM topographic representation of plasma-treated polymer banknotes where (a) is the control sample for (b) that has been treated by a plasma jet for 30 s and (c) is the control for (d) which has been treated by a plasma brush for 30 s all measured at a 5 μm scanning region.

It was decided it was worth obtaining this data to gain an insight into what plasma treatment on the surface would do to the surface properties. Unfortunately, due to project budgets, time and cost of analyses, several repeats of each measurement were not obtained. However, if in future these experiments could be repeated, it would allow for erroneous data points to be excluded and a more accurate observation of the surface modifications could take place. An average of several repeats would enable the measurements to indicate whether or not the amount of surface modification is significant in regards to the integrity of the surface and whether the plasma can be regarded as destructive or safe to the surface. Only a few measurements can at best, give an insight into these questions and one can only make an inference with limited certainty.

6.2.3 Fourier-Transform Infra-red Spectroscopy

Fourier-transform infra-red spectroscopy (FTIR) was performed on all of the above mentioned samples as FTIR measures the absorbance of infra-red light at different wavelengths of the functional groups on the surface, allowing a comparison of the characteristics of each sample to be drawn. For polypropylene it is expected that COO- and C=O groups will be seen at 1548 cm^{-1} and 1697 cm^{-1} respectively and a weak broad absorption observed between 3500-3700 cm^{-1} for O-H as a direct result of

plasma treatment [86]. Furthermore, similar absorptions are to be expected for cotton paper as carbonyl and carboxyl groups are also formed at the surface of cotton [87,88].

FTIR spectra for samples of polypropylene (a), cotton paper (b) and polymer banknotes (c) that have been treated by a plasma jet for various times are shown in Fig. 6.5. The absorbances at 2978-2815 cm^{-1}, 1472-1432 cm^{-1} and 1384-1345 cm^{-1} all increase as a direct result of plasma interaction and are likely to be due to C-H, O-H and possibly CH_3 respectively. Furthermore, weak absorbances can be seen at approximately 1553 cm^{-1}, 1643 cm^{-1} and 1728 cm^{-1} due to COO- and C=O, and another weak but broad absorption can be seen at 3460-3115 cm^{-1} characteristic of an O-H group.

Most of the changes in absorbance values occur straight away (i.e. after 10 s) and appear to reach their strongest values at 30 s. This evidence suggests that the plasma has enough energy to modify the surface and create bonds such as carboxyl and carbonyl bonds almost instantaneously. Therefore, it is reasonably safe to assume that any polypropylene or polymer banknote sample that is subjected to plasma for a few seconds is likely to undergo some surface modifications that will lead to an increase in surface bonds and hydrophilicity.

The FTIR spectra of the polymer banknotes are strikingly different from pure polypropylene which may not be a surprise given the inks and other chemicals used to produce a banknote. The majority of the main absorption peaks are the same but the intensities are very different. The absorbance for C-H at 2978-2815 cm^{-1} is much lower than with polypropylene, however, it does still increase after plasma interaction. The weak and broad absorption for O-H at 3574-3144 cm^{-1} is much more visible due to the scale but also shows an increase. Absorbances at 1759-1687 cm^{-1} and 1479-1432 cm^{-1} also increase which correlate to C=O and COO- respectively [89, 90]. The lower absorbance values may suggest that the polymer banknote is more stable than polypropylene which could be a result of a process within the manufacturing or printing stage. However, there is a large difference between polypropylene and polymer banknotes at the lower end of the spectrum which is likely to be due to C-O and C-H groups formed at the surface.

In all the FTIR data obtained in this study, there is a small absorption at 2387-2292 cm^{-1} which is vividly different from the controls, as the controls have a much lower absorption value at this wave number. This absorption appears to be seldom reported however, it is most likely to correspond to a C-N bond.

Finally, the cotton paper results were unsurprisingly very different from the polymer based spectra in 6.6. The cotton paper did not manifest a broad absorption for O-H,

Jet FTIR.jpg

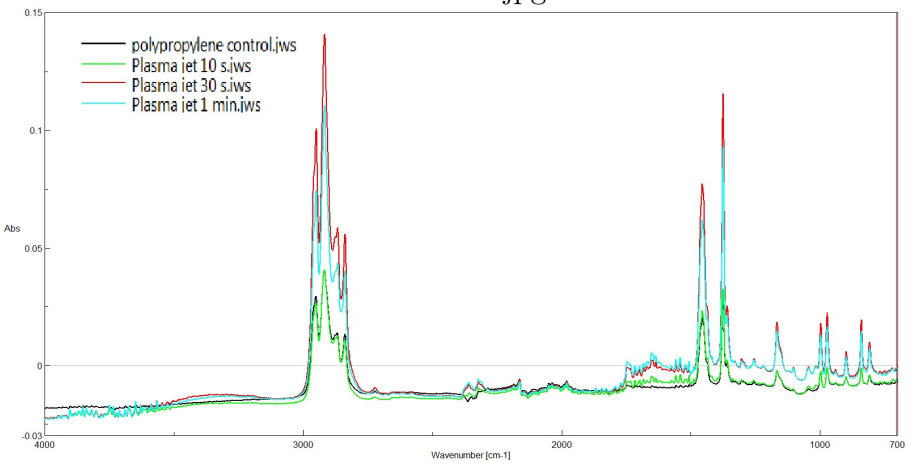

(a)

Brush FTIR.jpg

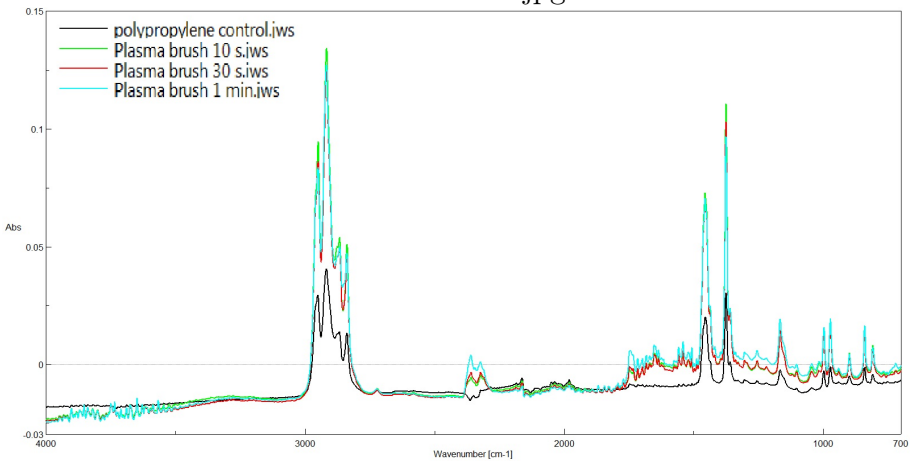

(b)

Banknote FTIR.jpg

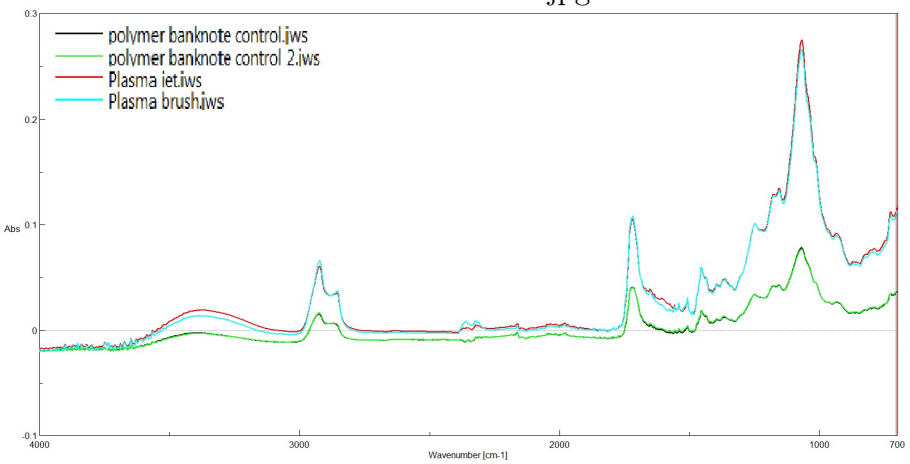

(c)

Figure 6.5. FTIR spectra of polypropylene (a), Cotton paper (b) and polymer banknotes (c) that have been treated with a plasma jet and brush for various lengths of time.

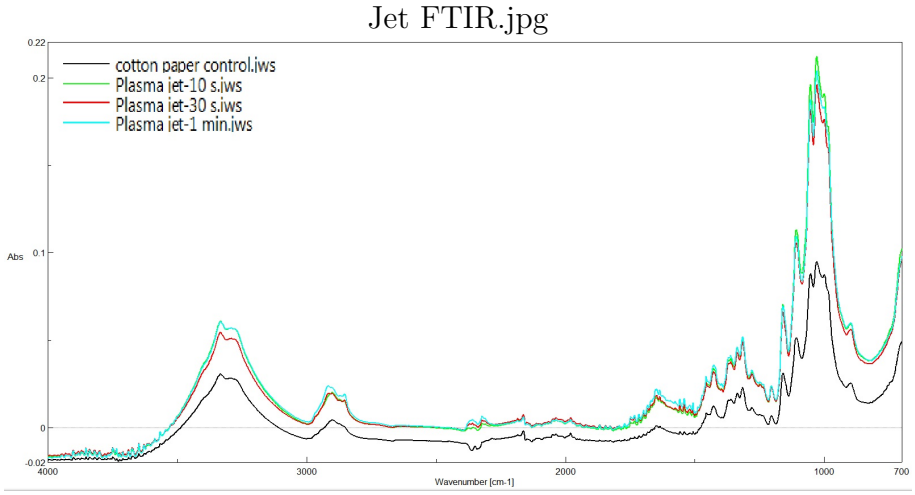

(a)

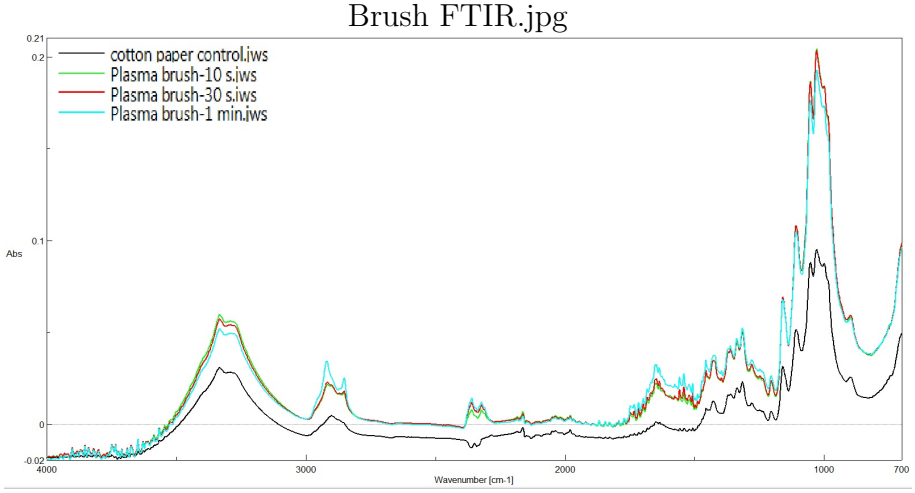

(b)

Figure 6.6. FTIR spectra of cotton paper that has been treated by a plasma jet (a) and a plasma brush (b).

instead it exhibits a strong absorption at 3130-3505 cm^{-1} which is characteristic of the N-H bond. Despite this absorbance, the majority of other absorbances are the same as seen before except for the peak at 1687-1570 cm^{-1} which may also be an N-H functional group. Equally, there is no apparent differences or discrepancies across the plasma source types.

The results obtained by FTIR corroborated what would have been expected from the literature and demonstrate that the plasma does interact with the surface and modifies its properties. As mentioned above, it is unlikely when analysing a polymer banknote for the presence of drugs that the polymer will be exposed to the plasma for any more than a few seconds. However, it is evident that even after 10 s there is significant surface modification. Despite this, the samples do not display any visual degradation or denaturing before 1 minute nor does the surface actually become porous and so it can be concluded that the plasma does not damage the polymer banknote beyond use. A final analysis by x-ray photoelectron spectroscopy was conducted on these samples which should reinforce the understanding of the surface modification.

6.2.4 X-Ray Photoelectron Spectroscopy

The before mentioned studies all aid with the conclusion that the surface properties of polypropylene, polymer banknotes and cotton paper are all modified as a direct result of plasma treatment. Plasma treatment of the surface results in new bonds forming at the surface such as carbonyl and carboxyl bonds. Furthermore, AFM studies suggest that the surfaces increase in roughness and WCA measurements indicate an increase in hydrophilicity. Using x-ray photoelectron spectroscopy (XPS) it is possible to measure the binding energies of the bonds formed and how they differ between non-treated and treated samples. The aim of this study is to look at the $C1_s$ and $O1_s$ orbitals and compare them to the literature [82, 91]. In Figure 6.7(a) it can be seen that an untreated sample of polypropylene predominantly contains C-C/C-H bonds with very little C-O, this is corroborated by current literature [81, 83]. Treated samples of polypropylene such as in Figure 6.7 b) and c) show many more C-O bonds but also the creation of C=O/O-C-O and C=O-O bonds due to plasma treatment which is also reported in the literature [81, 83, 86]. The XPS data for polypropylene also matches the peaks observed in the FTIR spectrum discussed above.

The binding energies of cotton paper that has been treated by a plasma jet and a plasma brush are shown in Fig. 6.8. As expected, the cotton paper results are vividly different to polypropylene as the binding energies of the cotton paper control are very

J B Control XPS.JPG

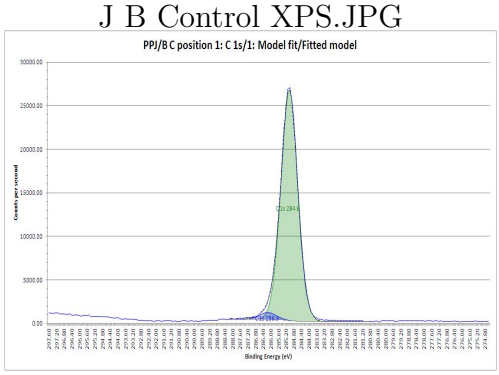

(a)

Jet XPS.JPG

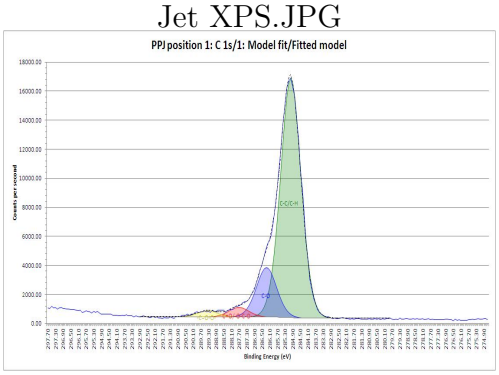

(b)

Brush XPS.JPG

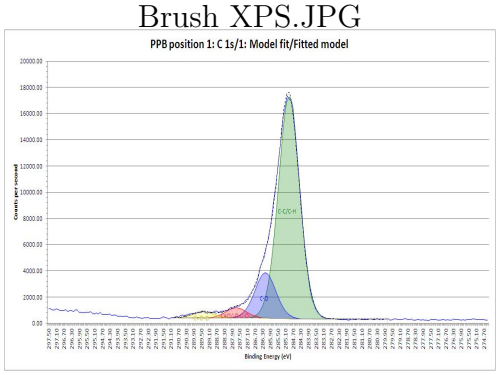

(c)

Figure 6.7. XPS binding energies of a) untreated polypropylene, b) plasma jet treated polypropylene and c) plasma brush treated polypropylene

similar to a treated polypropylene sample with the C-O/C-O-C and C-C-C-H bonds being reasonably similar in intensity. The treated samples of cotton paper display a reduction in the C-C/C-H bonds and increase in both the C=O/O-C-O and C=O-O bonds. For this XPS analysis, only the $C1_s$ and $O1_s$ orbitals were analysed so it does not confirm an increase of N-H functional groups as suggested in FTIR. The current literature suggests that using plasma to treat cotton and textile surfaces does result in a decrease of the C-C/C-H bonds and an increase in C=O/O-C-O and C=O-O bonds, therefore these results are to be expected [84, 92]. The increase in the carboxyl groups at the surface is caused by a break up of fibres and a modification of both physical and chemical properties at the surface of the cotton which helps to explain the AFM images obtained in Figure 6.3.

Finally, the polymer banknote are a difficult surface to analyse. This is because it contains many variations along the surface such as different ink patterns, textures and ridges e.t.c. Therefore, for every measurement (including the previous techniques) a control was used for each measurement taken from the same corresponding area of a second banknote. The results in Figure 6.9 are again very different to the polypropylene due to the various surface types as it is not as homogeneous as polypropylene. It would appear comparing figures a) control and b) for jet treatment that all of the bonds

paper JB Control XPS.JPG

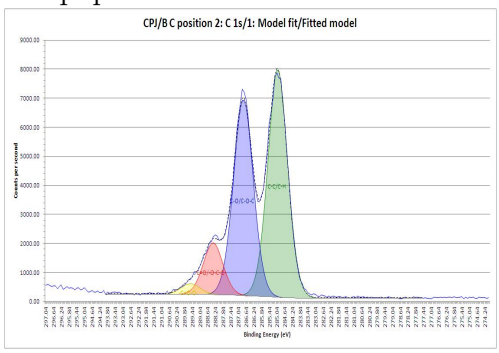

(a)

paper jet XPS.JPG

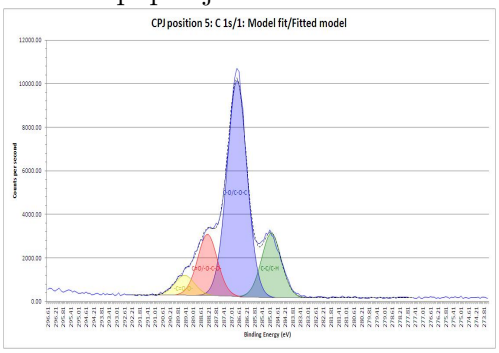

(b)

paper Brush XPS.JPG

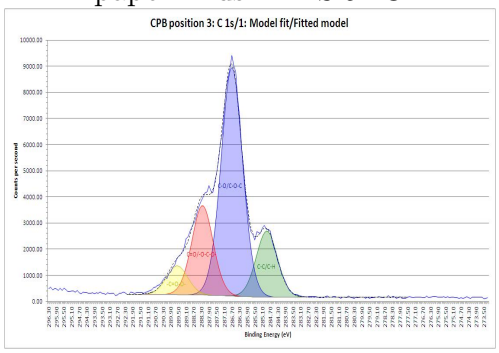

(c)

Figure 6.8. XPS binding energies of a) untreated cotton paper, b) plasma jet treated cotton paper and c) plasma brush treated cotton paper

decrease in intensity after treatment which may suggest other functional groups are being created. The plasma brush data is similar too in that the control is very nearly all C-C/C-H and C-O bonds, but after treatment by the plasma brush, the C-C/C-H bonds are dramatically reduced and although the C-O and C=O/O-C-O bonds are slightly increased, their increase is not significant and does not make up for the loss of the C-C/C-H intensity, suggesting that there are other species generated at the surface that have not been targeted in this study.

The XPS data above confirms all of the other corroboratory techniques used within this study to conclude that the surface properties are modified by plasma treatment. The plasma brush seemed to have a slightly reduced effect in comparison to the jet but this could be due to being operated under exactly the same conditions as the jet but over a larger surface area. Therefore, the helium metastables that are generated in the plasma, are distributed over a larger surface than the jet, resulting in less modification at the local scale.

banknote jet control XPS.JPG

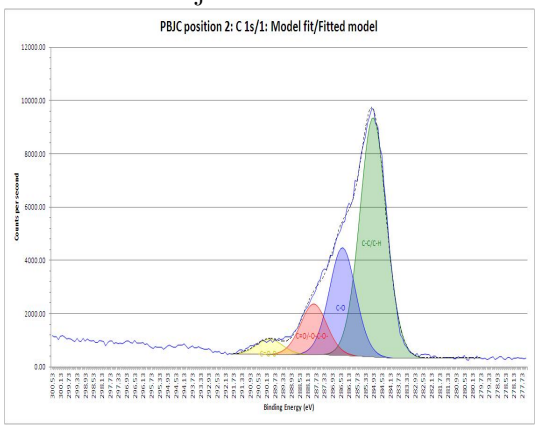

(a)

banknote jet XPS.jpg

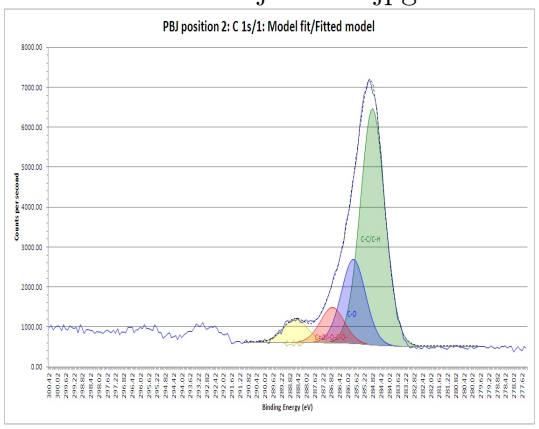

(b)

banknote brush control XPS.JPG

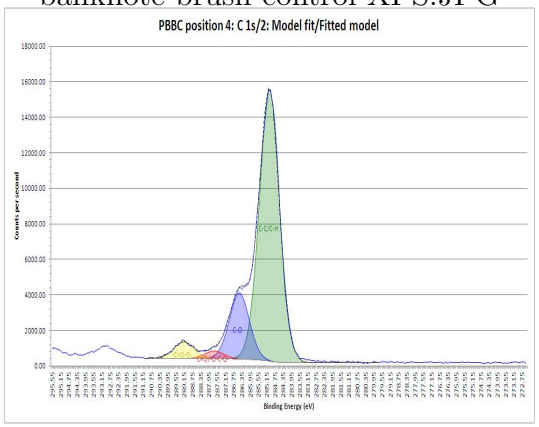

(c)

banknote brush XPS.JPG

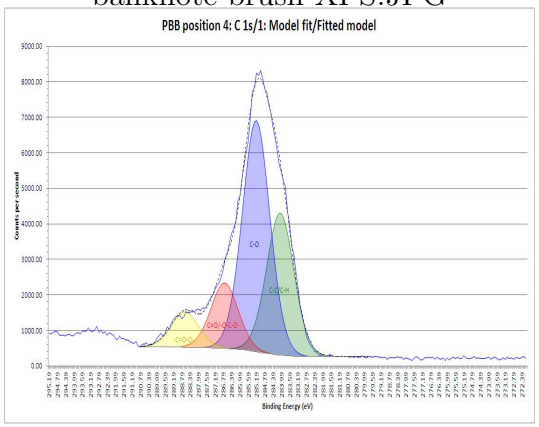

(d)

Figure 6.9. XPS binding energies of a) untreated polymer banknote jet control, b) plasma jet treated polymer banknote, c) untreated polymer banknote brush control and d) plasma brush treated polymer banknote

6.2.5 Conclusions

The data from WCA, FTIR, AFM and XPS confirm that surface properties are modified as a direct result of plasma treatment for polypropylene, cotton paper and polymer banknotes. The surface modification is due to breaking of the bonds at the surface and creating carbonyl and carboxyl bonds to form, these new bonds help to increase the hydrophilicity of the surface. Despite the hydrophilicity increasing, even after 10 minutes of plasma treatment, the samples (with the exception of cotton paper) do not become porous and therefore, the integrity of the polymer banknote would remain intact. Furthermore, degradation of the polypropylene and polymer banknote samples was not visible until at least after 30 seconds of plasma treatment but for drugs on money analysis, the banknote will only be subjected to the plasma for a maximum of 5 seconds.

These results are a good indication that using plasma with the polymer banknotes is safe providing the length of treatment is not significantly greater than 10 seconds.

However, for these results to be definitive, further research including several repeats of each sample would be required to eliminate any erroneous data points. Finally, it would be useful to conduct this research with the dielectric barrier discharge (DBD) ionisation source that is discussed in section 7 as this source operated in air instead of helium, at a higher temperature and the sample is exposed to the powered electrode.

The above surface measurements reflect the literature in that plasma treatment results in a modification to the surface which is especially important for applications where a hydrophobic or hydrophilic surface is required as plasma treatment may have adverse affects on that surface. Furthermore, the surface modification may be of interest to an application where it would be ideal for the surface properties to be modified. For the application of drugs on money, these measurements were important to indicate if the surface properties change on the banknote as this may reduce the lifetime of the note, or even effect the mechanism of how the banknotes are contaminated with drugs in future once they are reintroduced into general circulation.

Chapter 7

Development of a Surface Barrier Discharge Ionisation Source

This chapter will describe the development of a surface barrier discharge to a Technology Readiness Level-4 (TRL) prototype, detailing the design modifications made over the course of the project.

7.1 Introduction

The plasma brush and plasma array did not appear to be sufficient as an ionisation source for the application of drugs on money and explosive detection and so it was decided to see whether it was possible to couple a surface barrier discharge (SBD) with a mass spectrometer. The SBD was designed in the form of a plasma actuator. A plasma actuator, as described in section 3.1.4, usually consists of two offset electrodes (one driven and one ground) separated by an insulating dielectric barrier. The discharge caused by applying a high-voltage AC signal across the powered electrode ionises the molecules in the ambient air surrounding the electrode and accelerates them through the electric field, resulting in a chordwise ionic wind consisting of electrons, ions and neutrals as shown in Fig. 3.5.

Typically, plasma actuators were developed for aerodynamic flow control largely due to the lack of mechanical parts, but they are considered for many other applications typically considering flow control. While dielectric barrier discharges such as plasma jets and low temperature plasma probes have been used previously with mass spectrometry, plasma actuators are seldom coupled with mass spectrometry. Therefore, the use of a plasma actuator or surface barrier discharge with mass spectrometry is a novel application.

7.2 Development Stages of a Surface Barrier Discharge Ionisation Source

As a plasma actuator had not been used with mass spectrometry before, it was important to prove that a) the plasma actuator would work as an ionisation source, b) that it would be possible to safely harvest the ions generated and detect them within the mass spectrometer and c) that more than one pair of electrodes could be used to increase the sampling surface area. The initial proof of concept was performed by applying a pair of electrodes to a piece of ceramic to ensure that plasma was formed at the surface and a chordiwise ionic wind was induced. The simple form of a plasma actuator worked and therefore, it was important to couple it to a mass spectrometer.

To enable integration with a mass spectrometer, an old electrospray ionisation source was disassembled and modified to allow for a plasma actuator to be aligned with the orifice of the mass spectrometer. Following this quick experiment, positive background ions were detected suggesting that the plasma actuator was capable of ionisation and transporting them into the mass spectrometer. However, the intensity of the ions were low and the surface area of the plasma was much smaller than desired. To overcome a smaller surface area, sheets of mica (100 x 100 x 0.15 mm) were obtained to use as the dielectric barrier between the electrodes as mica has a very good dielectric constant.

As the application was to either analyse swabs for explosives or banknotes for drugs, the design was based on an existing thermal extraction ion source (TEIS) previously used by Mass Spec Analytical Ltd [29]. In Ebejer *et al*, two heated brass blocks (separated by 4 mm) are used to thermally desorb and volatilise drugs molecules on the surface before drawing them through a transfer line into an atmospheric pressure chemical ionisation (APCI) needle where the molecules are ionised before entering the mass spectrometer for detection [29]. Three pairs of electrodes (three actuators) were attached to the mica and another sheet of mica was made up to be an exact copy of the first. The sheets were then separated by 4 mm using fibre washers but with the powered electrodes on each mica sheet facing one another as if a mirror image.

As the powered electrodes were facing each other, when the plasma formed on the surface of each mica sheet and induce a chordwise ionic wind, the two sheets created a wind tunnel in the direction of the ground electrode. The mica sheets were then placed on top of the old electrospray front end to allow integration with the mass spectrometer. The mica SBD ionisation source can be seen in Fig. 7.1. Plasma forms on each mica sheet within the gap between both sheets creating a sampling surface area greater than 500 mm ^{2}. Plasma actuators in this format have never been seen with mass spectrometry

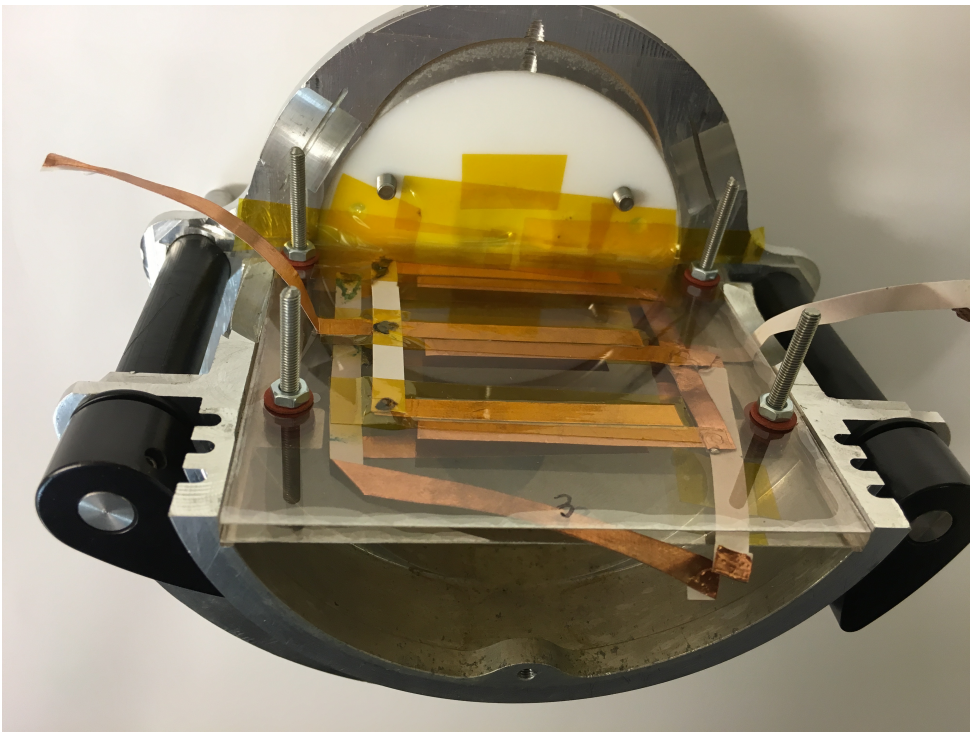

Figure 7.1. Early SBD prototype coupled with mass spectrometer on a modified electrospray ionisation source.

and therefore, this application is completely novel, leading to a British patent application No. 1717618.1.

It can be seen in Fig. 7.1 that there was a PTFE disc that has a 5 mm orifice which when attached, was directly aligned with the curtain plate and mass spectrometer orifice. However, it appeared that the PTFE orifice caused some issues especially for negative ions. The SBD was capable of a high intensity of positive ions and could even detect cocaine from polypropylene as shown in Fig. 7.2, but very few ions could be detected in negative ion mode.

The lack of negative ions was likely due to the PTFE orifice as it may have built up a static charge, a hypothesis that was confirmed by lining the orifice with aluminium foil which was connected to ground. Negative ions were then detected with the mica sheets and the positive ion background intensity was increased by an order of magnitude. The signal intensities can be seen in Fig. 7.3. There are fewer ions seen in the negative ion background but they are of larger intensity than the positive ions suggesting that the SBD ionisation source would be very capable of the detection of ions in both positive and negative ion modes.

The electrode design was arbitrarily chosen to be straight due to ease of application and the copper tape was bought as a 10 mm wide strip. However, it is thought that as

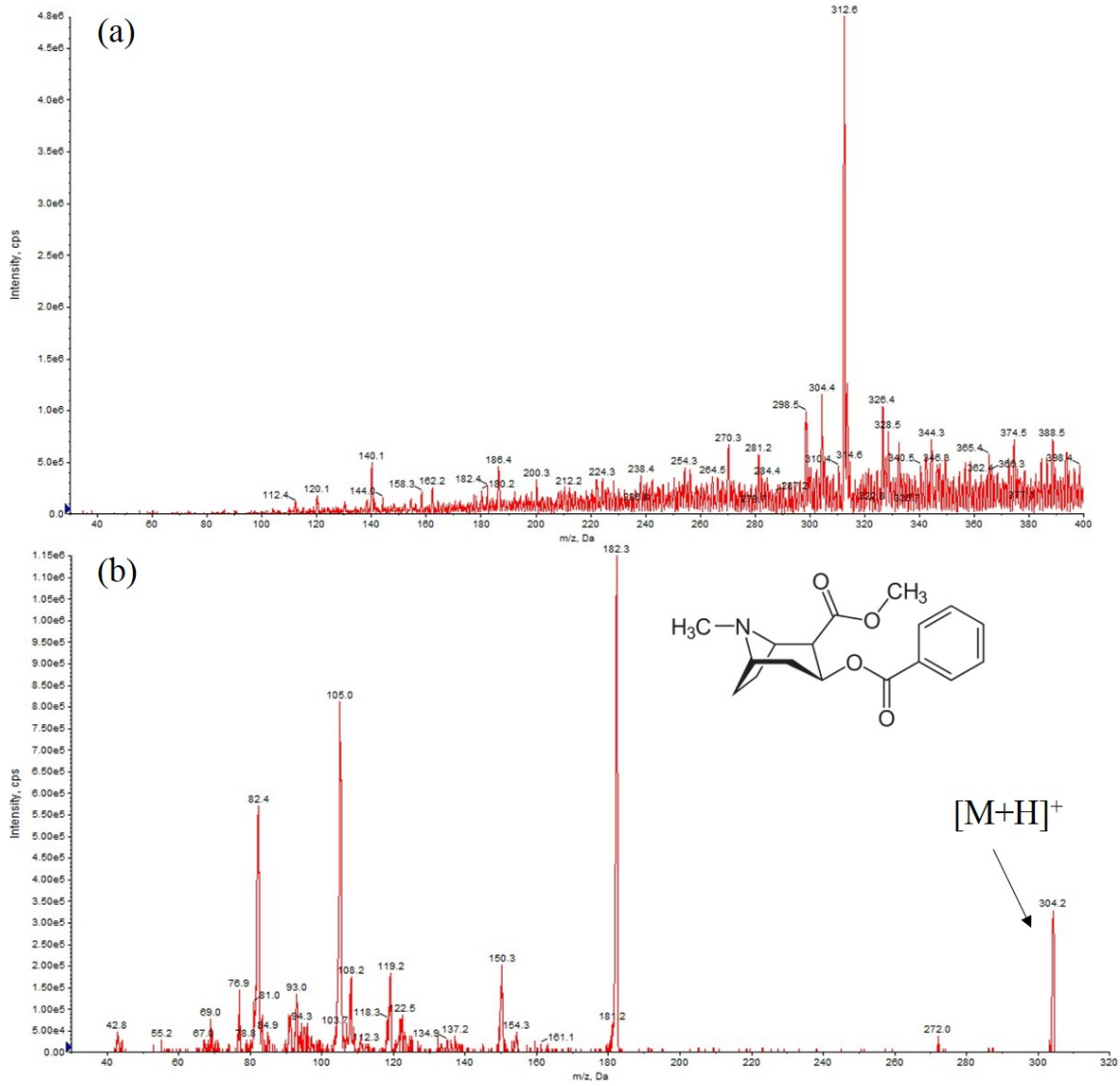

Figure 7.2. Mass spectra of positive ions in ambient air using an SBD ionisation source (a) and a product ion scan for cocaine (products of m/z 304 for $[M+H]^+$) with characteristic product ions at m/z 182 and 105 (b).

the ionic wind travels in the direction of the electrodes, the electrodes could be designed to focus the ions towards the orifice which may lead to an increase in sensitivity. To explore this, a comparison was performed between straight/linear electrodes as described and chevron shaped electrodes. The chevron electrodes were made from the same 10 mm wide copper tape and cut to 5 mm as before, except they were cut to include a chevron shape which can be seen in Fig. 7.4.

The comparisons between the electrodes consisted of measuring the ion intensity that was detected in the ambient air (background) in a Q1 scan and also by performing cocaine detection from a polypropylene surface using a selected reaction monitoring (SRM) method. These provided contrasting results as the background for the straight

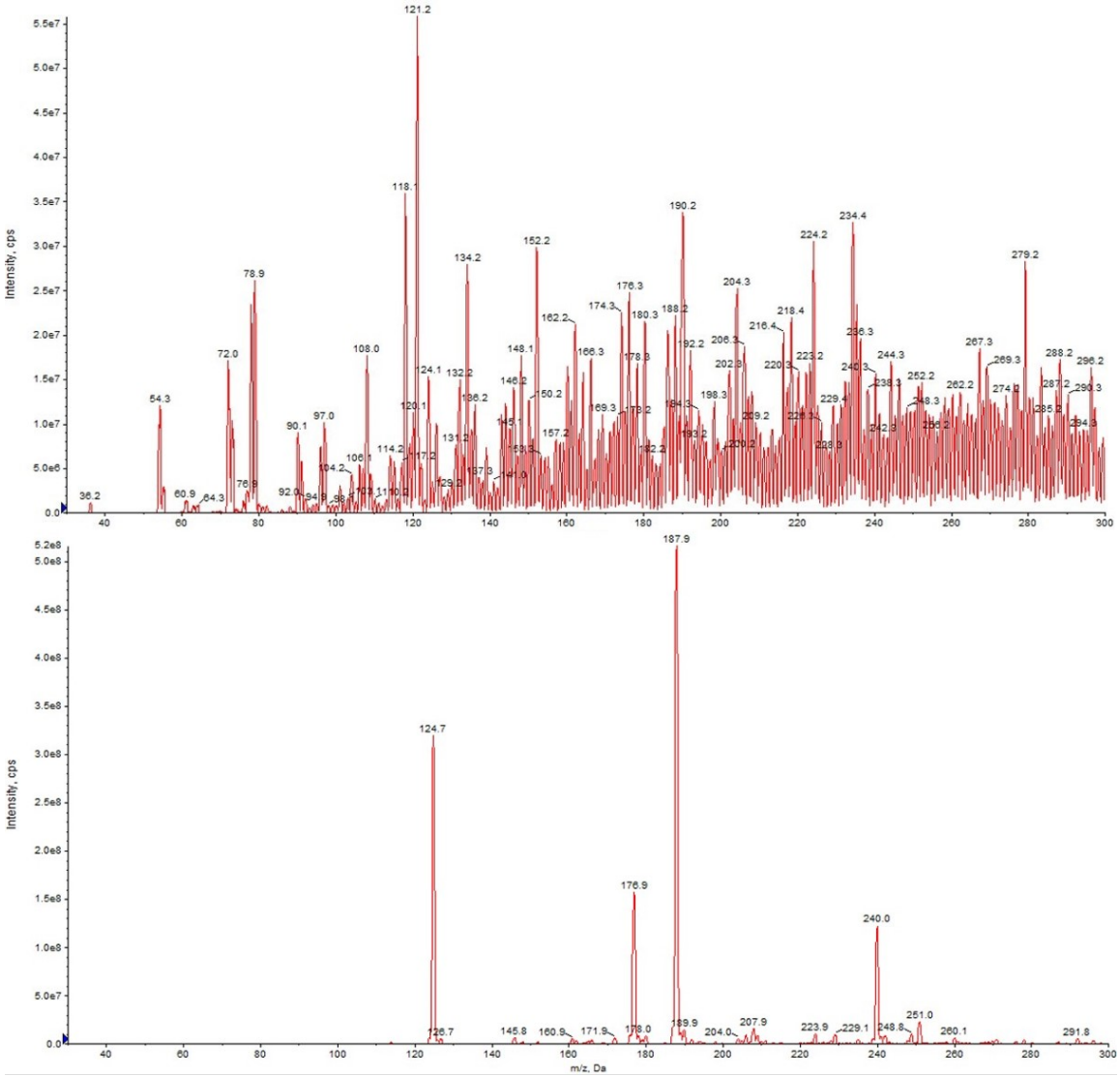

Figure 7.3. Mass spectra of a background scan of ambient air in positive ion mode using an SBD ionisation source showing an abundance of positive ions (a) and a background scan of ambient air in negative ion mode showing some of the nitrates generated in the plasma at m/z 125 and 188 (b).

electrodes was significantly higher but the sample detection of cocaine was significantly worse. There are several contributing factors that are likely to explain this. Firstly, the chevron angles were not optimised to direct the ions towards the mass spectrometer and the angles of the chevrons were likely to be so extreme that the ions were directed across the orifice. This may have resulted in a crossover of chordwise ionic winds from either side of the electrodes, resulting in additional, unwanted collisions of the ions forcing them to lose their charge resulting in a lower intensity background spectrum.

Secondly, the increased signal intensity for cocaine with chevron electrodes could be down to the nature of the electrode shape. As the electrodes are a chevron shape, there are a few sharp edges where the electrodes bend and the electric field is stronger

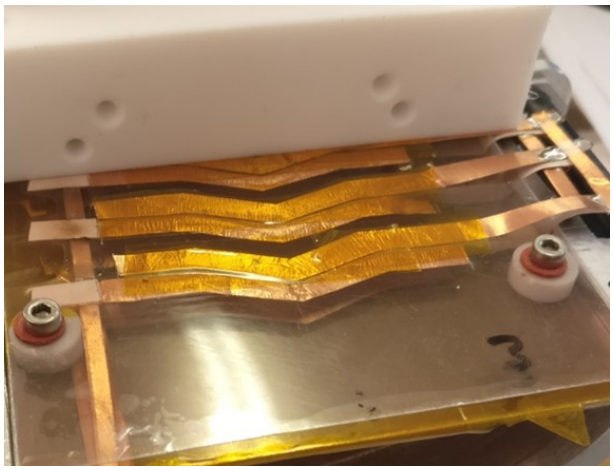

Figure 7.4. Image showing the chevron shaped electrodes used to compare against straight electrodes.

at sharp edges due to a higher density of electrons in a short space, resulting in a much hotter plasma. The heat of the chevron electrode SBD ionisation source is much greater than the straight electrode version, and will be more capable of thermal desorption. An increase in desorption from the surface will lead to a higher amount of molecules that can be ionised and therefore a higher intensity.

Although the sensitivity was greater for a sample with the chevron electrodes, the temperature increase was too great and would have resulted in permanent damage to a surface such as polymer banknotes and therefore, would not be suitable for the application. However, in future it would be beneficial to either experimentally or theoretically (using modelling and simulations) vary the electrode shape and angles to focus the ions into the mass spectrometer, but also find a more suitable and reproducible way of manufacturing the electrode which should result in a more capable SBD ionisation source. This unfortunately was not possible due to time and budget restraints but would be scope for future research. Straight electrodes were used in this project following these experiments, largely because the novelty of the ionisation source lies with the integration of the SBD to the mass spectrometer and the detection of analytes, but also because they are much easier to reproduce reliably.

As further experiments were undertaken, it was quickly realised that mica was not a suitable substrate to be used in the application as the dielectric. Mica is a silicate material with a layered structure making it relatively soft and flexible, especially when subjected to heat. The heat of the plasma and the electrodes was enough to cause the mica to bend over a short operation time (less than 2 minutes). The bending of the mica was a concern because it meant that the two sheets would get too close to one another,

causing arcs between the powered electrode on one sheet and the ground electrodes on the other. Further, the bending of the bottom sheet caused a blockage of the orifice preventing any ions from entering the mass spectrometer. Additionally, the layered structure resulting caused flaking or delamination of the mica resulting in an uneven surface with air gaps and possible changes to the dielectric strength and gaps between the electrodes.

To overcome the issues presented by using mica, alumina was obtained to be the dielectric. Alumina was chosen because it has a higher dielectric constant, is relatively cheap and is much more rigid than mica. Quartz would have been great from a commercial point of view as its transparent nature would allow the plasma to be visible. This would be aesthetically pleasing and safer for an end user. However, quartz is much more expensive and brittle so would cost a lot more to replace if it were to be dropped or broken. The mica sheets were only 0.15 mm thick which is partially due to their layered structure and ease to manufacture, but it was decided that the alumina would be 0.5 mm thick. As alumina is quite brittle, it would be more difficult to manufacture much thinner than 0.5 mm but also, the extra thickness would allow for better heat insulation preventing the plasma from becoming too hot for a polymer banknote.

As there was no injection port and it would not be possible to use a metal syringe tip due to the exposed powered electrodes, a sample could not be directly injected into the source. Instead, samples were spotted onto a glass slide and allowed to dry (or the solvent to evaporate) before swabbing it and analysing the swab by inserting it directly into the plasma. Consequently, it was important to determine what swabbing media would be best to render the highest level of sensitivity. A study of the intensity of cocaine swabbed from a glass slide at the same concentration with various swabbing media was conducted with the following materials: polypropylene, cotton paper, shark paper, PTFE, Nomex and Teflon coated fibreglass.

Polypropylene was considered to be the best swabbing medium due to its smooth surface and therefore, liberation of the sample occurred in a much shorter space of time resulting in a short sharp peak of high intensity. Textile based swabs resulted in broad peaks of lower intensity suggesting that polypropylene would be best to achieve the highest limits of detection. In an operation context it may be beneficial to sacrifice sensitivity and use a textile based swab as their collection efficiency is likely to reflect the make-up of their matrix (pores and fibres etc.). Also, the desorption rate is less efficient in comparison to polypropylene allowing the potential for the swab to be subjected to more than one type of analyses as after the first analysis it is very likely that some sample will remain on the swab after the first analysis.

It is interesting that polypropylene was the more efficient swabbing medium as polymer banknotes are made from polypropylene, so any analyses that could be conducted with polypropylene swabs should in theory, be suitable for polymer banknotes too. This evidence suggests that the plasma would be suitable for the analysis of polymer banknotes if it was capable of detecting analytes from polypropylene without inflicting too much damage.

Alumina was used as the new dielectric layer and a new prototype front end was built to replace the old electrospray housing. The entire housing was made from aluminium so there would no longer be an issue with the transportation of negative ions, the whole housing would be safely grounded and also, the distance the ions would have to travel from plasma to mass spectrometer by making the orifice plate much thinner. The reduction of the distance the ions had to travel did result in a slight improvement in signal intensity but not a significant increase; this led to another hypothesis that it could be possible that the ions are still losing their charge through collisions in the air and through forming clusters. Consequently, this hypothesis had to be proved or disproved before establishing limits of detection, because if the hypothesis were to be true, it would have a significant negative impact on the limit of detection.

In an attempt to establish whether or not the distance between the plasma ionisation region and the mass spectrometer was too great; the SBD was coupled with a custom-made plenum chamber by removing the brass blocks used in the TEIS source previously described [29]. Although it will have inevitably increased the distance between the plasma ionisation region and the mass spectrometer, the APCI needle was not removed and was used as a post-ionisation source to ionise any ions that had lost their charge and break up any clusters that may have formed. The plenum chamber was 70 mm in depth from the SBD to the curtain plate of the mass spectrometer.

The introduction of a plenum chamber and APCI needle had a significant positive impact on the intensity of the ions detected and it was decided that the APCI needle was integral to the success of being able to detect ions with a reasonable level of sensitivity. Firstly though, it was important to ensure that the SBD itself was forming the ions. To satisfy this, the SBD was coupled with the molecular beam mass spectrometer (MBMS) because, as described in section 4.2, the MBMS has no internal ionisation source or sample pump meaning that if any ions are detected, the SBD itself is responsible for the ionisation and also the transportation of the ions via its chordwise ionic wind.

The negative ion data for the SBD on the MBMS shows two dominant peaks for m/z

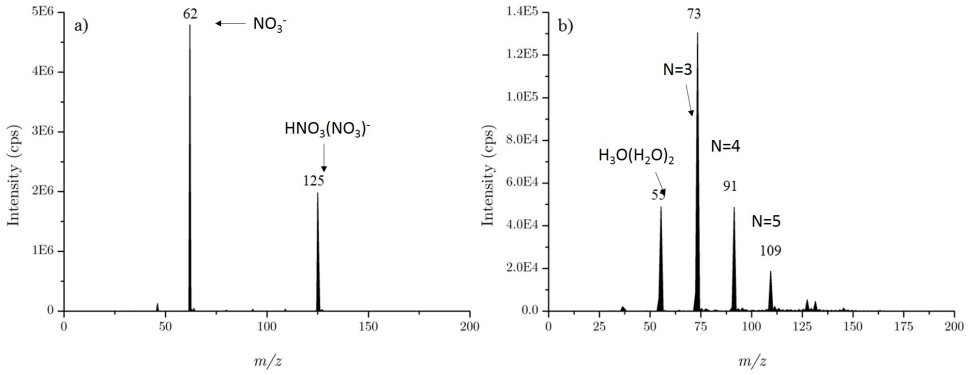

Figure 7.5. MBMS data of negative ions showing the nitrate ions generated at *m/z* 62 and 125 (a) and positive ions formed within the plasma from interaction with the ambient air mainly composed of water clusters of $[H_3O(H_3O)_n]^+$ starting from *m/z* 55 for $[H_3O(H_3O)_2]^+$.

62 and 125 ions in Fig. 7.5(a), presumed to be NO_3^- and $[HNO_3(NO_3)]^-$ respectively. The intensity of the NO_3^- ion is orders of magnitude higher than it was with the plasma jet in Fig. 7.6 and in both the positive and negative ion data for the SBD, the majority of ambient air peaks such as oxygen, nitrogen and argon are diminished when compared to the plasma jet data in Fig. 7.6. The positive ion data from the SBD largely consists of water clusters for $[H_3O(H_2O)_n]^+$, where n= 2, 3, 4 and 5 respectively at *m/z* 55, 73, 91 and 109, shown in Fig. 7.5(b). The presence of these water clusters could be important in the protonation of molecules in positive ion mode as the main precursor ion detected is $[M+H]^+$ [38].

This experiment with the MBMS demonstrates that the SBD is capable of ionisation on its own without the APCI needle and additionally, the SBD is capable of transporting ions into the mass spectrometer without the need for suction towards the mass spectrometer. Furthermore, it is possible to suggest that the ionisation mechanisms are slightly different to the plasma jet, but it is important to take into account that different gases were used i.e. the plasma jet uses helium and therefore largely consists of helium metastables $[He^*]$. The helium metastables are largely responsible for the liberation of the sample from a surface in a plasma jet, suggesting that it is likely that molecules are not desorbed from the surface as a result of thermal desorption (as the temperature of the SBD is less than 100 ^oC), but from other excited species in the air (as a result of plasma interaction) through a transfer of their potential energy to the surface [14, 34, 60, 65].

An SBD consisting of linear/straight electrodes was considered as the final design for the rest of this project but with further research it is likely that straight electrodes are not optimum. If the electrodes were to be manufactured in such a way that they were reproducible every time, without introducing errors or sharp edges, then it is likely that

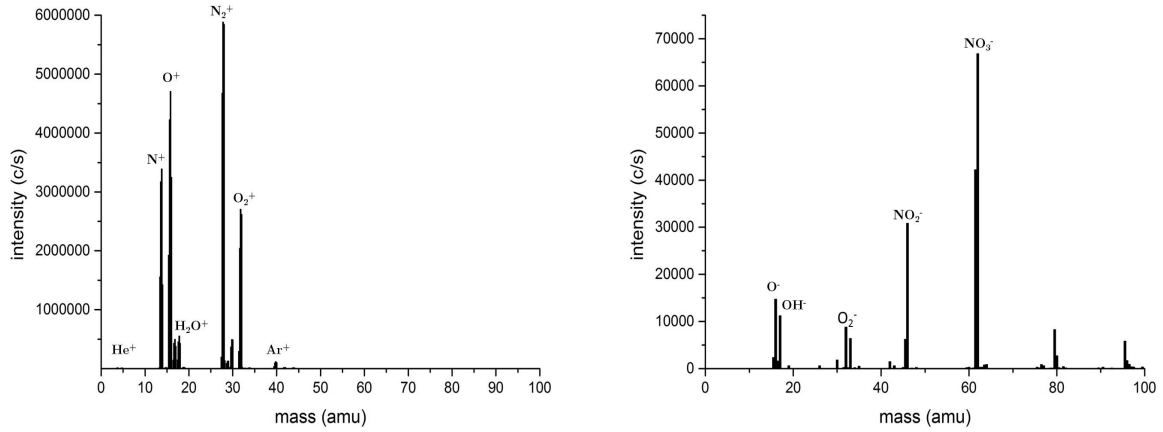

(a) **(b)**

Figure 7.6. Mass spectra acquired for ions generated in ambient air with a plasma jet couple to an MBMS in positive mode for the signal intensity (a) and the negative ion spectrum for intensity (b).

the electrodes would be better if curved towards the orifice. Simulations or modelling of the ionic wind produced in the SBD may be considered the best way to decide what shape would be best for the electrodes. As the amount of variables is so great, to do it experimentally would be too time consuming and costly. It is presumed that parabolic shaped electrodes would provide the optimum design as the front electrodes would probably require a steep curve to focus towards the orifice, whilst the other electrodes would require a much reduced curve.

The electrode design has many limitations that future development would overcome. A lot of the limitations stem from the use of the adhesive copper tape. The copper tape is readily oxidised by the plasma and after a short while, the copper starts to discolour and become soiled. Further, the adhesive used to secure the electrodes spoils under the heat resulting in the copper tape lifting from the surface of the alumina, creating air gaps and the concern of possible arcing. Finally, as the SBD is used for swab and banknote analysis, the thickness of the tape can cause the swab to snag and become caught in the electrode. In an attempt to overcome this issue, an experiment to sputter the electrodes by thin film deposition of tungsten on to the surface of the alumina via a low pressure magnetron was attempted. This process involves a low pressure magnetron containing a tungsten target and a helium based plasma. When the plasma ignites, the helium atoms bombard the tungsten surface causing the tungsten to break off. When there are other surfaces within the magnetron, such as alumina, the tungsten particles are then deposited onto the surface in a process called sputtering.

The thickness of the tungsten after sputtering onto a surface can be a few microns

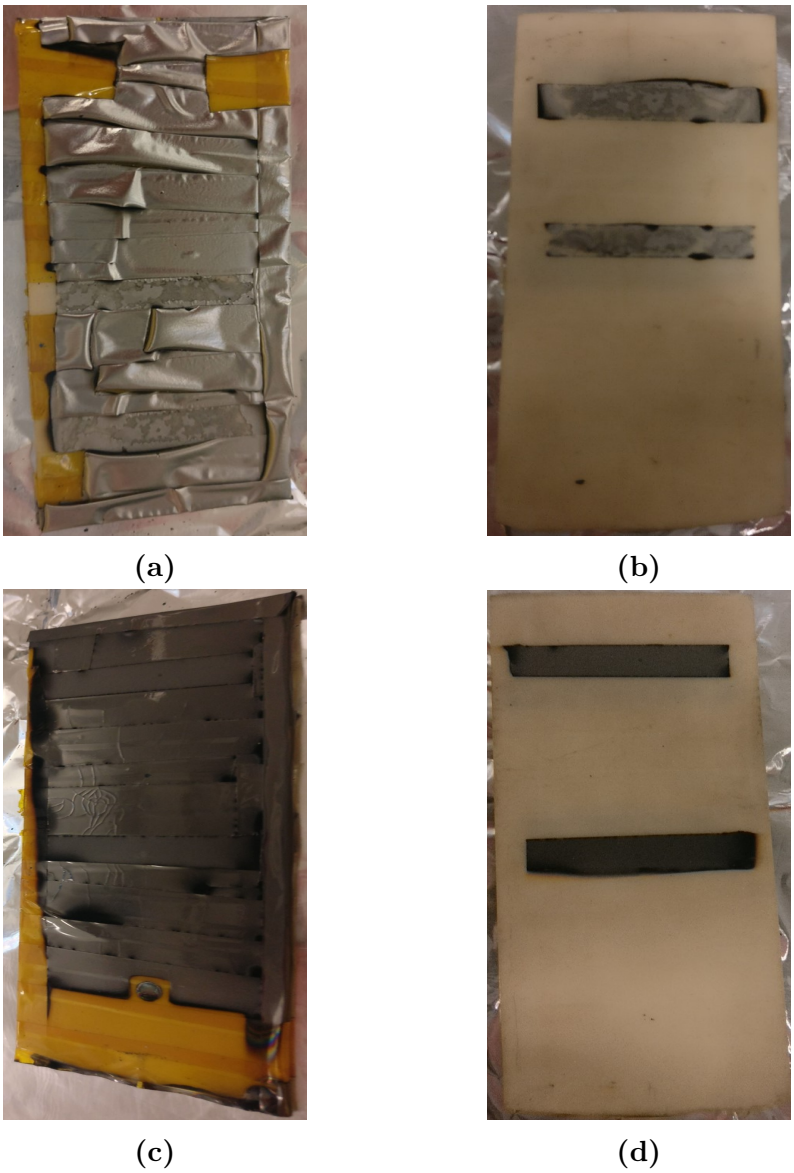

(a) **(b)**

(c) **(d)**

Figure 7.7. Alumina with Kapton tape wrapped around to form electrodes in lower power with helium (a) with the resulting sputtered electrodes with Kapton removed (b), and higher power with argon (c) with the resulting sputtered electrodes with Kapton tape removed (d).

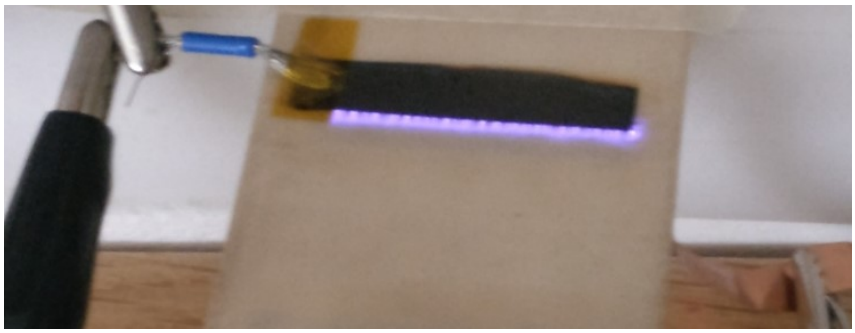

Figure 7.8. Plasma formed at the surface of alumina using sputtered electrodes from Fig. 7.7 (b) and (d).

and therefore overcoming the snagging problem. Also, sputtering circumvents the need for an adhesive and tungsten oxidises much less than copper which should prolong the lifetime of the electrodes. This process was attempted at the University of Liverpool by using a piece of alumina that had been pre-covered with Kapton tape so that only the exposed surface of the alumina would become sputtered, and the Kapton tape would protect the rest of the surface. Unfortunately however, this was an untested experiment and the parameters chosen were arbitrary and so the resulting electrodes were not likely to be the best result possible. The results of sputtering under various conditions can be seen in in Fig. 7.7 where (a) was obtained at higher pressure with helium (16.28 mTorr, 50.6 sccm (helium), power 100 W, 314 V, 0.32 A for 2 hours), (c) at lower pressure and with argon (6.8 mTorr, 28 sccm (argon) 400 W, 426 V, 0.94 A, 2 hours 5 minutes). Figures 7.7 (b) and (d) are the resulting electrodes once the Kapton tape was removed.

The sputtered electrodes at a higher temperature and lower pressure were unfortunately not suitable to be used as an electrode as the tungsten did not adhere to the alumina very well, and air bubbles occurred causing arcing. The electrodes in Fig. 7.7 (b) and (d) however worked sufficiently as an electrode, as the deposited tungsten was very smooth, adhered well to the surface and was also very thin. These electrodes are demonstrated in Fig. 7.8, where an AC high voltage was applied to them, and a copper adhesive electrode was used as a ground on the reverse, to produce a plasma on the surface of the alumina. This experiment suggests that alternative methods such as sputtering may be suitable to improve the design and composition of the electrodes and potentially with the use of a template, provide a much more reliable method of applying electrodes to the alumina.

7.3 Obtaining the Power Dissipated Within a Filamentary Mode Dielectric Barrier Discharge

The power measured using Ohm's law equation P = I x V (where P = power, V voltage and I = ampere) would result in a mass of errors as these measurements do not take into account the many losses within the SBD/DBD such as capacitance. Therefore, it is important to measure the power that is dissipated in the plasma itself as opposed to the whole circuit. In order to measure the power that is dissipated in the DBD, the capacitance of the DBD (Cdbd) is estimated by using the area and number of the electrodes and in this case, each dielectric sheet contained 5 electrodes. The length of all electrodes was 60 mm and the overlap between the powered electrode and ground electrode on either side was 1 mm, represented in Fig. 7.10. Therefore, the capacitance can be calculated by,

$$\frac{1}{C_{dbd}} = \frac{1}{C_{alumina}} + \frac{1}{C_{alumina}} + \frac{1}{C_{air}} \tag{7.1}$$

Where C = capacitance and alumina is the dielectric surface

$$C_{alumina} = \frac{\text{Dielectric constant of alumina (k) x permittivity } (\epsilon)}{\text{thickness of dielectric (meters)}} Area \tag{7.2}$$

Where dielectric constant of alumina (k) =10, ϵ = 8.85 x 10^{-12} farad per meter (F/m), thickness of the dielectric is 0.5 mm in metres, resulting in:

$$C_{alumina} = \frac{10 \text{ x } (8.85 \text{ x } 10^{-12})}{0.5 \text{ x } 10^{-3}} Area \tag{7.3}$$

For C_{air} where the air gap of 3.5 mm creates a capacitive effect:

$$C_{air} = \frac{1 \text{ x } (8.85 \text{ x } 10^{-12})}{3.5 \text{ x } 10^{-3}} Area \tag{7.4}$$

The area was calculated by,

$$Area = \text{(electrode overlap (m)) x (length of electrode (m)) x (number of electrodes)} \tag{7.5}$$

Where there were 5 electrodes with an overlap of 1 mm and the length of each electrode was 60 mm, the area is calculated by:

$$Area = (1 \text{ x } 10^{-3}) \text{ x } (60 \text{ x } 10^{-2}) \text{ x } 5 \text{ m}^2 \tag{7.6}$$

Therefore,

$$C_{alumina} = 5.31 \text{ x } 10^{-11} \text{ F, and } C_{air} = 7.59 \text{ x } 10^{-13} F \tag{7.7}$$

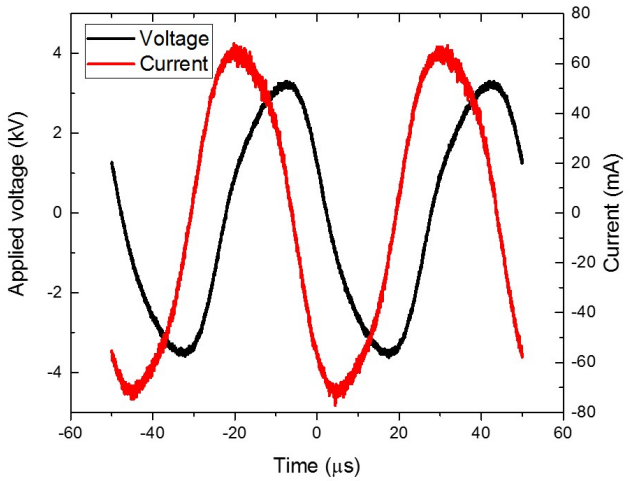

Figure 7.9. Applied voltage and measured current through the DBD circuit with the filamentary current being shown at the top and bottom of the current duty cycles.

The capacitance of the DBD is calculated by,

$$\frac{1}{C_{dbd}} = \frac{1}{5.31 \text{ x } 10^{-11}} + \frac{1}{5.31 \text{ x } 10^{-11}} + \frac{1}{7.59 \text{ x } 10^{-13}} \tag{7.8}$$

Which is equal to

$$C_{dbd} = 1.36 \text{ x } 10^{12} F \tag{7.9}$$

The collection of coefficients is the overall capacitance of the DBD which is the inverse of the elastance matrix, calculated by,

$$C_{inv} = \frac{1}{1.36 \text{ x } 10^{12}} = 7.38 \text{ x } 10^{-13} = 0.74 \text{ pF} \tag{7.10}$$

A 10 nF capacitor and a 1 kΩ resistor was situated on the ground path of the DBD. The peak current through the circuit was measured at 80 mA, resulting in a peak voltage drop of 80 V for an applied peak-to-peak voltage signal and therefore, the voltage drop is insignificant compared to the total applied voltage. The resistor was inserted to provide a resistor-capacitor time constant (10 μs) in an effort to smooth the discharge current fluctuations caused by the filamentary mode plasma within the DBD, as shown in Fig. 7.9. A schematic representation of the resulting circuit is shown in Fig. 7.10.

The value of the capacitor used in the circuit, 10 nF, was more than 10,000 times greater than the capacitance in the DBD, 0.74 pF. The power of the circuit was measured via a Lissajous plot 7.11. The charge on the capacitor, Qm, was calculated as the product of Cm and Vm where Vm is the voltage measured across the capacitor and Cm is the

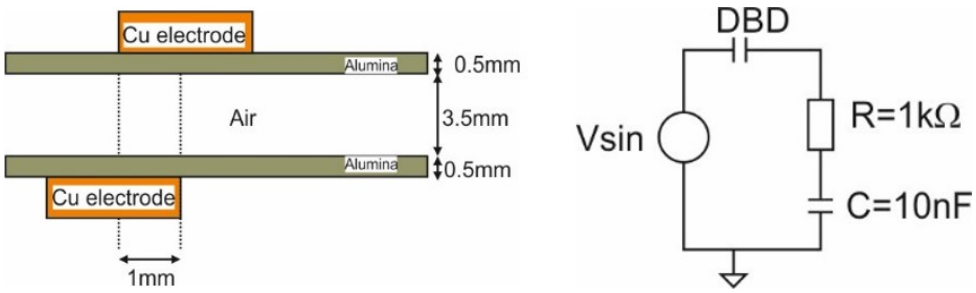

Figure 7.10. Figure showing the schematic of the DBD (left) and schematic of the measurement circuit.

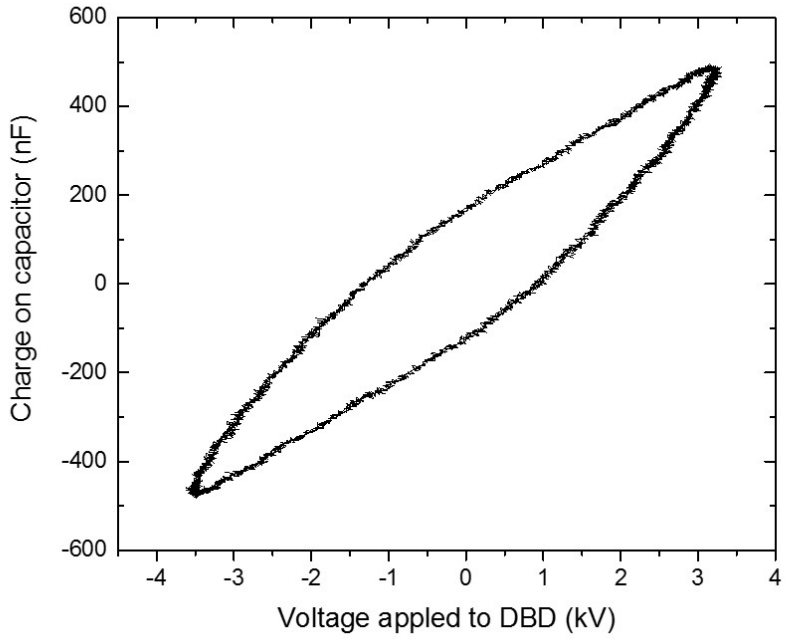

Figure 7.11. Lissajous plot of Voltage (kV) measure across the DBD against the charge on the capacitor (nF).

value of the capacitor (10 nF). The values of Qm were averaged over 3 measurements and each measurement was obtained 10 minutes apart.

The power is equal to:

$$Power = \frac{1}{\mathrm{T}} \int_0^T V_{app} dQm \tag{7.11}$$

Or the area in the Lissajous plot multiplied by the period, i.e. 20 kHz [93, 94]. Using the current and voltage measurements alone from Fig. 7.9, the RMS voltage and current are equal to 3.4 kV and 46 mA respectively, resulting in a power of 110 W. The measured current is composed of a displacement current and the plasma discharge current. Assuming

that the DBD Capacitance is 0.74 pF, and

$$Displacement(i) = C\frac{\mathrm{dV}}{\mathrm{Dt}} \tag{7.12}$$

Where the C is the capacitance (0.74 pF), and dv/dt is the instantaneous rate of voltage change (volts per second)

$$V(t) = V_o sin(wt) \tag{7.13}$$

Where Vo is the peak voltage, i.e 3.4 kV and so,

$$Idisp = \mathrm{C}_{DBD} \text{ x } \mathrm{V}_o \text{ x } \omega \text{ x } \sin(\omega \mathrm{t}) \tag{7.14}$$

Where ω is the angular frequency, and therefore,

$$Power = \mathrm{V}_{rms} \text{ x } (\mathrm{I}_{rms} \text{ - } \mathrm{Idisp}_{rms}) \tag{7.15}$$

The resultant power is 110 W which is not an accurate estimation of the power dissipated in the plasma. However, by calculating the area within the Lissajous plot in Fig. 7.11 as a function of time, the resultant power is equal to 26 W, more than 4 times less than when calculated by voltage and current measurements alone.

7.4 Conclusions

An SBD was developed from a simple plasma actuator to several plasma actuators in a wind tunnel formation to create a large surface area of more than 500 mm^2, operating with a low power of 26 W. The SBD has been coupled to a plenum chamber and APCI for optimum signal intensity and can be fully integrated to a mass spectrometer. The SBD has been proven to be capable of detecting ions from various swab matrices including polypropylene suggesting that it would be capable of detecting drugs on polymer banknotes and explosives on swabs. The development of the SBD has been shown to generate more data than both the plasma array and the plasma jet and therefore, the SBD was chosen as the ionisation source to develop further for drugs and explosive detection. The use of the SBD with a mass spectrometer in this way is entirely novel and a patent application is under way for a DBD Ion Source (as named in the patent) and therefore, the following chapters will refer to this ionisation source as a DBD Ion Source.

The DBD Ion Source described in this chapter was developed as part of a collaboration with Mass Spec Analytical Ltd. and funded by the Innovative Research Call 2016 for Explosives and Weapons Detection. This is a Cross-Government programme sponsored by

a number of Departments and Agencies under the UK Government's CONTEST strategy in partnership with the US Department of Homeland Security, Science, and Technology Directorate. The foreground IP for this DBD Ion Source is covered by British Patent Application No. 1717618.1.

Chapter 8

Detection of Explosives using a Surface Barrier Discharge Ion Source

This chapter will discuss the use of the DBD Ion Source developed in section 7 for the detection of explosives as part of the IRC 2016 for explosives and weapons detection. However, the DBD used within this chapter is an adaptation of that described in 7 as shown in Fig. 8.1.

8.1 Introduction

The ability to detect and identify explosives is crucially important, especially in forensic science [72,95,96] and aviation security [97], but also for environmental monitoring [98,99], and public safety [100]. While ion mobility is ubiquitously used for rapid screening of explosives, forensic analysis for confident identification of explosives often relies on mass spectrometric techniques for their high sensitivity, selectivity and speed. More recently, the interest in the potential to derive mass spectral information from analytes within the ambient environment (ambient ionisation mass spectrometry) has grown significantly.

A plethora of ambient ionisation techniques, where the ionisation occurs externally from the mass spectrometer, have been recently developed with the aim to reduce sample preparation to a minimum. The first fully acknowledged technique of its kind was atmospheric pressure chemical ionisation (APCI) [101] followed by desorption electrospray ionisation (DESI). This was described in 2004 and uses an electrospray and high voltages to produce charged solvent ions which collide with the sample, consequently initiating desorption/ionisation [16]. Shortly after the introduction of DESI, direct analysis in real time (DART), which ionises analytes through collisional interactions with electronically excited species such as helium metastables (He^*) [14] was introduced.

As a result of these two techniques, many subsequent plasma based ambient ionisation techniques were to rapidly follow (as mentioned in 2), all with the aim of becoming a reliable ionisation source to be used with mass spectrometry. DESI and DART enjoy greater advantages than many of the other ionisation techniques owing to the fact that they are commercially available, used by many and well described in the literature. The main disadvantages of all the ambient ionisation sources as described are that they require expensive discharge gases, such as helium and solvents which can be environmentally unfriendly which can be expensive consumables. They also require safety training for their use, but possibly their greatest limitation is that they all have a fairly small sampling surface area, typically less than 10 mm^2.

There have however, been some ionisation sources that have been developed to overcome the small surface area, such as a plasma array consisting of a number of plasma jets but still, disadvantages persist. For example, in Dalgleish *et al*, the flow of helium was increased when the number of probes increased but also, the effective sampling area was still relatively small due to the diameter of the probes used [57]. Additionally, within plasma arrays there is a divergence between each stream due to the strong repulsion forces which can result in a non-uniform, non-reproducible ionisation source for sample analysis [78]. Uniformity of the plasma is important for an analysis procedure where a swab is analysed because a non-uniform plasma would reduce the confidence that the area analysed was fully investigated.

Further, a smaller sampling surface area for swab analysis would require several repeat analyses to ensure that all of the swabbing media had been investigated as the analyte of interest could be on any part of that swab. A larger sampling surface area with a uniform plasma allows for a larger percentage or even a whole swab to be analysed in a single step, increasing throughput and confidence that the swab did or did not contain the analyte of interest.

Explosive detection typically requires an adduct forming reagent which increases identification confidence and sensitivity (detection probability). Routinely for nitroesters such as pentaerythritol trinitrate (PETN) and nitroglycerin and nitroamines, such as cyclotrimethylene trinitramine (RDX) an acidic reagent containing chlorine, formate or acetate ions is used to adduct to the explosive molecule to form adducted species such as $[M+Cl]^-$ [72]. This chapter introduces the DBD Ion Source for the detection of explosives that operates in ambient air with a surface area greater than 500 mm^2. This not only produces an ionic wind for ion transportation, but also produces an NO_3^- ion through ozone interactions [102], which can be used to form an adduct with an explosive molecule, thereby producing an ionisation source that detects explosives without the

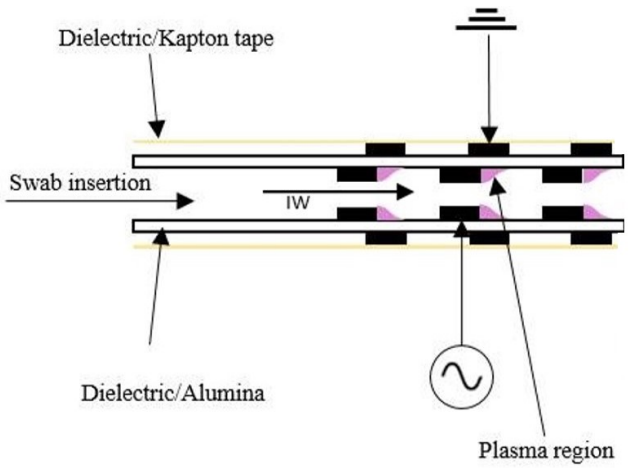

Figure 8.1. Schematic representation of DBD ion source with two alumina sheets each containing three pairs of electrodes. Chordwise ionic wind direction is labelled by IW.

need for adduct forming reagents, solvents, sample preparation or expensive discharge gases.

8.2 Experimental Setup

The experimental conditions used for the DBD Ion Source were as described at the end of section 7. The DBD Ion Source consisted of two alumina plates 91 x 79 x 0.5 mm; on each plate were three pairs of electrodes (three powered, three ground) 60 mm long and 5 mm wide, separated by 7 mm from one another. The powered and ground electrodes were on reverse sides of the alumina and overlapped by 1 mm as previously described. The two sheets of alumina were separated by 4 mm with the powered electrodes facing one another as shown in Fig. 8.1. The offset electrodes result in a chordwise ionic wind in the direction of the ground electrode. The velocity of the ionic wind was not recorded in this study but previous literature of a similar configuration, consisting of one pair of electrodes, document the velocity to be 2 m/s [62]. It is suggested in the literature that additional actuators (electrode pairs) can increase the flow velocity up to 10 m/s [61,64].

A sinusoidal AC high voltage (7 kV, 20 kHz) was applied to the powered electrodes using an audio amplifier driven by a digital function generator. A custom-built step-up transformer was connected to the output stage to enable high voltages required for gas breakdown (plasma ignition). A high voltage probe was used to measure the voltage on the powered electrodes which was displayed on a dual trace oscilloscope. The operating temperature of the DBD Ion Source was recorded to be roughly 100 ^{o}C, measured using

a hand-held infrared thermometer on the ground electrodes and therefore, it is possible that the temperature within the DBD Ion Source is slightly higher, but it has been shown to not damage a polymer banknote within 3 seconds of direct interaction.

The DBD Ion Source was successfully integrated to several analytical mass spectrometers such as a molecular beam mass spectrometer (MBMS) as described in 3.2.1, an AB Sciex API 2000 tandem mass spectrometer 3.2.3 and a Sciex X500R QTOF 3.2.4. These experiments were performed to show the versatility of the DBD Ion Source in that it can be easily integrated with various detectors, but also to obtain analytical data such as proof of ionisation and ionic wind (MBMS), limits of detection and analyte identification (MS/MS) and exact mass measurements (QTOF). The samples used in this study are described in section 3.4.

8.3 Results and Discussion

8.3.1 DBD Ion Source with Molecular Beam Mass Spectrometer

The objectives of this study were to establish what ions, if any, were produced by the DBD Ion Source and whether the ionic wind was significant enough to result in successful ion transportation from the DBD into the mass spectrometer. Due to the operating conditions of the molecular beam mass spectrometer (MBMS) as laid out in section 3.2.1, any ions detected within the MBMS must have come from an external ionisation source and they must have entered by their own transportation means i.e. the ionic wind, focussed by varying the skimmer cone voltages. The DBD Ion Source was integrated with the MBMS without a plenum chamber or APCI by directly aligning the two alumina sheets to the orifice, with the bottom sheet roughly 1 mm below the orifice. As the DBD Ion Source operates in ambient air, it was anticipated that enough detectable reactive species would be present to demonstrate ion production.

Data was obtained with the MBMS in both positive and negative ion mode over a range of m/z 0 to 200. Five repeats of each cycle were obtained which were then averaged to produce the mass spectra shown in Fig. 8.2. The negative ion data in Fig. 8.2 (a) is dominated by peaks at m/z 62 presumed to be NO_3^- and 125 presumed to be$[HNO_3(NO_3)]^-$. The positive ion data in Fig. 8.2 (b) primarily consists of (presumed) water clusters at m/z 55, 73, 91 and 109 for $[H_3O(H_2O_n)]^+$, where n = 2, 3, 4 and 5 respectively.

The data obtained with the MBMS demonstrates that the DBD Ion Source is

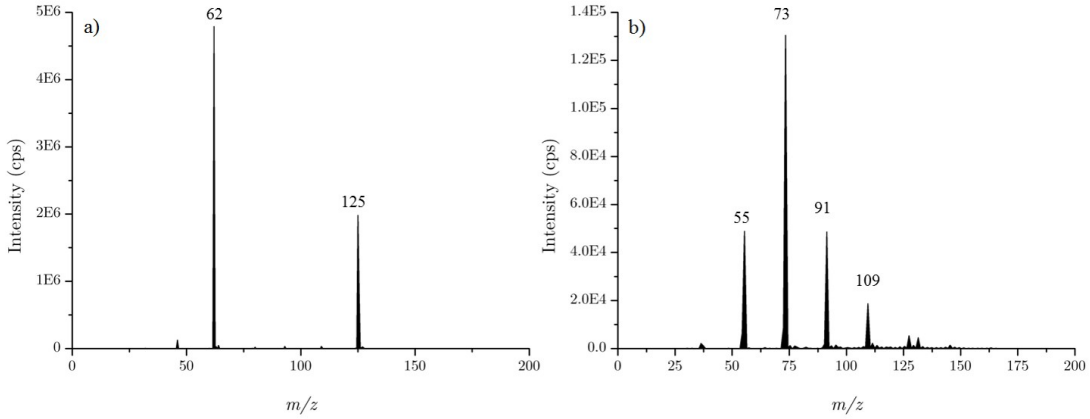

Figure 8.2. MBMS data of DBD ion source in negative ion mode (a) and positive ion mode (b).

capable of operating in ambient air, without additional gas flows, and produces negative and positive ions. Further, the resulting chordwise ionic wind generated by the DBD is sufficient enough for ion transportation in the direction of the mass spectrometer, however, it is not known how efficient the ionic wind is for ion transportation. It is assumed that even if the induced flow is directed in the downstream direction, (or in the direction of the ground electrodes) there must be some opposite, upstream flow too due to the ion motions within each half cycle of the sine applied voltage that may result in a reduction in ion transportation efficiency [64].

8.3.2 DBD Ion Source with AB Sciex API 2000 Tandem Mass Spectrometer

Optimisation of samples were performed using diluted solutions (in methanol) of trinitrotoluene (TNT), PETN and RDX (100 ng/μL) and hexamethylene triperoxide diamine (HMTD) (50 ng/μL) and then infused using a syringe drive at 0.60 mL/hr through a glass capillary with the exit 1 mm in front of the powered electrode closest to the mass spectrometer, centrally located in front of the mass spectrometer orifice. The surface discharge (plasma) was then used to volatilise the samples before the formed ions were entrained through a ceramic transfer line to an APCI needle. Although the previous study demonstrated that the DBD Ion Source was capable of ionisation without an APCI needle, it is assumed that these ions form clusters between the point of ionisation by the DBD and the mass spectrometer and therefore, the APCI needle is used to break up these clusters leading to a significant increase in ion sensitivity.

The addition of an APCI needle acts as a post-ionisation source and offers the

prospect of remote sampling whereby the DBD Ion Source can be taken further away from the mass spectrometer to analyse a surface by liberating and ionising the sample before its transfered through a tube towards the APCI needle, similar to mechanisms previously described in other techniques within the literature [103, 104].

The assumption of the APCI needle acting as a post-ionisation source was corroborated by integrating the DBD Ion Source with the mass spectrometer on a separate custom built front end that did not contain a plenum chamber or APCI needle. Analyte ions were detected with this set-up but the intensity was significantly reduced by roughly one order of magnitude. However, this study also shows that analyte ions are formed within the plasma as opposed to the plasma being responsible for liberating the sample from the surface (or volatilising a liquid sample) before being ionised at the APCI needle. This experiment demonstrates that the ions produced do not arise from an aspirator effect caused by the sample pump (as described in section 3.2.3) as the DBD Ion Source has been proven to liberate and ionise a sample without the APCI needle.

It is anticipated that further design improvements to the DBD Ion Source such as electrode shapes, composition and plenum chamber designs will likely result in higher reproducibility and sensitivity, as mentioned in section 10.2. The future improvements should result in an increased ion transmission by focussing the ion wind toward the orifice and will improve the reproducibility of the electrodes by eliminating the use of a copper adhesive tape. Currently, the plenum chamber is at ambient temperature, except for any temperature rise due to heat transfer from the DBD, and the internal ceramic transfer line is not heated. However, if they were heated, this may decrease any condensation of the samples on the walls and increase ion transmission and therefore, sensitivity.

The ions observed in the mass spectrum are different to those that would be typically expected with APCI alone; and as for TNT, the dominant molecular ion observed was $[M\text{-}NO{+}HNO_3]^-$ at m/z 260, for this reason, this molecular ion was chosen for TNT. In APCI however, the dominant molecular ions detected for TNT are typically $[M]^-$ and $[M\text{-}H]^-$ at m/z 227 and 226 respectively, and while these ions are observed with the DBD, their intensity is significantly lower than $[M\text{-}NO{+}HNO_3]^-$ at m/z 260. It is not uncommon to see the $[M\text{-}NO{+}HNO_3]^-$ at m/z 260 for TNT where the ionisation occurs in ambient air however [18, 105, 106]. This suggests a different ionisation mechanism from APCI which is likely to be due to the fact that when a plasma is allowed to interact with ambient air, an abundance of ozone is generated which, in turn, is responsible for the reduction in the proton abstraction reaction and thus limiting the amount of $[M\text{-}H]^-$ for TNT [105, 106].

The product ions observed for TNT due to collisionally activated dissociation (CAD)

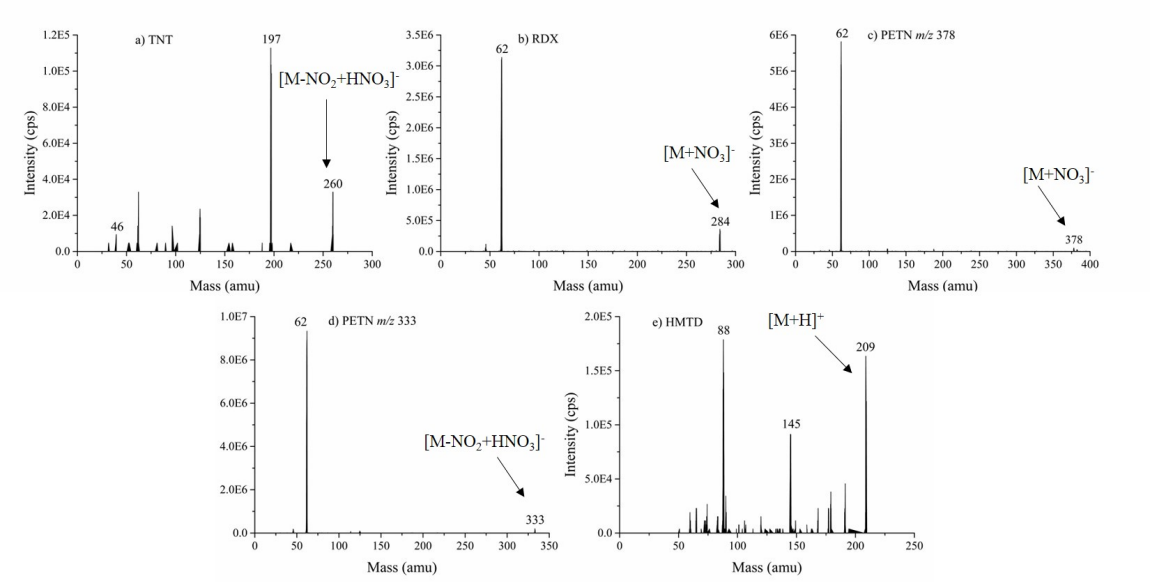

Figure 8.3. MS/MS mass spectra of explosives infused by capillary for 60 seconds, over a range of collision energies (5-60 eV) for (a) TNT (100 ng/μL) detected as [M-NO+HNO_3]$^-$ at m/z 260, (b) RDX (100 ng/μL) detected as [M+NO_3]$^-$ at m/z 284, (c) PETN (100 ng/μL) products of [M+NO_3]$^-$ at m/z 378, (d) PETN (100 ng/μL) products of [M-NO_2+HNO_3]$^-$ at m/z 333, and (e) HMTD (50 ng/μL) detected in positive ion mode for the [M+H]$^+$ ion at m/z 209.

or collision-induced dissociation (CID) were the usual characteristic ions for [M-NO]$^-$ at m/z 197 and NO_2^- at m/z 46 as shown in Fig. 8.3(a). For RDX the major ion detected was [M+NO_3]$^-$ at m/z 284. For APCI, typically an adduct is added for the detection of these compounds such as a formate, acetate or chloride ion and therefore, this molecular ion is different to APCI considering the NO_3^- ion was not introduced by means of an adduct forming reagent. The resulting product ions for RDX at m/z 284 were found at m/z 62 and 46 for NO_2^- and NO_3^- respectively, as shown in Fig. 8.3(b).

The major ions detected for PETN were [M+NO_3]$^-$ at m/z 378 and [M-NO_2+HNO_3]$^-$ at m/z 333. Two ions were used for the identification of PETN as for tandem mass spectrometry, it is recommended that a 3-ion criterion is used to ensure a reliable identification, reducing the chances of a false positive [107–109]. Two separate ions were used as each precursor produced a strong NO_3^- product ion at m/z 62, much stronger than any other observed product ion. Each precursor and respective product ion for PETN are shown in Fig. 8.3(c) and (d). HMTD was detected in positive ion mode in the form of the protonated molecule ion [M+H]$^+$ at m/z 209, with two dominant product ions observed at m/z 145 for [M-CH_4O_3]$^+$ (due to a loss of formaldehyde and hydrogen peroxide) and at m/z 88 for [$C_2H_6O_2N$]$^+$ [110].

Although some of the product ions reported above are often observed in APCI such as NO_3^- and NO_2^- at m/z 62 and 46 respectively for explosives such as RDX and PETN,

and the $[M\text{-}CH_4O_3]^+$ for HMTD at m/z 145, the dominance of the NO_3^- ion at m/z 62 that is observed with the DBD Ion Source is seldom seen in APCI. Additionally, it is uncommon that the product at m/z 88 for HMTD is reported in the literature with APCI, largely because other higher mass products have the tendency to dominate the APCI product ion spectrum instead, such as the $[M\text{-}CHO]^+$ and $[M\text{-}CH_4O_3]^+$ ions at m/z 179 and 145 respectively.

For the detection of nitrogen-containing explosives, such as RDX and PETN, when using APCI an adduct forming reagent is added to the explosive molecule aiding ease of identification as mentioned above. A commonly encountered adduct is a chloride ion because not only do they provide their own product ions for tandem mass spectrometry with products at m/z 35 and 37 for the chlorine isotopes ^{35}Cl and ^{37}Cl respectively, but their isotopic patterns are very characteristic due to their relative abundance, adding additional information and increasing the confidence level for identification [111].

The limits of detection (LODs) were ascertained for each explosive by applying a known concentration of solution onto a glass slide and allowing the solvent to evaporate. Once the solvent had evaporated, the slide was firmly swabbed with a polypropylene strip which was analysed by placing it within the DBD Ion Source for direct interaction with the plasma for 2-3 seconds. The limits of detection for each explosive are shown in Fig. 8.4. It can be seen in Fig. 8.4 that the LOD for RDX and PETN could be lower than the reported 100 pg for the product ion shown, however, the LOD is given at 100 pg due to the 3-ion criterion for identification and having both precursor-product ion transitions above 3.5 x signal-to-noise ratio.

The signal-to-noise ratio was obtained by measuring the peak-to-peak noise between 3 separate peaks from 3 separate swabs. The limit of detection was measured at at least 3.5 times greater than the noise signal for both transitions. This approach is very much a qualitative and does not achieve the exact lower limit of detection, instead, a best estimate. A more appropriate method to measure the limits of detection would be to perform serial dilutions of the target analyte and perform many more repeats at each concentration. The average peak heights or areas can be plotted as a calibration curve and the LOD would be measured through interpolation of the graph as described previously in the literature [112, 113]. The limits of detection were not performed using this method as the DBD is still in an early prototype stage and will likely undergo many more variations and modifications. A full validation of the LODs and detection probability i.e. false positive rate, would be required before commercialisation can take place.

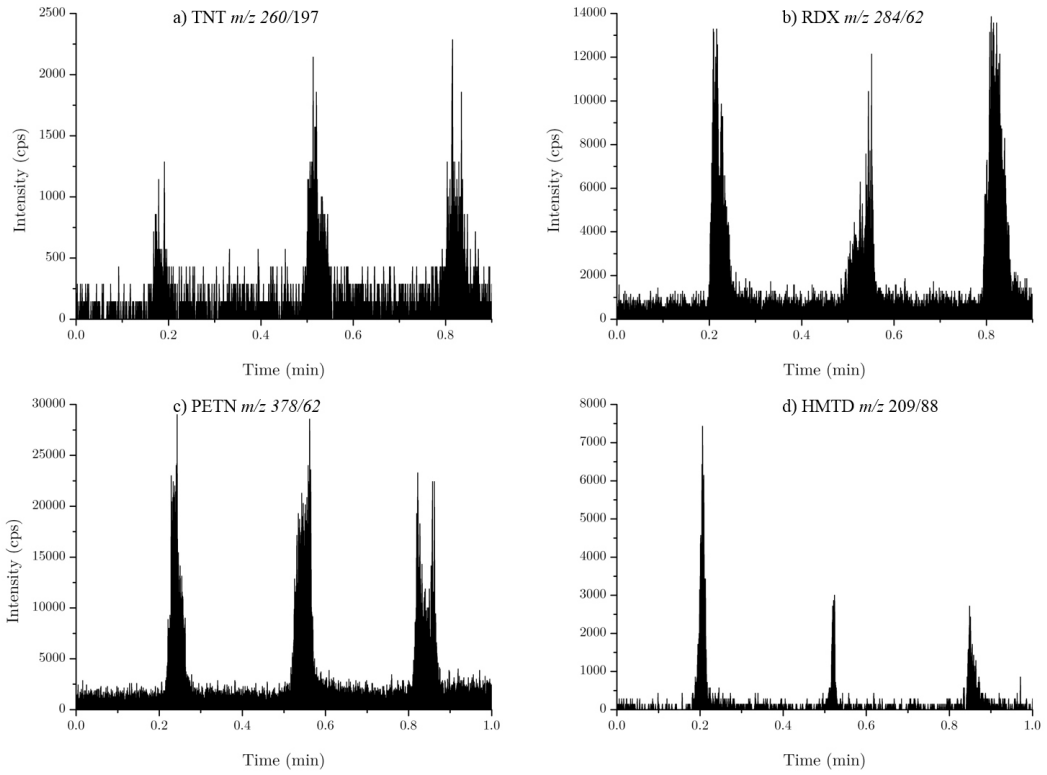

Figure 8.4. MRM scan data for the limits of detection using polypropylene swabs of samples deposited onto a glass slide (1 μL) for (a) 5 ng/μL TNT *m/z* 260/197, (b) 100 pg/μL RDX *m/z* 284/62, (c) 100 pg/μL PETN *m/z* 378/62, and (d) 1 ng/μL HMTD *m/z* 209/88. LODs calculated by measuring the peak-to-peak noise and the signal being at least 3.5 x the signal-to-noise ratio for both transitions for each explosive.

Polypropylene was used as the swabbing medium due to its smooth surface as this will likely cause any swabbed analytes to remain on the surface of the polypropylene, resulting in a much more efficient liberation of the analytes than if the swab was made from a textile for example. The quicker desorption rate of the polypropylene resulted in much higher signal intensities than with PTFE, shark paper, cotton paper, Nomex and Teflon coated fibreglass swabs. The LODs established for RDX and PETN were 100 pg, HMTD was 1 ng and TNT was 5 ng. It is important to remember that these LODs were obtained after a secondary transfer step (swab of a slide) as opposed to a direct injection and therefore, could be much improved if a direct injection was possible. Unfortunately a direct injection is not feasible with the current design due to the exposed powered electrodes, however, the design could be easily modified to allow for a direct injection as discussed in section 10.2.

In an operational context, it may be beneficial to use a textile based swab as opposed to polypropylene as the collection efficiency of the swab is likely to reflect the make-up of the matrix (textile based swabs contained pores and fibres etc. resulting in

a higher retention of the analytes), as the desorption rate is likely to be less efficient that polypropylene. While for most forensic applications this would be viewed as a disadvantage, it could be advantageous in allowing the prospect for the swab to be analysed with one technique such as the DBD Ion Source, and then subsequently re-analysed with another technique as some of the sample will remain on the swab unlike with polypropylene. This would be most beneficial in scenarios where there was little sample to begin with, but it would come at a compromise to sensitivity.

It is important to understand how efficiently the DBD Ion Source can analyse swabs that have been taken from various surfaces that are likely to be encountered in a real world environment for example, a search of a building. In order to replicate a scenario where several surface types may or may not have become contaminated with explosives; a government stakeholder of the IRC 2016 provided assistance for a blind study. The blind study consisted of four test boards, each board contained a metal door handle, a plastic light switch and a melamine board. The government stakeholder, handled a mobile phone that had been heavily contaminated with Semtex using a gloved hand. With one gloved finger, the government stakeholder pressed their finger onto a piece of paper 9 times and then placed the 10^{th}, 11^{th} and 12^{th} fingerprint onto one door handle, one plastic light switch and one melamine board at random, leaving all other surfaces blank.

The surfaces that had been contaminated were not known to the analyst and were only confirmed after analysis. The mass spectra shown in Fig. 8.5 were obtained using polypropylene as a swabbing medium and note that the peaks are short in time and high in intensity, suggesting a rapid desorption rate (unlike those shown in 8.6 from textile based swabs) and demonstrates that the DBD Ion Source is self-purging, evident to the fact that the peak returns back to baseline levels. This blind study was designed to replicate real-world scenarios using a real manufactured explosive (Semtex) as opposed to a certified reference standard, suggesting that the sample will be a complex matrix of dyes, taggants, plasticisers and other compounds.

It can be seen in Fig. 8.5 that there is only one peak in each spectrum other than (b) which was the blank test board; this suggests that the DBD Ion Source has correctly identified the contaminated surface as being positive for Semtex (RDX and PETN) and the other surfaces as being blank, ruling out false positives and cross-contamination. In forensic and detection applications, it is important to minimise false positives as they are often expensive and time consuming requiring the investigation of a sample further. In Fig. 8.6, the same surfaces were re-analysed without contaminating the surfaces again, therefore, any sample that is detected had remained since the first analysis. For this

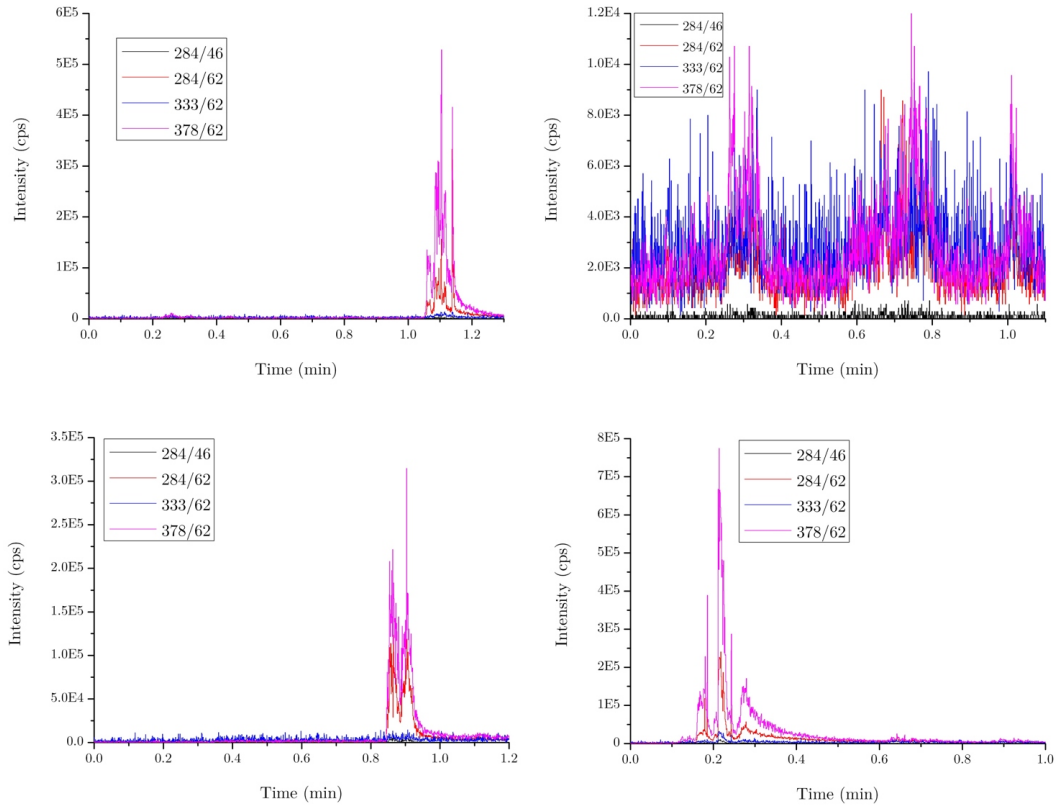

Figure 8.5. All multiple reaction monitoring (MRM) spectra for RDX and PETN taken from a blind study of Semtex deposited on various surfaces. All spectra show 3 swabs from 3 different surfaces in the order: handle, light switch, melamine board, taken with polypropylene swabs. Top left shows PETN and RDX detected on the melamine board, top right shows all 3 surfaces are blank, bottom left shows contamination on the light switch, and bottom right shows contamination on the handle. All other surfaces correctly identified as being blank.

subsequent analysis, Teflon coated fibreglass and Nomex swabs were used instead of polypropylene. It can be seen in Fig. 8.6 that the same surfaces were identified as having Semtex contamination even after the fourth transfer step (deposit and three swabs) of the 10^{th}, 11^{th} and 12^{th} fingerprints. The blind study presented here demonstrates the ability of DBD Ion Source to detect explosives from a variety of materials and surface types, presenting itself as a versatile ionisation source to be coupled with mass spectrometry and potentially other detection techniques.

8.3.3 DBD Ion Source with Sciex X500R QTOF Mass Spectrometer

It was decided that it would be useful to demonstrate that the DBD Ion Source could be easily integrated with other mass spectrometers and so it was coupled to a Sciex X500R

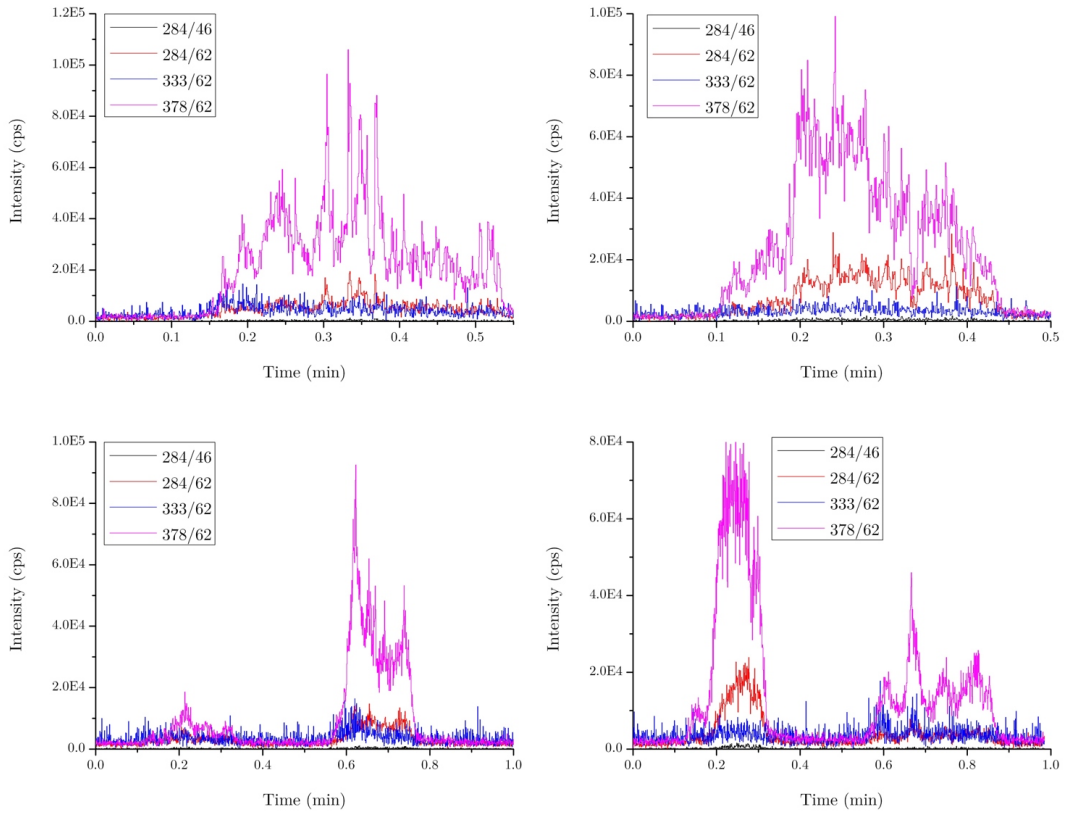

Figure 8.6. MRM mass spectra of the same surfaces being reanalysed using different swabbing materials. Top left is a Teflon coated fibreglass (TCFG) swab on the melamine board, top right is a Nomex swab of the melamine board, bottom left is TCFG and Nomex swabs of the light switch, and bottom right is TCFG and Nomex swabs of the handle.

QTOF for this purpose, and to ascertain whether using accurate mass could be used in the detection of explosives as it may provide further information such as likely molecular formula. Additionally, it is possible to perform retrospective data analysis and therefore, it could provide a useful means of better understanding the plasma and the explosives themselves by aiding identification of other detectable compounds within the samples.

Fig. 8.7 was obtained using a SWATH method as described in section 3.2.4. The mass spectrum in Fig. 8.7 was obtained by swabbing a glass slide that had been contaminated by a gloved finger which previously handled a mobile phone that had been heavily contaminated with Semtex. The data is not presented here but it is interesting to point out that this fingerprint was deposited immediately after contaminating the phone, but the 80^{th} fingerprint in a series of depositions (where every 10^{th} fingerprint was pressed onto a glass slide, and all other prints were pressed onto paper) was identified as containing both RDX and PETN, demonstrating great sensitivity even after many transfers. In Fig. 8.7, the exact mass for PETN was observed at m/z 378.0099 for the $[\text{M}+\text{NO}_3]^-$ precursor ion; the software formula finder identified the formula $\text{C}_5\text{H}_9\text{N}_5\text{O}_{15}$

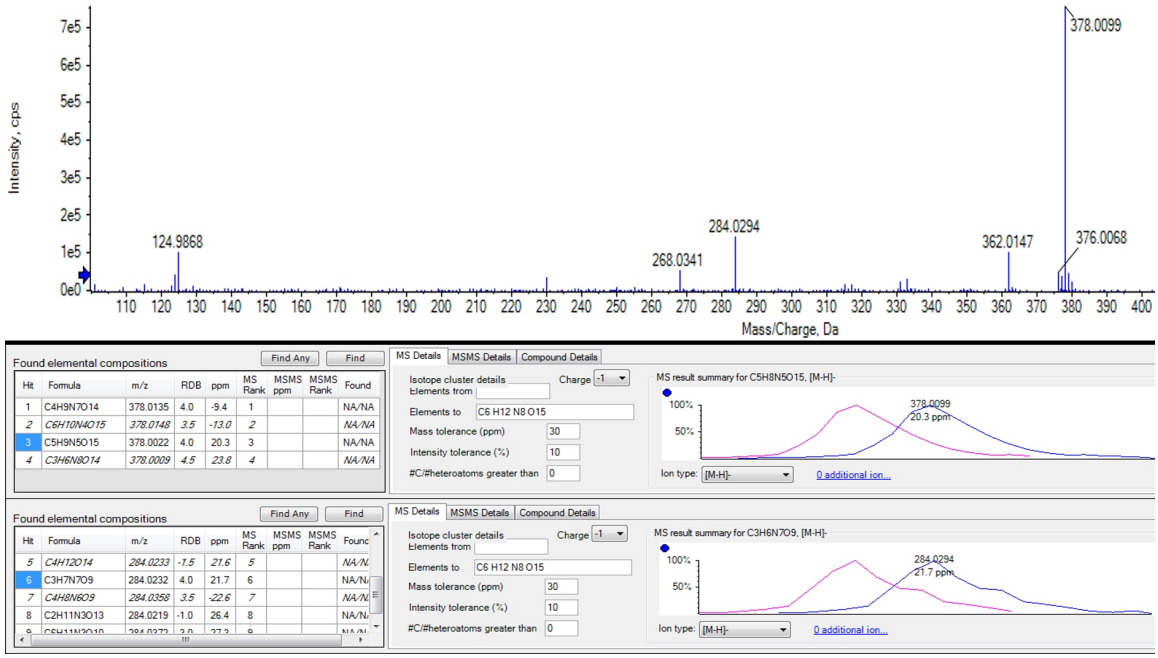

Figure 8.7. SWATH TOF/MS spectra of a Semtex sample on a glass slide with TOF/MS (top) and formula finder for PETN $[M + NO_3]^-$ (middle) and RDX $[M + NO_3]^-$ (bottom). Sample was analysed via DBD coupled with a Sciex X500R QTOF.

to have an exact mass of m/z 378.0022, suggestion a calibration shift of 20.3 ppm.

Calibration of the instrument was not conducted prior to this study as there was no method available for introducing a calibrant at the time and therefore, a calibration shift was to be expected. The purpose of this study intends to show proof of principle for successful integration of the DBD Ion Source with the Sciex X500R QTOF instrument. A background peak known to be $[HNO_3(NO_3)]^-$ was used as a calibration reference peak as it has a known exact monoisotopic mass of m/z 124.9840 and therefore, the calibration shift of this peak can be used to correct the calibration shift in the sample. The peak for $[HNO_3(NO_3)]^-$ was found at m/z 124.9870 which equates to a calibration shift of 23.9 ppm, shown in Fig. 8.8. The evidence of a calibration shift using the background reference peak suggests that the 20.3 ppm shift in the PETN is actually within 5 ppm of what would be expected (with 5 ppm of 23.9 ppm). For RDX, the calibration is also within 5 ppm of the calibration reference peak as the peak for RDX $[M+NO_3]^-$ was found at m/z 284.0294 despite the exact monoisotopic mass being m/z 284.0232.

LODs for the explosives have not yet been ascertained on the X500R QTOF but it is expected to parallel the sensitivity improvements made when using other ion sources, Additionally, the additional information such as exact mass, will circumvent the recommendation for the 3-ion criterion, allowing the use of the precursor ion and the much more abundant m/z 62 product ion for NO_3^-.

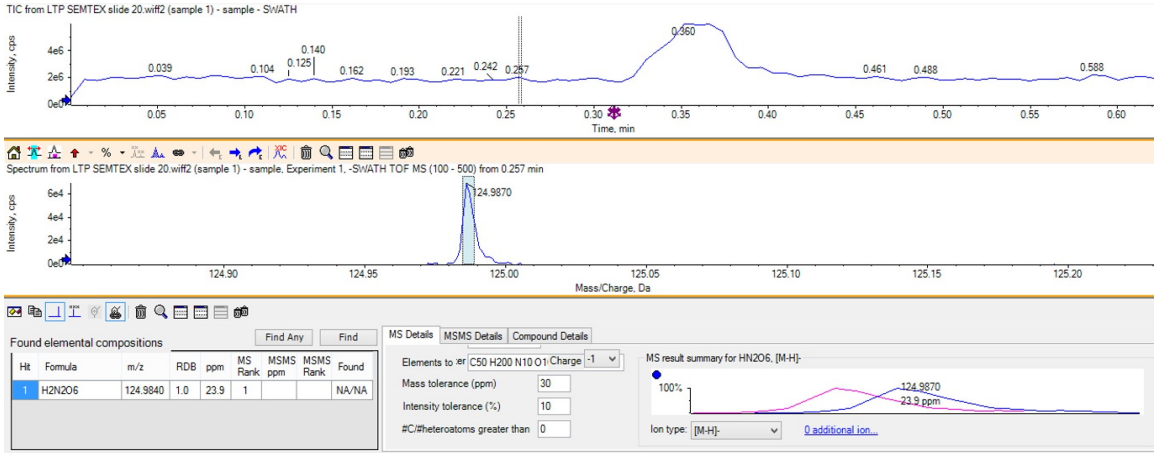

Figure 8.8. SWATH TOF/MS scan from a glass slide contaminated with Semtex where the sample is inserted between 0.30 and 0.40 min (top). Presented here (middle) is a background peak taken from ca. 0.25 min at m/z 124.9870 presumed to be $[HNO_3(NO_3)]^-$. Formula finder (bottom) identifies the peak to have the formula $H_2N_2O_6$ with a calibration shift of 23.9 ppm. Samples analysed via DBD coupled with a SCiex X500R QTOF.

8.4 Conclusions

This study demonstrated the DBD Ion Source as an ionisation source capable of being integrated to mass spectrometers (with the potential for other instrument types) for rapid screening and detection of explosives from various surfaces and swab matrices. The DBD Ion Source coupled with mass spectrometry enjoys high sensitivity, reproducibility, specificity and selectivity in laboratory and real-world scenarios. Most advantageously, the DBD Ion Source operates in ambient air, without the use of chromatography, solvents or adduct forming reagents, largely reducing sample preparation, analysis time and consumables whilst posing the possibility of being field-portable. Finally, the DBD Ion Source has presented evidence that it is capable of ionising samples in both positive and negative ion modes for small molecule analysis which could be applied to many other applications such as the detection of substance of abuse.

This study was performed as part of the Innovative Reserch Call 2016 for explosives and weapons detection. This is a cross-government programme sponsored by a number of departments and agencies under the UK government's CONTEST strategy in partnership with the US department of Homeland Security, Science, and Technology Directorate.

The foreground IP for this DBD Ion Source is covered by British Patent Application No. 1717618.1

Chapter 9

Detection of Controlled Substances with a Surface Barrier Discharge Ionisation source

This chapter will describe the detection of substances of abuse (controlled substances) from polymer banknotes using a slightly modified and improved design of the DBD Ion Source.

9.1 Introduction

Banknotes from crime scenes can be seized as evidence in cases where the defendant is suspected of being associated with drug related activities such as illicit drug dealing. The contamination levels found on the seized banknotes can be compared to the contamination found on banknotes from general circulation and any major discrepancies can result in an inference that the seized banknotes have been involved in drug related activity. The evaluation of the contamination adds weight to other circumstantial evidence in drug supply cases especially in cases where there are no drugs found at the scene. Traditionally, banknotes are analysed by a technique either involving separation such as liquid chromatography (LC) and gas chromatography (GC) [114, 115], or by direct analysis such as thermal desorption tandem mass spectrometry (TD-MS/MS) or ion mobility spectrometry (IMS) [116–118].

Direct analysis by TD-MS/MS using a thermal extraction ion source (TEIS), as mentioned in Ebejer *et al* [29], allows for rapid identification of drug analytes from a very complex matrix such as a banknote without any sample preparation unlike chromatographic techniques; GM/MS for example. A banknote can be analysed in as little as two seconds by subjecting it to thermal desorption which volatilises the drug

molecules on the surface, before being ionised using atmospheric pressure chemical ionisation (APCI); allowing identification using MS/MS. The use of TD-MS/MS has been used to determine drugs contamination on money in various scenarios such as the distribution of contamination due to counting machines [119], whether there are geographical trends in the contamination [120, 121] and using chemometrics methods to recognise patterns within drug distribution on banknotes [68, 122].

Using TD-MS/MS for the analysis of banknotes operates with a temperature of 285 ^{o}C to liberate the samples from the complex banknote matrix and while this works extremely well for paper banknotes, the temperature is far too great for any polymer banknotes such as those that have just recently been introduced in the UK and other countries. Polymer banknotes, due to their polypropylene composition, do not withstand temperatures greater than 120 ^{o}C and for this reason [123], it is imperative that a new technique is developed that allows for the detection of drug contamination on polymer banknotes without permanently degrading or destroying them.

Therefore, the DBD Ion Source previously documented throughout this project was developed with polymer banknote analysis in mind as a plasma based technique should have sufficient energies to liberate a sample from a surface whilst operating at relatively cool temperatures and thus, not being destructive to a banknote. The design of the DBD Ion Source was focussed on the TEIS as presented in Ebejer *et al* [29].

9.2 Experimental Setup

The DBD Ion Source used for the detection of controlled substances from polymer banknotes was similar to that described in the previous chapter (section 7) however, there were some modifications made to the design. Firstly, in section 7, the DBD Ion Source consisted of two dielectric surfaces, each containing three pairs of electrodes and a plenum chamber that was 70 mm in depth. The modified DBD Ion Source used for these experiments consisted of two dielectric surfaces each containing five pairs of electrodes, and a plenum chamber with a depth of 50 mm to reduce the distance the ions would have to travel to the APCI needle, in an attempt to increase ion intensity.

It is important to note that this plenum chamber was a rough prototype, and was not completely air-tight and contained air gaps. The DBD Ion Source was further developed in an attempt to increase safety to the user, improve its appearance and practicalities of use. The schematic for the modified electrode design can be seen in Fig. 9.1 that represents each dielectric surface containing 5 electrodes. The modified prototype as a whole

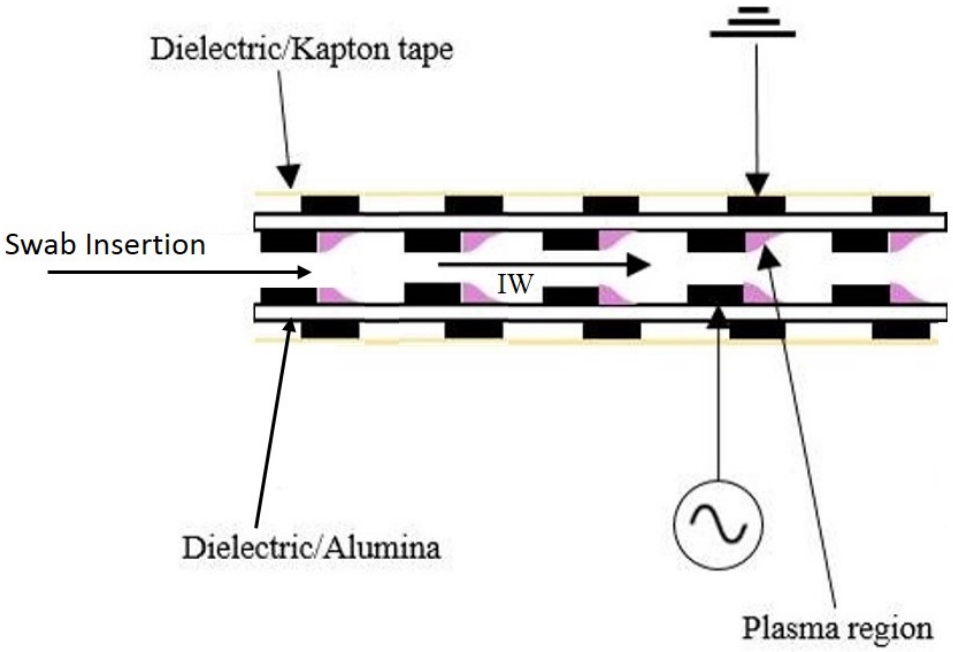

Figure 9.1. Schematic of DBD Ion Source with modified electrode design to include 5 electrodes per dielectric surface. Dielectric surface is alumina and the dielectric tape was Kapton tape. The chordwise ionic wind and direction of flow is depicted by IW.

can be seen in Fig. 9.2, complete with modified PTFE surround for added safety and ease of use. Further, Fig. 9.2 shows the APCI needle and ceramic transfer line arrangement and locking pins to interface to the mass spectrometer. With the additional pairs of electrodes, the sampling surface area of the DBD Ion Source was greater than 700 mm^2.

The DBD Ion Source depicted in Fig. 9.2 is a demonstrator that would satisfy technology readiness level (TRL) 5; suggesting that it is technologically ready for small scale trials/demonstrations but is not yet ready for full scale deployment. For banknote analysis, banknotes were entered from the right hand side, and passed through the source via the Queen's head end, holding in the centre for roughly 1 second amounting to a 2 second analysis time. A standard of cocaine at 10 ng/μL in methanol was used to deposit 2 μL onto a glass surface before being allowed to dry; the surface was then swabbed with polypropylene and analysed using the DBD Ion Source to provide validation that the equipment was working adequately before analysing any banknotes.

9.3 Results and Discussion

The analytes used in this study were methyl (1R,2R,3S,5S)-3- (benzoyloxy)-8-methyl-8-azabicyclo[3.2.1] octane-2-carboxylate (cocaine), 1-(1,3-benzodioxol-5-

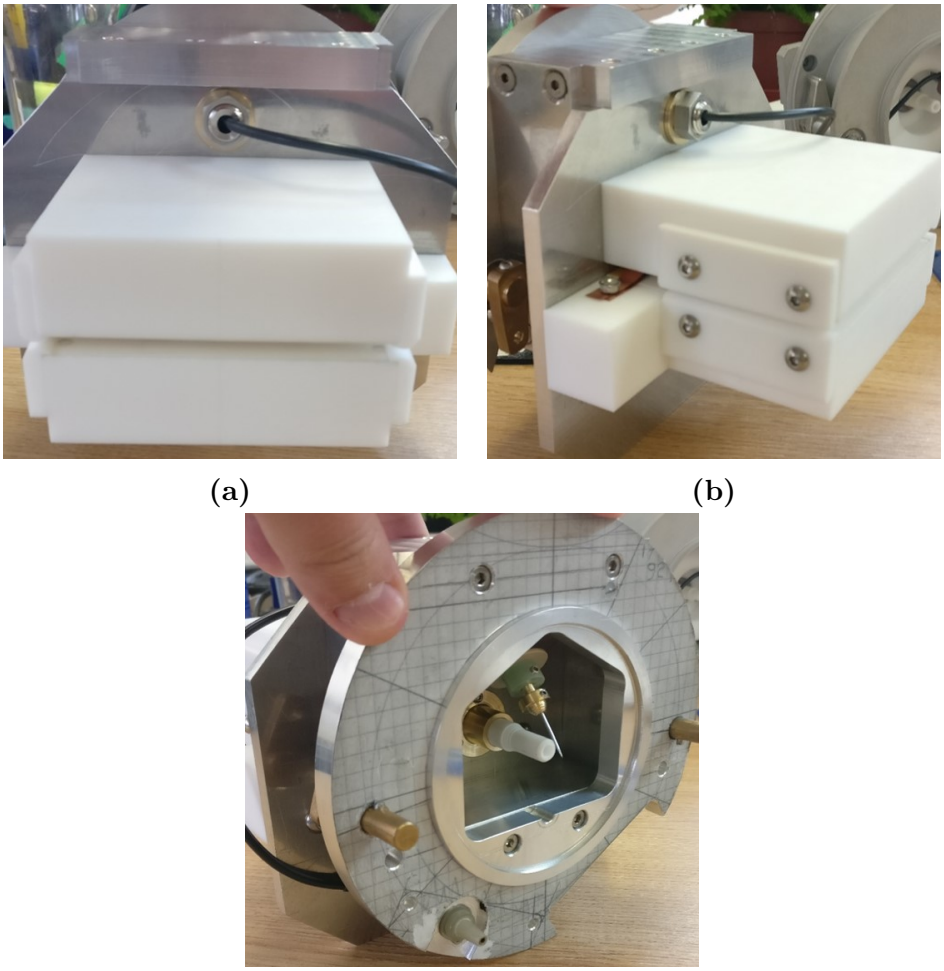

(a) **(b)**

(c)

Figure 9.2. Images of modified prototype for DBD Ion Source including new PTFE surround providing additional robustness and safety (a), reduced plenum chamber from Chapter 8 (b) and APCI needle arrangement with ceramic transfer line (c).

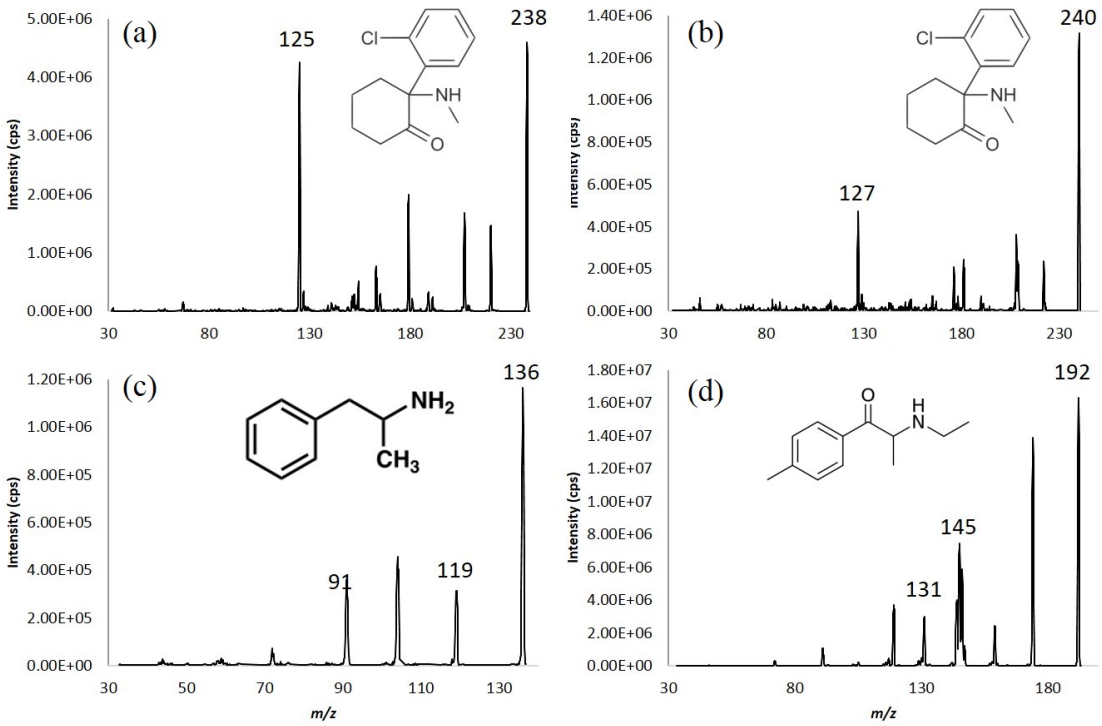

Figure 9.3. Positive product ion spectra using a 100 ng/μL solution for ketamine $[M+H]^+$ (a) at m/z 238, ketamine ^{37}Cl (b) at m/z 240, amphetamine $[M+H]^+$ (c) at m/z 136 and 4-MEC $[M+H]^+$ (d) at m/z 192. Product ion scans were performed over a range of collision energies between 5 and 60 eV.

yl)-N-methylpropan-2-amine (3,4-methylenedioxymethamphetamine (MDMA)), 1-phenylpropan-2-amine (amphetamine), 2-(ethylamino)-1-(4-methylphenyl)propan-1-one (4-methylethcathinone (4-MEC)), (RS)-2-methylamino-1-(4-methylphenyl)propan-1-one (4-methylmethcathninone (mephedrone)), 2-(2-chlorophenyl)-2-(methylamino)cyclohexan-1-one (ketamine) and N-phenyl-N-[1-(2-phenylethyl)piperidin-4-yl]propanamide (fentanyl). These analytes were chosen to encompass a variety of compound types such as alkaloids, opioids, amines, amphetamines and cathinones. All of these compounds were previously optimised in the same way that the explosive samples were, by means of an infusion of 0.60 L/hr through a glass capillary at the frontmost electrode.

All compounds were detected in positive ion mode by their protonated molecule $[M+H]^+$ with the exception of ketamine and two product ions were used for identification. Ketamine was detected at m/z 238 for $[M+H]^+$ with product ion m/z 125, and ketamine was also detected at m/z 240 due to the ^{37}Cl isotope with a product ion at m/z 127. The $[M+H]^+$ ion at m/z 238 had a greater intensity, largely due to the 3:1 ratio of ^{35}Cl to ^{37}Cl. Amphetamine was detected at m/z 136 with a product ion at m/z 91 and a product ion at m/z 119 and the protonated molecule found at m/z 192 was for 4-MEC with a product ion at m/z 145 and a product ion at m/z 131 shown in Fig. 9.3.

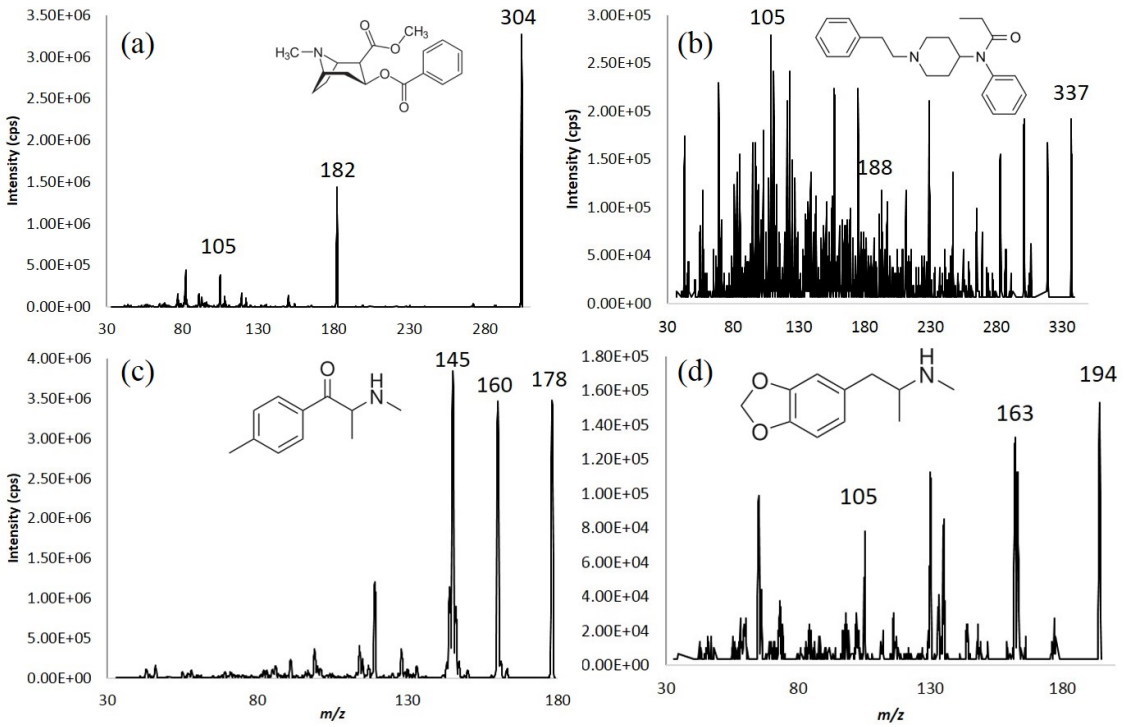

Figure 9.4. Positive product ion spectra using a 100 ng/μL solution for cocaine $[M+H]^+$ (a) at m/z 304, fentanyl $[M+H]^+$ (b) at m/z 337, mephedrone $[M+H]^+$ (c) at m/z 178 and MDMA $[M+H]^+$ (d) at m/z 194. Product ion scans were performed over a range of collision energies between 5 and 60 eV.

For cocaine, the protonated molecule was found at m/z 304 with characteristic ions at m/z 182 and m/z 105. MDMA was detected at m/z 194 with characteristic ions at m/z 163 and 105. Mephedrone was detected at m/z 178 for the $[M+H]^+$ ion with product ions of m/z 160 and 145 and finally, fentanyl was detected at m/z 337 with a product ion at m/z 105 and a product at m/z 188 shown in Fig. 9.4.

It can be seen in Fig. 9.4 that the fentanyl product ion spectra was dominated by other background peaks and therefore, the product ion data should be reacquired to show the true product ions formed as a result of fragmentation.

It is important to determine the limits of detection for each analyte and therefore, after optimisation, a series of different concentrations was made up of each sample, and analysed until the detection of the dominant ion was equal or greater than 3.5 multiplied by the signal to noise (S/N) ratio of the peak-to-peak noise. LODs were determined at 3.5 x S/N ratio following the IUPAC recommendation of the relative detection limit being the smallest amount of material detectable (3σ-criterion) in a matrix relative to the amount of material analysed [124, 125]. The limit of detection for ketamine was 100 pg, amphetamine and 4-MEC were detected at 250 pg, cocaine (shown in Fig. 9.5), fentanyl

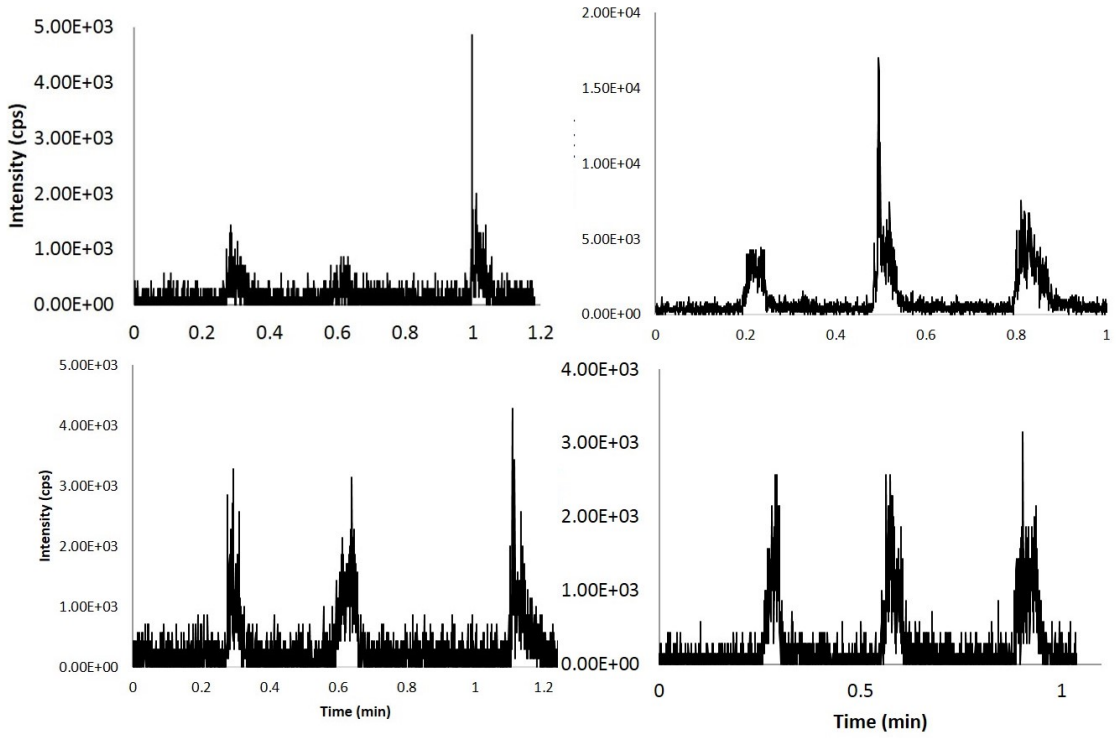

Figure 9.5. Mass Spectra showing limit of detection for ketamine 100 pg (a), amphetamine 250 pg (b), 4-MEC 250 pg (c) and cocaine 500 pg (d). LODs were measured by using the peak-to-peak noise with a signal-to-noise ratio of at least 3.5.

and mephedrone were detected at 500 pg and the limit of detection for MDMA was 4 ng and can be seen in Fig. 9.6. The limits of detection are at least in low nanogram range or mid picogram range, which is very good considering there is an additional transfer step involved (sample is spotted onto glass and swabbed as opposed to a direct injection) and also the plenum chamber is not completely sealed.

The LODs reported here were performed and measured in the same way as in Chapter 8 except they were recorded for the most abundant product ion as opposed to both transitions. This is important to note as for a safe identification, at least three characteristic ions have to be chosen and therefore, the LOD may be slightly higher than reported here. The LODs were measured in this way because the DBD Ion Source is not yet a finalised product and therefore, it is useful to obtain a rough estimate as to its capabilities. For a better estimation of the LODs, it is best to perform a series of dilutions and calculate the LODs by means of interpolation [112, 113].

Given that this prototype is at TRL-5, there is still room to improve the design of the electrodes and the plenum chamber which is likely to result in an increase in sensitivity. Furthermore, there is scope to modify the DBD Ion Source to allow for a direct injection which will remove the additional transfer step and eliminate the need for desorption

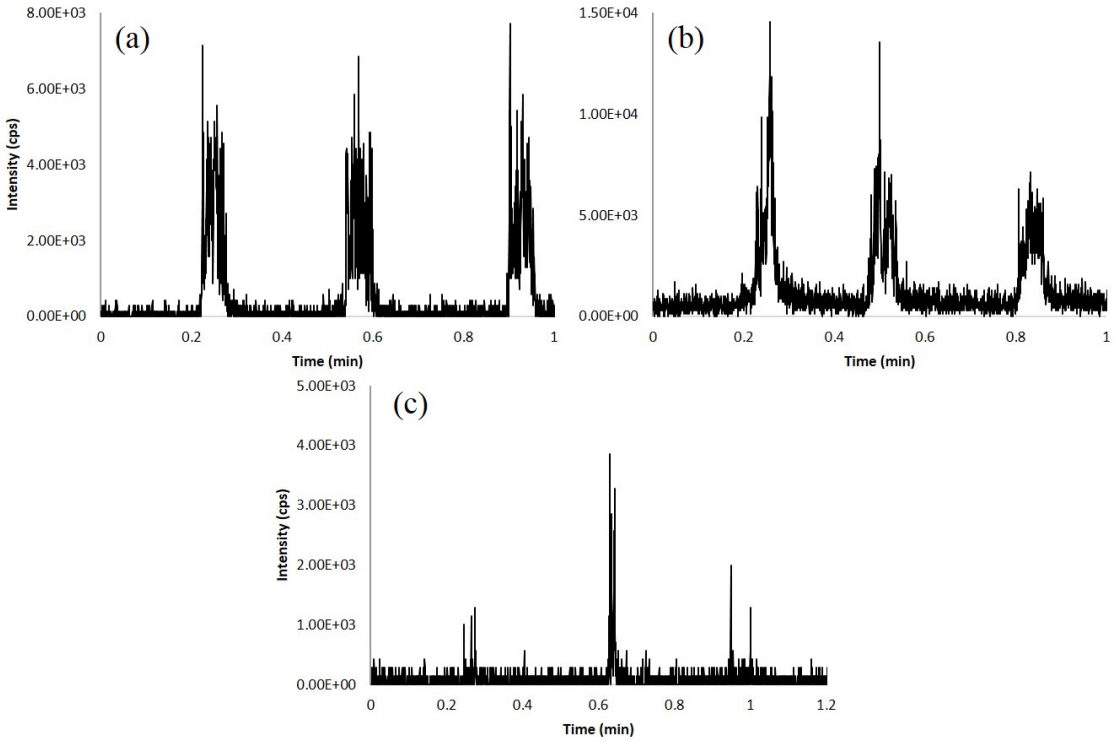

Figure 9.6. Mass spectra showing limits of detection for fentanyl 500 pg (a), mephedrone 500 pg (b) and MDMA 4 ng (c). LODs were measured by using the peak-to-peak noise with a signal-to-noise ratio of at least 3.5.

by introducing the molecules in the gas phase (volatilised liquid) likely leading to an increase in sensitivity as mentioned in section 10.2.

Once the limits of detection were established, the DBD Ion Source could be used to analyse banknotes for contamination. For these experiments, paper and polymer banknotes were obtained from Lloyds TSB in Patchway, Bristol, UK. Paper banknotes consisted of £1000 in mixed denominations of £50 and £20 notes and the polymer banknotes consisted of £1000 in mixed denominations of £10 and £5 notes. These samples are referred to as background samples. The samples were analysed using a multiple reaction monitoring (MRM) method that contained all seven drug analytes each with two ion pairs, resulting in 14 ion transitions.

For analysis, the banknotes were passed from right to left one at a time, by sliding them through the 4 mm gap in the DBD Ion Source and holding them in the centre for roughly 1 second, before removing again, resulting in an overall analysis time of roughly 2 seconds per banknote. The results from paper banknotes are much more difficult to compare to the data obtained with TEIS because liberation of the samples from paper with the DBD Ion Source is not as efficient as thermal desorption and therefore, the peaks are an order of magnitude different in intensity. However, the polymer background

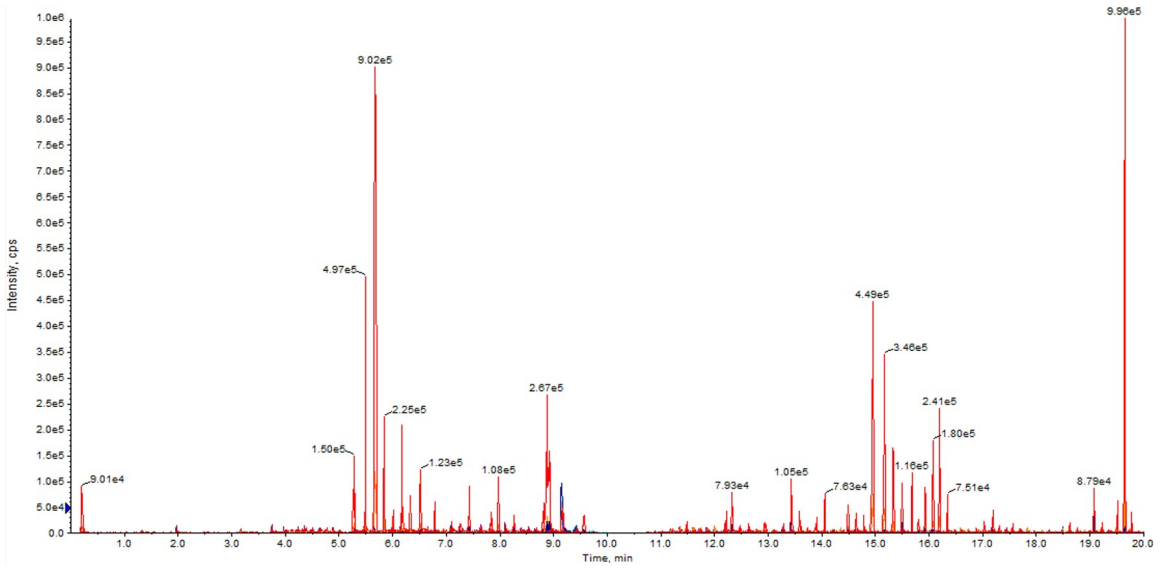

Figure 9.7. MRM scan data against time for paper banknotes analysed using DBD Ion Source. The trace in red is for the dominant transition of cocaine at m/z 304 to product ion m/z 105. The linear dynamic range for this instrument is 1 x 10^4 ion counts per second to 1 x 10^7 ion counts per second for cocaine. It is evident that the degree of contamination varies between each note.

sample can be compared rather easily. For the TEIS analysis of the polymer background the Queen's head side of notes were swabbed with a pre-tested piece of paper and the paper swab was subjected to the TEIS in the same way.

The predominant transition in Fig. 9.7 (coloured red) is for the m/z 304/182 cocaine transition, the other drugs are seldom seen on banknotes in general circulation however, there are a handful of banknotes in this sample that contain low levels of ketamine (not easily viewed in the data) which is normal for general circulation monies. It can be seen in Fig. 9.7 that the ion intensities of the transitions are quite low with only a few banknotes reaching higher intensities. This is evidence to the fact that some banknotes will contain more contamination than others and can therefore, be distinguished from banknotes containing low levels of contamination. In the background sample seen in Fig. 9.7, four or five banknotes are significantly higher in intensity than the rest. This equates to about 5% of banknotes, which is to be expected in general circulation. Any monies that have been involved in drug related activities would typically display a much higher percentage of high intensity banknotes allowing inference to be drawn on their source i.e. it would be unlikely that a sample containing many banknotes with high intensities of contamination would have originated directly from a general circulation source such as an ATM or a bank [69].

It is important to note that there are many other factors that determine whether a seized sample of banknotes could have come from a general circulation source or

whether it is likely they have been associated with drug related activities. Additional information such as number of banknotes, pattern distribution of the peaks and others must be taken into account before an experts' interpretation is given on the hypothesis.

In contrast, the polymer banknote background in Fig. 9.8 shows a much higher intensity of ions for all banknotes, this is due to the matrix of the polymer not being quite as complex as paper and the smooth surface of the polymer allows for desorption/liberation of the sample to occur more efficiently. However, a similar pattern emerges with the polymer banknote background than with paper in that there are only a couple of banknotes that have greater intensities, which is comparable to a separate polymer note background that had been analysed by TEIS via swabbing with paper swabs in Fig. 9.8 (b).

For the purpose of comparison, in Fig. 9.9 a seized exhibit is shown that has been analysed by swabbing and TEIS; this is a case where, due to the cocaine contamination support was given for the hypothesis that these banknotes (within the whole case, not based on this exhibit alone) had likely been involved with drug related activities. It is clear when comparing the cocaine intensities between Fig. 9.9 and Fig. 9.8 (b) that the intensities and quantity of high intensity banknotes is much greater in Fig. 9.9 suggesting that it does not conform to what one might expect to see in terms of the contamination of banknotes from general circulation. However, It is important to note that inference on case samples will not be drawn from comparing only one background sample, but a database of many. These figures are for understanding and visual purposes only.

Although only cocaine has been demonstrated for real-life samples, the data presented here suggests that the DBD Ion Source would be sufficient for the examination of polymer banknotes for drug contamination and would be a suitable technique to replace the TEIS, eliminating the need for thermal desorption. However, there is still some development required for compounds such as (5,6)-7,8-didehydro-4,5-epoxy-17-methylmorphinan-3,6-diol diacetate (diacetylmorphine/heroin) and ()-(6aR,10aR)-6,6,9-trimethyl- 3-pentyl-6a,7,8,10a-tetrahydro- 6H-benzo[c]chromen-1-ol (Δ^9-Tetrahydrocannabinol/THC) which have proved to be more difficult to detect with the DBD Ion Source than the other compounds.

9.4 Conclusions

The DBD Ion Source has demonstrated that it is capable of analysing target drug analytes of various structural formations from a polymer surface to reasonable limits of

detection. Further, the DBD Ion Source has exhibited its potential to replace current technologies for the purpose of drugs on money examinations without the need for any sample preparation or thermal desorption. Therefore, presented here is a DBD Ion Source capable of detecting analytes to reasonable limits of detection that is reliable, rapid and has a large sampling surface area. Despite this though, there are still further improvements that could be made to the DBD Ion Source which is discussed in the following chapter.

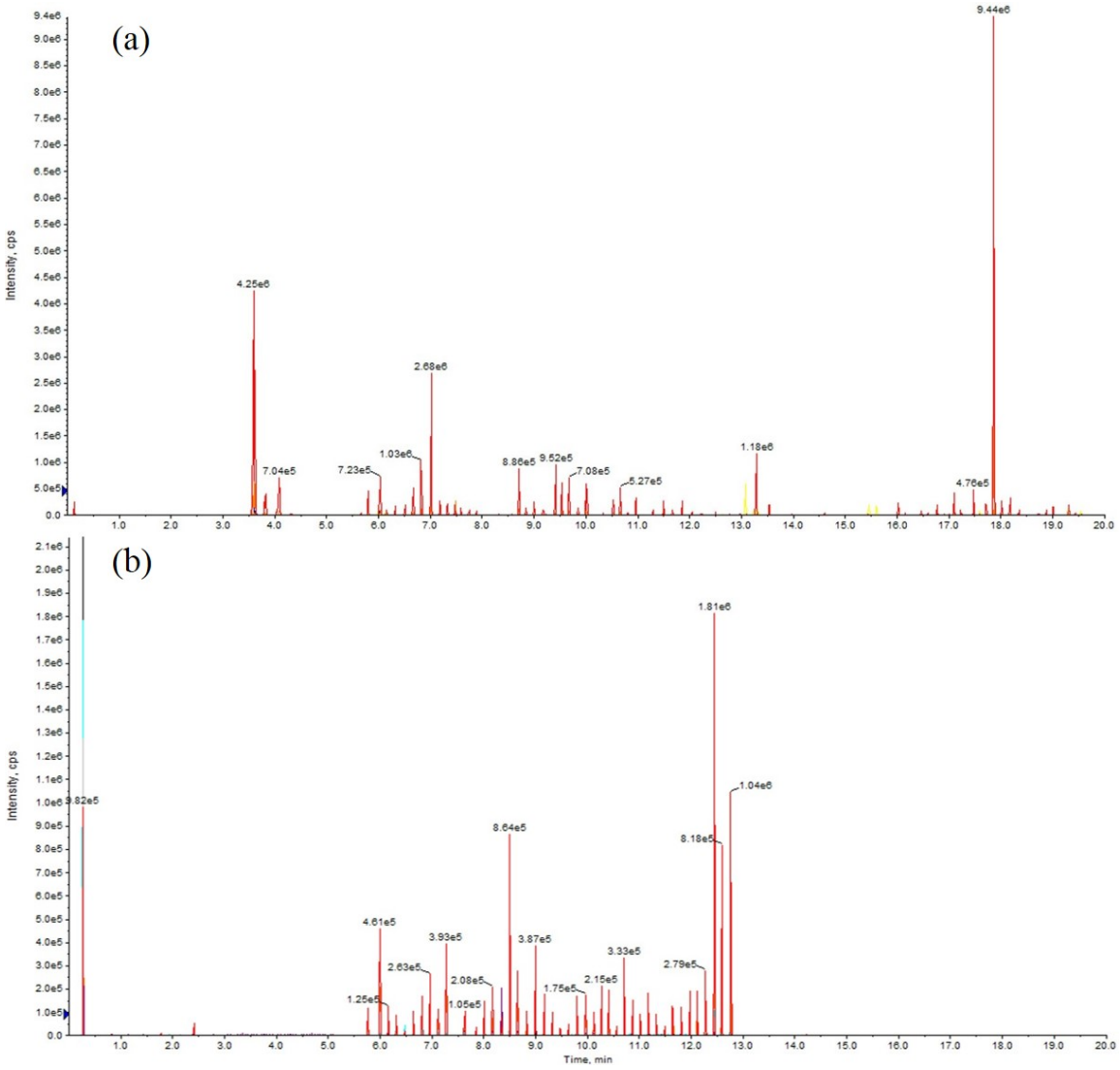

Figure 9.8. Data from MRM scans over time for polymer banknote background samples using a method containing 14 transitions, 2 for each analyte of interest. MRM data shown in (a) were polymer banknotes analysed using the DBD Ion source coupled with an AB Sciex API 2000 tandem mass spectrometer. MRM data shown in (b) were polymer banknotes analysed via using a dry paper swab and analysing using the TEIS couple with MS/MS. The major red trace shown in both (a) and (b) is for cocaine at m/z 304 to product ion m/z 105.

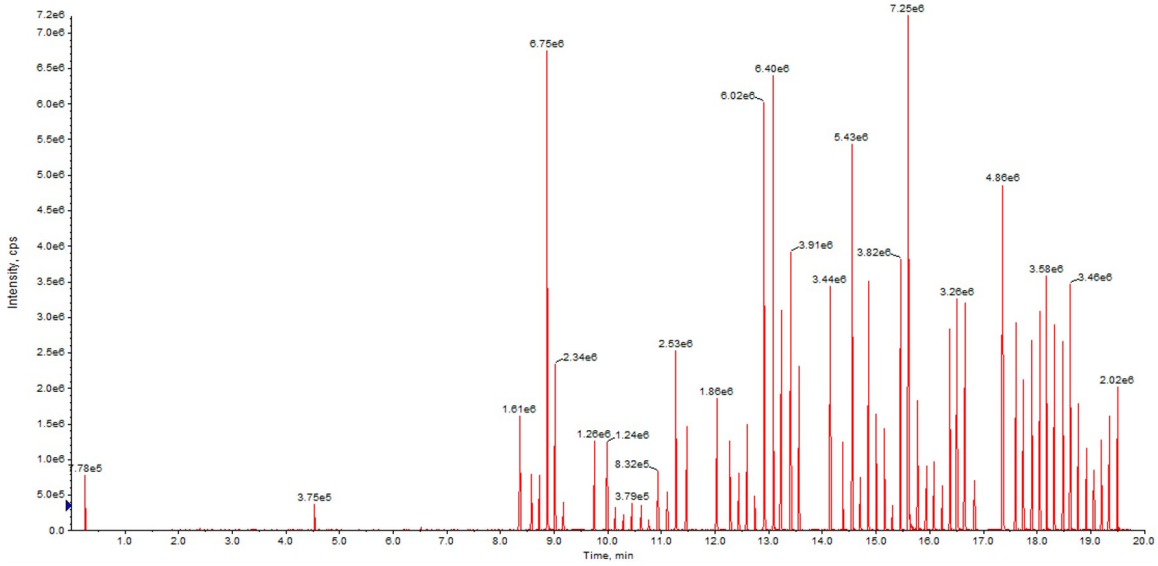

Figure 9.9. Data of an MRM scan of cocaine at m/z 304 to product ion m/z 105 from polymer banknotes that were seized as evidence in a criminal investigation and analysed using TEIS (via swabbing with paper). It can be seen that the intensity of the cocaine contamination is much greater than the polymer backgrounds analysed via TEIS, suggesting that these banknotes have become contaminated via contact with drug related activities.

Chapter 10

Conclusions

10.1 Summary

This thesis presents several novel plasma based ionisation sources for mass spectrometry. An extensive literature review was performed, bringing together a thorough comparison of many of the widely used ambient ionisation techniques. This literature review uncovered that the main disadvantages of the current techniques were that they all encompassed a small sampling surface area and nearly all required either a special discharge gas such as helium, or a solvent. This thesis focussed on developing a plasma based ionisation source that could analyse small molecules, typically drugs and explosives from various surfaces, with a large sampling surface area, minimal sample preparation and minimal consumables.

It was decided that a plasma jet (an existing plasma source from the literature) would be used as the premise for the development because other plasma based techniques such as DART and DESI were already commercially available, and a plasma jet is comparatively very simple in construction and operation. In order to satisfy the aims, it was decided an attempt to make the opening of the plasma jet wider would result in a suitable ionisation source, called the plasma brush. However, the plasma brush did not result in any ion formation or at least not any that was detected within a mass spectrometer. A likely explanation is that, due to the same power requirements as a much smaller plasma jet being used but now over a much wider area, locally and at the surface, the plasma ionisation potential was much reduced. As the desorption/ionisation is largely due to the excited helium metastables within the plasma, the spreading of these species resulted in no sample being detected.

Following the failure of the plasma brush, the idea that using several plasma jets as opposed to making the jets themselves larger was proposed, and an ionisation source referred to as a plasma jet array was developed. The plasma jet array was

slightly successful in that some ions were detected within the mass spectrometer however, it did have some major disadvantages. Firstly, it would be rather difficult to align the plasma jet array to the orifice of the mass spectrometer which has shown to be crucial as the orifice is only a few microns in diameter and the plasma array encompasses an area of roughly 500 mm^2. It would have been possible to introduce a pump to draw ions towards the orifice, however, this proved to be detrimental to the performance of the plasma jet array as it disturbed the helium flow resulting in an unstable plasma formation. Finally, the largest disadvantage of the plasma jet array was that it operated with a significantly higher flow of helium which is a declining natural source and so the plasma jet array was deemed not to be a viable ionisation source.

Despite having a large surface area, it was concluded that having a large flow of helium would not be suitable as it is a limited, non-renewable resource and high cost consumable. To overcome this issue, a surface barrier discharge ionisation source was developed. This type of ionisation source was novel in its design and application to be used with mass spectrometry, resulted in a Great Britain patent application which is pending. The surface barrier discharge referred to as the DBD Ion Source demonstrated versatility by being easily integrated with various mass spectrometers and also showed great promise for drug and explosive detection from picogram to low nanogram detection limits. The analysis of UK polymer banknotes for drug contamination is a novel application and may be suitable to replace current thermal desorption based techniques currently used for this application.

Furthermore, the DBD Ion Source demonstrated the ability to detect ions in both positive and negative ion modes, suggesting a potential for many other small molecule applications. Also, and most importantly, the DBD Ion Source operates with a large sampling surface area, in ambient air circumventing the need for any special discharge gases or solvents with minimal sample preparation or consumables resulting in a rapid, sensitive technique that when coupled with mass spectrometry, affords high specificity, selectivity and high-throughput analysis.

Should the DBD Ion Source be made commercially available, there are some elements that would need to be improved and addressed which would form the basis of future research and would consist of a more robust, reproducible design, with a much simpler, easier to use power supply that non-scientists could use without compromise to safety as discussed in the next section.

10.2 Future Development of DBD Ion Source

10.2.1 Electrode Composition

The electrodes are currently composed of a copper adhesive tape but there are many disadvantages to this. Firstly, there is great variation in each electrode due to the electrodes being cut by hand; secondly, the adhesives begin to spoil under the heat and plasma process which results in the electrodes lifting from the surface, creating air gaps and risk of arcing. Additionally, the copper tape itself is very susceptible to oxidation via ozone produced in the plasma, causing the copper to warp, discolour and become soiled, reducing its life span. Finally, when used in the format of the DBD Ion Source where a banknote or swab is analysed by means of passing them through the DBD Ion Source, the electrodes snag due to the raised height of the copper. Snagging of a swab or banknote could result in an erroneous result by subjecting them to the plasma far away from the orifice which may negatively effect the ion transmission into the orifice as well over-exposing the swab/banknote to the plasma potentially causing long term damage.

To overcome this, as before mentioned in chapter 7, the idea of sputtering electrodes within a low pressure magnetron has shown some potential. The sputtering process will result in a very thin layer of tungsten (or other material) on the alumina, in the order of few microns thick, which requires no adhesive, is thermally stable and much more resistant to oxidation. However, the experiments previously described are limited to proof of concept and this idea requires a thorough experimentation which would be a topic for future development. Sputtering may not be the only suitable technique for this application as electroplating and others may be possible and potentially more feasible.

10.2.2 Electrode Configuration

The design of the electrode may be important to influence several factors. Having more electrodes results in a larger plasma region (or regions where plasma occurs) and larger sampling surface area however, these plasma regions are further away from the mass spectrometer, resulting in low ion transmission. If the electrodes were smaller in width, the electrodes would then be able to be bunched closer together and closer to the mass spectrometer but again, a thinner electrode may negatively effect the ionic wind strength. While some experimentation has been conducted into the electrode size and shape, there are a large amount of unknowns which could still benefit the application, but may require a lot of research in order to be fully understood.

Previous experiments adopted a chevron shaped electrode which did work to a similar

extent to straight electrodes but it was decided that chevron shaped electrodes were not viable due to the increase in heat at the sharp edges and difficulty in making them. Despite this though, it is possible that shaping the electrodes in such a way that it focusses the ionic wind in the direction of the mass spectrometer could be advantageous as it may reduce some of the losses that may occur otherwise. However, to understand the effects that the shape of the electrodes have on the ionic wind, and the effects that the ionic wind has on the ions themselves will require a deep and thorough investigation coupling theoretical simulations with experimentation which would be rather time consuming.

Finally, as there are several electrodes within the DBD Ion Source, all connected to the same power supply, there does not seem to be an even share of the current between the electrodes. As a result, the powered electrode closest to the mass spectrometer, which is also nearest the power supply, reaches a temperature much higher than the other electrodes in the series. There have been previous studies using several plasma jets similar to the plasma array where it has been found that an individual ballast resistor or capacitative ballast enables every single jet to ignite, whereas without it, only a few jets may ignite [77, 78]. To eliminate the issue of variably heated electrodes, the prospect of introducing ballast resistors between each electrode might help to evenly distribute the current, allowing for more flexibility in operating conditions because the overall DBD Ion Source temperature will likely reduce.

10.2.3 Overall Source Design

It is still required for the plenum chamber to undergo further development and experimentation. It is understood that the further the ions have to travel from the plasma, the less ions make it to the mass spectrometer and therefore, reducing the length of the plenum chamber and transfer line could lead to an increase in sensitivity. Furthermore, it is well known that some samples, such as explosives, can condensate on the walls of a transfer line or plenum chamber if they are at ambient temperature which could add to additional losses in sensitivity. Experiments into a heating the plenum chamber and transfer line may be useful to increase ion sensitivity.

Currently, the limits of detection for both the drugs and explosives are limited by the fact that to introduce a sample into the DBD Ion Source, a solution is spotted onto a glass slide and then swabbed, introducing what is possibly an unnecessary transfer step. Eliminating the transfer step would inevitably increase the sensitivity and this could be achieved by direct injections of a liquid sample. Direct injections however, are not possible with the current design due to metal syringes and conducting solvents, as

an injection would be via the powered electrodes, posing a potential health risk to the analyst. Modifications to the source, may include an attachment that fits to the front of the DBD Ion Source containing a heated transfer line. This transfer line would be safe for the syringe as it will be far enough from the electrodes and if hot enough, would volatilise the solution into gaseous form whereby the gaseous molecules can be ionised by the DBD Ion Source.

Finally, safety for an end user is crucial for commercial success and currently, the connections to the power supply are exposed and pose an electrical safety concern. For the DBD Ion Source to be safer for an end user, the wires connected to the powered electrodes and the power supply should be embedded within the source housing where they cannot be touched or accidentally handled, ideally within an inert material. Embedding the electrodes should be relatively simple and this would also allow for an increased ease of operation for an analyst as it would reduce the amount of obstructions.

10.2.4 Bespoke Power Supply for an End User

The equipment used to supply an AC sinusoidal high voltage to the DBD Ion Source is rather large and complicated, especially for untrained personnel. Additionally, the power supply equipment has a vast array of functions that are not necessary for a likely end user of the DBD Ion Source and so, a bespoke power supply would be more suitable. The bespoke power supply would be capable of providing the same power requirements, coping with the current and load capacities, but without having as much variability in the parameters available. Limiting the options on the power supply will allow for a much more compact power supply with simple operation options such as 'ON/OFF', allowing a non-scientist to operate the DBD Ion Source easily and safely. To design a bespoke power supply will require a specific set of expertise, time, money and development that was not available for this project and will therefore, hopefully be a priority for future development.

10.2.5 Mass Spectrometric Investigations

As there is limited information of a DBD Ion Source or SBD being used with mass spectrometry, the technique is not yet fully understood. It is understood how the NO_3^- is created in negative mode for example, but it is not understood when during the AC sine wave duty cycles this is generated and whether or not further knowledge of this could be useful. For example, if time resolved mass spectrometry was used with the DBD Ion Source, where the mass spectrometer was able to detect when exactly in the duty cycle ions were produced, it may be able to present additional information. The NO_3^- can

be used as an adduct for some application such as explosives detection, but in scenarios where it is favourable that the NO_3^- ion is not produced, using time resolved mass spectrometry to establish when and how it is created may provide an insight into how the power supply could be manipulated in a way so that the NO_3^- ion is not produced for example, by changing the symmetry of the duty cycles.

Finally, a large feature for future development of the DBD Ion Source will consist of expanding the suite of compounds that can be readily detected. Currently, the DBD Ion Source has demonstrated detection of at least seven drugs and four explosives which is not an exhaustive list and therefore, it would be of interest to add more analytes, especially ones of interest to other applications but also of sample states such as gas vapours. The addition of an attachment that allows for direct injections will be essential to increase the range of detectable analytes and direct injections would enable much more reproducible results when optimising and establishing limits of detection.

Bibliography

[1] Stout, P. R., Bynum, N. D., Mitchell, J. M., Baylor, M. R., and Ropero-Miller, J. D. (2009) A comparison of the validity of gas chromatography- mass spectrometry and liquid chromatography- tandem mass spectrometry analysis of urine samples for morphine, codeine, 6-acetylmorphine, and benzoylecgonine. *Journal of analytical toxicology*, **33**, 398–408.

[2] Stout, P. and Bynum, N. (2010) A comparison of the Validity of Gas Chromatography-Mass Spectrometry and Liquid Chromatography-Tandem Mass Spectrometry Analysis of Urine Samples II: Amphetamine, Methamphetamine. *Journal of analytical toxicology*, **34**, 430–443.

[3] Marin, S. J., Hughes, J. M., Lawlor, B. G., Clark, C. J., and McMillin, G. A. (2012) Rapid screening for 67 drugs and metabolites in serum or plasma by accurate-mass LC-TOF-MS. *Journal of analytical toxicology*, **36**, 477–86.

[4] Borsdorf, H., Mayer, T., Zarejousheghani, M., and Eiceman, G. A. (2011) Recent developments in ion mobility spectrometry. *Applied Spectroscopy Reviews*, **46**, 472–521.

[5] Fletcher, C. M. and Sleeman, R. (2016) Rapid identification of seized controlled substances and related compounds by tandem mass spectrometry without chromatography. *Rapid Communications in Mass Spectrometry*, **30**, 908–916.

[6] M. Lindström (1991) Improved enantiomer separation using very short: Capillary columns coated with permethylated β-cyclodextrin. *Journal of High Resolution Chromatography*, **14**, 765–767.

[7] Statheropoulos, M., Tzamtzis, N., and Mikedi, K. (1998) Short column gas chromatographymass spectrometry and principal component analysis for the identification of coeluted substances in doping control analysis. *Journal of Chromatography B: Biomedical Sciences and Applications*, **706**, 245–251.

[8] Ewing, R. (2001) A critical review of ion mobility spectrometry for the detection of explosives and explosive related compounds. *Talanta*, **54**, 515–529.

[9] Hill, H. H. and Simpson, G. (1997) Capabilities and limitations of ion mobility spectrometry for field screening applications. *Field Analytical Chemistry & Technology*, **1**, 119–134.

[10] Goldston, R. J. and Rutherford, P. H. (1995) *Introduction to plasma physics*. CRC Press.

[11] Lu, X., Laroussi, M., and Puech, V. (2012) On atmospheric-pressure non-equilibrium plasma jets and plasma bullets. *Plasma Sources Science and Technology*, **21**, 034005.

[12] Märk, T. D. (1995) Dissociative ionization by electron impact. *Electron Impact Ionization of Plasma Edge Atoms*, **34**, 2083–2090.

[13] Shang, J. J. S. (2018) Modeling Plasma via Electron Impact Ionization. *Aerospace*, **5**, 1–25.

[14] Cody, R. B., Laramée, J. A., and Durst, H. D. (2005) Versatile new ion source for the analysis of materials in open air under ambient conditions. *Analytical chemistry*, **77**, 2297–302.

[15] Jjunju, F. P. M., Maher, S., Li, A., Syed, S. U., Smith, B., Heeren, R. M. A., Taylor, S., and Cooks, R. G. (2015) Hand-Held Portable Desorption Atmospheric Pressure Chemical Ionization Ion Source for in Situ Analysis of Nitroaromatic Explosives. *Analytical chemistry*, **87**, 10047–10055.

[16] Takáts, Z., Wiseman, J. M., Gologan, B., and Cooks, R. G. (2004) Mass spectrometry sampling under ambient conditions with desorption electrospray ionization. *Science (New York, N.Y.)*, **306**, 471–3.

[17] Harper, J. D., Charipar, N. A., Mulligan, C. C., Zhang, X., Cooks, R. G., and Ouyang, Z. (2008) Low-temperature plasma probe for ambient desorption ionization. *Analytical chemistry*, **80**, 9097–104.

[18] Na, N., Zhang, C., Zhao, M., Zhang, S., Yang, C., Fang, X., and Zhang, X. (2007) Direct detection of explosives on solid surfaces by mass spectrometry with an ambient ion source based on dielectric barrier discharge. *Journal of Mass Spectrometry*, **42**, 1079–1085.

[19] Ratcliffe, L. V., Rutten, F. J. M., Barrett, D. A., Whitmore, T., Seymour, D., Greenwood, C., Aranda-Gonzalvo, Y., Robinson, S., and McCoustra, M. (2007) Surface analysis under ambient conditions using plasma-assisted desorption/ionization mass spectrometry. *Analytical chemistry*, **79**, 6094–101.

[20] Stoffels, E., Flikweert, A. J., Stoffels, W. W., and Kroesen, G. M. W. (2002) Plasma needle: a non-destructive atmospheric plasma source for fine surface treatment of (bio)materials. *Plasma Sources Science and Technology*, **11**, 383–388.

[21] Symonds, J. M., Galhena, A. S., Fernández, F. M., and Orlando, T. M. (2010) Microplasma discharge ionization source for ambient mass spectrometry. *Analytical chemistry*, **82**, 621–7.

[22] Iwai, T., Kakegawa, K., Okumura, K., Kanamori-Kataoka, M., Miyahara, H., Seto, Y., and Okino, A. (2014) Fundamental properties of a touchable high-power pulsed microplasma jet and its application as a desorption/ionization source for ambient mass spectrometry. *Journal of mass spectrometry : JMS*, **49**, 522–8.

[23] Shelley, J. T., Ray, S. J., and Hieftje, G. M. (2008) Laser ablation coupled to a flowing atmospheric pressure afterglow for ambient mass spectral imaging. *Analytical chemistry*, **80**, 8308–13.

[24] Andrade, F. J., Shelley, J. T., Wetzel, W. C., Webb, M. R., Gamez, G., Ray, S. J., and Hieftje, G. M. (2008) Atmospheric pressure chemical ionization source. 2. Desorption-ionization for the direct analysis of solid compounds. *Analytical chemistry*, **80**, 2654–63.

[25] Andrade, F. J., Shelley, J. T., Wetzel, W. C., Webb, M. R., Gamez, G., Ray, S. J., and Hieftje, G. M. (2008) Atmospheric pressure chemical ionization source. 1. Ionization of compounds in the gas phase. *Analytical chemistry*, **80**, 2646–53.

[26] Polyakova, O. V., Mazur, D. M., Artaev, V. B., and Lebedev, A. T. (2013) Determination of polycyclic aromatic hydrocarbons in water by gas chromatography/mass spectrometry with accelerated sample preparation. *Journal of Analytical Chemistry*, **68**, 1099–1103.

[27] Moore, D. S. (2004) Instrumentation for trace detection of high explosives. *Review of Scientific Instruments*, **75**, 2499–2512.

[28] Wang, H., Manicke, N. E., Yang, Q., Zheng, L., Shi, R., Cooks, R. G., and Ouyang, Z. (2011) Direct analysis of biological tissue by paper spray mass spectrometry. *Analytical chemistry*, **83**, 1197–201.

[29] Ebejer, K. A., Brereton, R. G., Carter, J. F., Ollerton, S. L., and Sleeman, R. (2005) Rapid comparison of diacetylmorphine on banknotes by tandem mass spectrometry. *Rapid communications in mass spectrometry : RCM*, **19**, 2137–43.

[30] Liu, Y., Lin, Z., Zhang, S., Yang, C., and Zhang, X. (2009) Rapid screening of active ingredients in drugs by mass spectrometry with low-temperature plasma probe. *Analytical and bioanalytical chemistry*, **395**, 591–9.

[31] Martínez-Jarquín, S. and Winkler, R. (2013) Design of a low-temperature plasma (LTP) probe with adjustable output temperature and variable beam diameter for the direct detection of organic molecules. *Rapid communications in mass spectrometry : RCM*, **27**, 629–34.

[32] Chan, G. C.-Y., Shelley, J. T., Jackson, A. U., Wiley, J. S., Engelhard, C., Cooks, R. G., and Hieftje, G. M. (2011) Spectroscopic plasma diagnostics on a low-temperature plasma probe for ambient mass spectrometry. *Journal of Analytical Atomic Spectrometry*, **26**, 1434–1444.

[33] McKay, K., Salter, T. L., Bowfield, A., Walsh, J. L., Gilmore, I. S., and Bradley, J. W. (2014) Comparison of three plasma sources for ambient desorption/ionization mass spectrometry. *Journal of the American Society for Mass Spectrometry*, **25**, 1528–37.

[34] Salter, T. L., Gilmore, I. S., Bowfield, A., Olabanji, O. T., and Bradley, J. W. (2013) Ambient Surface Mass Spectrometry Using Plasma-Assisted Desorption Ionization: Effects and Optimization of Analytical Parameters for Signal Intensities of Molecules and Polymers. *Analytical Chemistry*, **85**, 1675–1682.

[35] Walsh, J. L., Shi, J. J., and Kong, M. G. (2006) Contrasting characteristics of pulsed and sinusoidal cold atmospheric plasma jets. *Applied Physics Letters*, **88**, 171501.

[36] Walsh, J. L. and Kong, M. G. (2008) Contrasting characteristics of linear-field and cross-field atmospheric plasma jets. *Applied Physics Letters*, **93**, 111501.

[37] Shelley, J. T., Stindt, A., Riedel, J., and Engelhard, C. (2014) Time-resolved mass-spectral characterization of ion formation from a low-frequency, low-temperature plasma probe ambient ionization source. *Journal of Analytical Atomic Spectrometry*, **29**, 359–366.

[38] Klee, S., et al. (2014) Are clusters important in understanding the mechanisms in atmospheric pressure ionization? Part 1: Reagent ion generation and chemical control of ion populations. *Journal of the American Society for Mass Spectrometry*, **25**, 1310–21.

[39] Chen, C.-H., Lin, Z., Garimella, S., Zheng, L., Shi, R., Cooks, R. G., and Ouyang, Z. (2013) Development of a mass spectrometry sampling probe for chemical analysis in surgical and endoscopic procedures. *Analytical chemistry*, **85**, 11843–50.

[40] Dalgleish, J. K., Hou, K., Ouyang, Z., and Cooks, R. G. (2012) In Situ Explosive Detection Using a Miniature Plasma Ion Source and a Portable Mass Spectrometer. *Analytical Letters*, **45**, 1440–1446.

[41] Hendricks, P. I., et al. (2014) Autonomous in situ analysis and real-time chemical detection using a backpack miniature mass spectrometer: concept, instrumentation development, and performance. *Analytical chemistry*, **86**, 2900–8.

[42] Wiley, J. S., Shelley, J. T., and Cooks, R. G. (2013) Handheld low-temperature plasma probe for portable "point-and-shoot" ambient ionization mass spectrometry. *Analytical chemistry*, **85**, 6545–52.

[43] Abd-Allah, Z., Sawtell, D. A. G., McKay, K., West, G. T., Kelly, P. J., and Bradley, J. W. (2015) Mass spectrometric investigation of the ionic species in a dielectric barrier discharge operating in helium-water vapour mixtures. *Journal of Physics D: Applied Physics*, **48**, 085202.

[44] Oh, J.-S., Bryant, P. M., and Bradley, J. W. (2011) Discharge and Plasma Bullet Formation in a Capillary DBD Atmospheric-Pressure Microplasma Jet. *IEEE Transactions on Plasma Science*, **39**, 2352–2353.

[45] Walsh, J. L., Olszewski, P., and Bradley, J. W. (2012) The manipulation of atmospheric pressure dielectric barrier plasma jets. *Plasma Sources Science and Technology*, **21**, 034007.

[46] Hayen, H., Michels, A., and Franzke, J. (2009) Dielectric barrier discharge ionization for liquid chromatography/mass spectrometry. *Analytical chemistry*, **81**, 10239–45.

[47] Bowfield, A., Barrett, D. A., Alexander, M. R., Ortori, C. A., Rutten, F. M., Salter, T. L., Gilmore, I. S., and Bradley, J. W. (2012) Surface analysis using a new plasma assisted desorption/ionisation source for mass spectrometry in ambient air. *The Review of scientific instruments*, **83**, 063503.

[48] McKay, K., Oh, J.-S., Walsh, J. L., and Bradley, J. W. (2013) Mass spectrometric diagnosis of an atmospheric pressure helium microplasma jet. *Journal of Physics D: Applied Physics*, **46**, 464018.

[49] Brewer, T. M. and Verkouteren, J. R. (2011) Atmospheric identification of active ingredients in over-the-counter pharmaceuticals and drugs of abuse by atmospheric pressure glow discharge mass spectrometry (APGD-MS). *Rapid communications in mass spectrometry : RCM*, **25**, 2407–17.

[50] Marcus, R. K., Burdette, C. Q., Manard, B. T., and Zhang, L. X. (2013) Ambient desorption/ionization mass spectrometry using a liquid sampling-atmospheric

glow discharge (LS-APGD) ionization source. *Analytical and bioanalytical chemistry*, **405**, 8171–84.

[51] Marcus, R. K., Quarles, C. D., Barinaga, C. J., Carado, A. J., and Koppenaal, D. W. (2011) Liquid sampling-atmospheric pressure glow discharge ionization source for elemental mass spectrometry. *Analytical chemistry*, **83**, 2425–9.

[52] Shelley, J. T., Wiley, J. S., and Hieftje, G. M. (2011) Ultrasensitive ambient mass spectrometric analysis with a pin-to-capillary flowing atmospheric-pressure afterglow source. *Analytical chemistry*, **83**, 5741–8.

[53] Pfeuffer, K., Schaper, J., and Shelley, J. (2013) Halo-Shaped Flowing Atmospheric Pressure Afterglow: A Heavenly Design for Simplified Sample Introduction and Improved Ionization in Ambient Mass Spectrometry. *Analytical chemistry*, **85**, 7512–7518.

[54] Schaper, J., Pfeuffer, K., and Shelley, J. (2012) Drop-on-Demand Sample Introduction System Coupled with the Flowing Atmospheric-Pressure Afterglow for Direct Molecular Analysis of Complex Liquid Microvolume. *Analytical chemistry*, **84**, 9246–9252.

[55] Albert, A., Shelley, J. T., and Engelhard, C. (2014) Plasma-based ambient desorption/ionization mass spectrometry: state-of-the-art in qualitative and quantitative analysis. *Analytical and bioanalytical chemistry*, **406**, 6111–27.

[56] Shelley, J. T. and Hieftje, G. M. (2010) Ionization matrix effects in plasma-based ambient mass spectrometry sources. *Journal of Analytical Atomic Spectrometry*, **25**, 345–350.

[57] Dalgleish, J. K., Wleklinski, M., Shelley, J. T., Mulligan, C. C., Ouyang, Z., and Graham Cooks, R. (2013) Arrays of low-temperature plasma probes for ambient ionization mass spectrometry. *Rapid communications in mass spectrometry : RCM*, **27**, 135–42.

[58] Jõgi, I., Talviste, R., Raud, J., Piip, K., and Paris, P. (2014) The influence of the tube diameter on the properties of an atmospheric pressure He micro-plasma jet. *Journal of Physics D: Applied Physics*, **47**, 415202.

[59] Chen, W., Huang, J., Du, N., Liu, X.-D., Wang, X.-Q., Lv, G.-H., Zhang, G.-P., Guo, L.-H., and Yang, S.-Z. (2012) Treatment of enterococcus faecalis bacteria by a helium atmospheric cold plasma brush with oxygen addition. *Journal of Applied Physics*, **112**, 013304.

[60] Fletcher, C., Sleeman, R., Luke, J., Luke, P., and Bradley, J. W. (2017) Explosive Detection Using a Novel Dielectric Barrier Discharge Ionisation Source for Mass Spectrometry. *Journal of Mass Spectrometry*, **53**, 214–222.

[61] Thomas, F. O., Corke, T. C., Iqbal, M., Kozlov, A., and Schatzman, D. (2009) Optimization of Dielectric Barrier Discharge Plasma Actuators for Active Aerodynamic Flow Control. *AIAA Journal*, **47**, 2169–2178.

[62] Erfani, R., Zare-Behtash, H., Hale, C., and Kontis, K. (2015) Development of DBD plasma actuators: The double encapsulated electrode. *Acta Astronautica*, **109**, 132–143.

[63] Robinson, M. (1962) A History of the Electric Wind. *American Journal of Physics*, **30**, 366–372.

[64] Forte, M., Jolibois, J., Pons, J., Moreau, E., Touchard, G., and Cazalens, M. (2007) Optimization of a dielectric barrier discharge actuator by stationary and non-stationary measurements of the induced flow velocity: Application to airflow control. *Experiments in Fluids*, **43**, 917–928.

[65] Shelley, J. T., Wiley, J. S., Chan, G. C. Y., Schilling, G. D., Ray, S. J., and Hieftje, G. M. (2009) Characterization of direct-current atmospheric-pressure discharges useful for ambient desorption/ionization mass spectrometry. *Journal of the American Society for Mass Spectrometry*, **20**, 837–44.

[66] Davide, B. and Buck, U. (1988) Atomic and molecular beam methods. Scoles, G. (ed.), *Atomic and Molecular Beam Methods*, vol. 1, pp. 499–524, Oxford university press, g. scoles edn.

[67] Horcas, I., Fernández, R., Gómez-Rodríguez, J. M., Colchero, J., Gómez-Herrero, J., and Baro, A. M. (2007) WSXM: A software for scanning probe microscopy and a tool for nanotechnology. *Review of Scientific Instruments*, **78**, 013705.

[68] Dixon, S. J., Brereton, R. G., Carter, J. F., and Sleeman, R. (2006) Determination of cocaine contamination on banknotes using tandem mass spectrometry and pattern recognition. *Analytica Chimica Acta*, **559**, 54–63.

[69] Wilson, A., Aitken, C., Sleeman, R., and Carter, J. (2014) The evaluation of evidence relating to traces of cocaine on banknotes. *Forensic science international*, **236**, 67–76.

[70] Oh, J.-S., Aranda-Gonzalvo, Y., and Bradley, J. W. (2011) Time-resolved mass spectroscopic studies of an atmospheric-pressure helium microplasma jet. *Journal of Physics D: Applied Physics*, **44**, 365202.

[71] McKay, K., Walsh, J. L., and Bradley, J. W. (2013) Observations of ionic species produced in an atmospheric pressure pulse-modulated RF plasma needle. *Plasma Sources Science and Technology*, **22**, 035005.

[72] Evans, C. S., Sleeman, R., Luke, J., and Keely, B. J. (2002) A rapid and efficient mass spectrometric method for the analysis of explosives. *Rapid Communications in Mass Spectrometry*, **16**, 1883–1891.

[73] Tang, J., Cao, W., Zhao, W., Wang, Y., and Duan, Y. (2012) Characterization of stable brush-shaped large-volume plasma generated at ambient air. *Physics of Plasmas*, **19**, 013501.

[74] Li, X., Bao, W., Jia, P., and Di, C. (2014) A brush-shaped air plasma jet operated in glow discharge mode at atmospheric pressure. *Journal of Applied Physics*, **116**, 023302.

[75] Chen, Z., Zheng, X., Xia, G., Li, P., Hu, Y., Du, Z., Zhu, L., Liu, M., Chen, M., and Hu, X. (2014) A 30 mm Wide DC-Driven Brush-Shaped Cold Air Plasma Without Airflow Supplement. *Plasma Science and Technology*, **16**, 329–334.

[76] Chen, Q. and Ichiki, T. (2015) 80 mm-wide cold atmospheric-pressure plasma generated by two parallel but horizontally separated electrodes. *Plasma Sources Science and Technology*, **24**, 025022.

[77] Cao, Z., Walsh, J. L., and Kong, M. G. (2009) Atmospheric plasma jet array in parallel electric and gas flow fields for three-dimensional surface treatment. *Applied Physics Letters*, **94**, 021501.

[78] Ghasemi, M., Olszewski, P., Bradley, J. W., and Walsh, J. L. (2013) Interaction of multiple plasma plumes in an atmospheric pressure plasma jet array. *Journal of Physics D: Applied Physics*, **46**, 052001.

[79] Niu, J., Liu, D., Ji, L., Xia, Y., Bi, Z., Song, Y., Ma, Y., Huang, Y., Wang, W., and Yang, W. (2015) Propagation of brush-shaped He/O<inf>2</inf> plasma plumes in ambient air. *IEEE Transactions on Plasma Science*, **43**, 1993–1998.

[80] Cappella, B. and Dietler, G. (1999) Force-distance curves by atomic force microscopy. *Surface Science Reports*, **34**, 1–104.

[81] Navaneetha Pandiyaraj, K., Deshmukh, R., Arunkumar, A., Ramkumar, M., Ruzybayev, I., Ismat Shah, S., Su, P.-G., Periayah, M. H., and Halim, A. (2015) Evaluation of mechanism of non-thermal plasma effect on the surface of polypropylene films for enhancement of adhesive and hemo compatible properties. *Applied Surface Science*, **347**, 336–346.

[82] Pandiyaraj, K. N., Selvarajan, V., Deshmukh, R., and Gao, C. (2009) Modification of surface properties of polypropylene (PP) film using DC glow discharge air plasma. *Applied Surface Science*, **255**, 3965–3971.

[83] Kostov, K. G., Nishime, T. M. C., Castro, A. H. R., Toth, A., and Hein, L. R. O. (2014) Surface modification of polymeric materials by cold atmospheric plasma jet. *Applied Surface Science*, **314**, 367–375.

[84] Inbakumar, S., Morent, R., de Geyter, N., Desmet, T., Anukaliani, A., Dubruel, P., and Leys, C. (2010) Chemical and physical analysis of cotton fabrics plasma-treated with a low pressure DC glow discharge. *Cellulose*, **17**, 417–426.

[85] Gomathi, N. and Neogi, S. (2009) Surface modification of polypropylene using argon plasma: Statistical optimization of the process variables. *Applied Surface Science*, **255**, 7590–7600.

[86] Cheng, C., Liye, Z., and Zhan, R.-J. (2006) Surface modification of polymer fibre by the new atmospheric pressure cold plasma jet. *Surface and Coatings Technology*, **200**, 6659–6665.

[87] Malek, R. and Holme, I. (2011) The effect of plasma treatment on some properties of cotton. *I*, **2**, 271–280.

[88] Nithya, E., Radhai, R., Rajendran, R., Shalini, S., Rajendran, V., and Jayakumar, S. (2011) Synergetic effect of DC air plasma and cellulase enzyme treatment on the hydrophilicity of cotton fabric. *Carbohydrate Polymers*, **83**, 1652–1658.

[89] Müller, M., Rieser, T., Lunkwitz, K., Berwald, S., Meier-Haack, J., and Jehnichen, D. (1998) Anin-situ ATR-FTIR study on polyelectrolyte multilayer assemblies on solid surfaces and their susceptibility to fouling. *Macromolecular Rapid Communications*, **19**, 333–336.

[90] Bhat, N. V. and Upadhyay, D. J. (2002) Plasma-induced surface modification and adhesion enhancement of polypropylene surface. *Journal of Applied Polymer Science*, **86**, 925–936.

[91] Leroux, F., Campagne, C., Perwuelz, A., and Gengembre, L. (2008) Polypropylene film chemical and physical modifications by dielectric barrier discharge plasma treatment at atmospheric pressure. *Journal of Colloid and Interface Science*, **328**, 412–420.

[92] Sun, D. and Stylios, G. K. (2006) Fabric surface properties affected by low temperature plasma treatment. *Journal of Materials Processing Technology*, **173**, 172–177.

[93] Pons, J., Moreau, E., and Touchard, M. (2005) Asymmetric surface dielectric barrier discharge in air at atmospheric pressure: electrical properties and induced airflow characteristics. *Journal of Physics D: Applied Physics*, **38**, 3635–3642.

[94] Biganzoli, I., Barni, R., Gurioli, A., Pertile, R., and Riccardi, C. (2014) Experimental investigation of Lissajous figure shapes in planar and surface dielectric barrier discharges. *Journal of Physics: Conference Series*, **550**, 012039.

[95] Xu, X., Koeberg, M., Kuijpers, C.-J., and Kok, E. (2014) Development and validation of highly selective screening and confirmatory methods for the qualitative forensic analysis of organic explosive compounds with high performance liquid chromatography coupled with (photodiode array and) LTQ ion trap/Orbitrap ma. *Science & Justice*, **54**, 3–21.

[96] Demoranville, L. T. and Brewer, T. M. (2013) Ambient pressure thermal desorption ionization mass spectrometry for the analysis of substances of forensic interest. *The Analyst*, **138**, 5332–7.

[97] Singh, S. and Singh, M. (2003) Explosives detection systems (EDS) for aviation security. *Signal Processing*, **83**, 31–55.

[98] Crowson, C. A., Cullum, H. E., Hiley, R. W., and Lowe, A. M. (1996) A Survey of High Explosives Traces in Public Places. **41**, 980–989.

[99] Cullum, H. E., Mcgavigan, C., Uttley, C. Z., Stroud, M. A. M., and Warren, D. C. (2004) A Second Survey of High Explosives Traces in Public Places . **49**, 1–7.

[100] Cotte-Rodríguez, I. and Cooks, R. G. (2006) Non-proximate detection of explosives and chemical warfare agent simulants by desorption electrospray ionization mass spectrometry. *Chem. Commun.*, **0**, 2968–2970.

[101] French, J. B., Thomson, B. A., Davidson, W. R., Reid, N. M., and Buckley, J. A. (1985) *Atmospheric Pressure Chemical Ionization Mass Spectrometry*, pp. 101–121. Springer US.

[102] Sekimoto, K. and Takayama, M. (2010) Negative ion formation and evolution in atmospheric pressure corona discharges between point-to-plane electrodes with arbitrary needle angle. *The European Physical Journal D*, **60**, 589–599.

[103] Balog, J., et al. (2013) Intraoperative Tissue Identification Using Rapid Evaporative Ionization Mass Spectrometry. *Science Translational Medicine*, **5**, 194ra93–194ra93.

[104] Balog, J., et al. (2015) In Vivo Endoscopic Tissue Identification by Rapid Evaporative Ionization Mass Spectrometry (REIMS). *Angewandte Chemie International Edition*, **54**, 11059–11062.

[105] Usmanov, D. T., Chen, L. C., Yu, Z., Yamabe, S., Sakaki, S., and Hiraoka, K. (2015) Atmospheric pressure chemical ionization of explosives using alternating current corona discharge ion source. *Journal of Mass Spectrometry*, **50**, 651–661.

[106] Usmanov, D. T., Yu, Z., Chen, L. C., Hiraoka, K., and Yamabe, S. (2016) Low-pressure barrier discharge ion source using air as a carrier gas and its application to the analysis of drugs and explosives. *Journal of Mass Spectrometry*, **51**, 132–140.

[107] Sphon, J. A. (1978) Use of mass spectrometry for confirmation of animal drug residues. *Journal - Association of Official Analytical Chemists*, **61**, 1247–1252.

[108] SWGDRUG (2011) Scientific working Group for the Analysis of Seized Drugs (SWGDRUG) Recommendations. **6**, 1–62.

[109] SWGDRUG (2014) Scientific Working Group for the Analysis of Seized Drugs (SWGDRUG) Recommendations. Tech. rep.

[110] Peña-Quevedo, A. J. and Hernández-Rivera, S. P. (2009) Mass spectrometry analysis of hexamethylene triperoxide diamine by its decomposition products, may. vol. 7303, p. 730303.

[111] Popov, I. A., Chen, H., Kharybin, O. N., Nikolaev, E. N., and Cooks, R. G. (2005) Detection of explosives on solid surfaces by thermal desorption and ambient ion/molecule reactions. *Chemical Communications*, **2**, 1953–1955.

[112] Miller, J. N. and Miller, J. C. (2004) *Statistics and Chemometrics for Analytical Chemistry*, vol. 46. 6th edn.

[113] Bethem, R. A. and Boyd, R. K. (1998) Mass spectrometry in trace analysis. *Journal of the American Society for Mass Spectrometry*, **9**, 643–648.

[114] Aaron, R. and Lewis, P. (1987) Cocaine residues on money. *Crime Laboratory Digest*, **14**, 18–18.

[115] Esteve-Turrillas, F. A., Armenta, S., Moros, J., Garrigues, S., Pastor, A., and De La Guardia, M. (2005) Validated, non-destructive and environmentally friendly determination of cocaine in euro bank notes. *Journal of Chromatography A*, **1065**, 321–325.

[116] Roberts, D., Carter, J., Sleeman, R., and Burton, I. (1997) Application of tandem mass spectrometry to the detection of drugs on cash. *Spectroscopy Europe*, **9**, 16–22.

[117] Sleeman, R., Burton, F., Carter, J., Roberts, D., and Hulmston, P. (2000) Peer Reviewed: Drugs on Money. *Analytical Chemistry*, **72**, 397 A–403 A.

[118] Armenta, S. and de la Guardia, M. (2008) Analytical methods to determine cocaine contamination of banknotes from around the world. *TrAC - Trends in Analytical Chemistry*, **27**, 344–351.

[119] Carter, J. F., Sleeman, R., and Parry, J. (2003) The distribution of controlled drugs on banknotes via counting machines. *Forensic Science International*, **132**, 106–112.

[120] Ebejer, K. A., Lloyd, G. R., Brereton, R. G., Carter, J. F., and Sleeman, R. (2007) Factors influencing the contamination of UK banknotes with drugs of abuse. *Forensic Science International*, **171**, 165–170.

[121] Aitken, C. G., Wilson, A., Sleeman, R., Morgan, B. E., and Huish, J. (2017) Distribution of cocaine on banknotes in general circulation in England and Wales. *Forensic Science International*, **270**, 261–266.

[122] Sleeman, R., Carter, J., and Ebejer, K. (2005) Drugs on money and beyond: Tandem mass spectrometry in the forensic sciences. *Spectroscopy Europe*, **17**, 10–13.

[123] Bank of England (2016), Bank of England: Polymer Banknotes.

[124] Morrison, G. H., Cheng, K. L., and Grasserbauer, M. (1979) General Aspects of Trace Analytical MethodsIv. Recommendations for Nomenclature, Standard Procedures and Reporting of Experimental Data for Surface Analysis Techniques. *Pure and Applied Chemistry*, **51**, 2243–2250.

[125] Mallet, A. and Down, S. (2010) *Dictionary of mass spectrometry*. John Wiley & Sons.